https://doi.org/10.1016/j.rser.2023.113861

Operation of rechargeable metal-ion batteries in low-temperature environments

Xingyi Shi[#, a], Guangzhe Li[#, a], Ruihan Zhang[a], Oladapo Christopher Esan[a], Xiaoyu Huo[a], Qixing Wu[b, *], Liang An[a, c, d, *]

[a] Department of Mechanical Engineering, The Hong Kong Polytechnic University, Hung Hom, Kowloon, Hong Kong SAR, China

[b] Shenzhen Key Laboratory of New Lithium-ion Batteries and Mesoporous Materials, College of Chemistry and Environmental Engineering, Shenzhen University, Shenzhen, 518060, Guangdong Province, China

[c] Research Institute for Smart Energy, The Hong Kong Polytechnic University, Hung Hom, Kowloon, Hong Kong SAR, China.

[d] Research Institute for Advanced Manufacturing, The Hong Kong Polytechnic University, Hung Hom, Kowloon, Hong Kong SAR, China

[#] These authors contributed equally to this work.

* Corresponding authors.

Email: qxwu@szu.edu.cn (Q. Wu)

Email: liang.an@polyu.edu.hk (L. An)

Abstract

Rechargeable metal-ion battery is regarded as one of the most effective technologies for energy storage and conversion, and its booming development has led to its increasing applications in the emerged next-generation electric equipment, such as portable electronics and electric vehicles. However, at low temperatures (< 0 °C), performance deterioration of batteries usually occurs, which significantly hinders the wide adoption of metal-ion batteries, especially in high-latitude regions. Such undesirable issue is mainly attributed to the sluggish ion transport in battery systems at

low temperatures. Following this crucial consideration, extensive efforts have been made to tackle the ion-transport issues from various aspects. Resultantly, remarkable progress has been achieved, in recent years, on the development of metal-ion battery systems suitable for low-temperature operations. However, up to date, there is no existing systematic review that covers the latest research outcomes and advances on these metal-ion batteries operating at low temperatures. To this end, we first present the ion-transport phenomena in a typical metal-ion battery and discuss the prominent methods for revealing the rate-limiting step of ion transport. Critical ion-transport issues in the battery system at low temperature are also summarized while the corresponding strategies to effectively address these lingering issues are highlighted. In addition, other novel methods for tackling each ion-transport step for enhancing the low temperature performance of metal (Li, Na, K, Al, Zn)-ion batteries are also reviewed. Finally, the remaining challenges as well as relevant directions for future research on these battery systems are highlighted.

Keywords: Metal-ion batteries; Low temperature; Ion-transport issues; Rate-limiting steps; Thermal activation

Nomenclature

Abbreviations:

MIB	Metal-ion battery
LIB	Lithium-ion battery
SEI	Solid electrolyte interphase
CV	Cyclic voltammetry
EIS	Electrochemical impedance spectroscopy

GITT	Galvanostatic intermittent titration technique
SIBs	Sodium-ion batteries
PIBs	Potassium-ion batteries
AIBs	Aluminum-ion batteries
ZIBs	Zinc-ion batteries
CEI	Cathode electrode interface
DFT	Density functional theory

Symbols:

A	Arrhenius constant
c_p	Specific heat capacity
D_i	Diffusion coefficient
E_A	Activation energy of electrochemical reactions
E_h	Activation energy for the ion mobility
E_m	Activation energy for diffusion
e	Unit charge of electrons
I_A	Current
k	Reaction rate
k_B	Boltzmann factor
m	Mass
n_i	Free ion number
R	Gas constant
T	Temperature

U_0	Thermal equilibrium potential
u_i	Ionic mobility
V_A	Cell voltage during activation
v^*	Effective vibrational frequency
x	Distance of diffusion step
Z_i	Valence order
σ	Ionic conductivity
Γ	Movement frequency
τ_A	Activation time

1. Introduction

Tremendous advancements have been made towards the development and adoption of renewable resources, such as solar and wind power, to tackle the energy and environmental challenges caused by the overuse of primary energy sources.[1-4] However, due to their intermittent nature, the energy gleaned from these resources inevitably requires storage systems for continuous and sustainable end use. As a result of this, considerable efforts have been employed towards the development of advanced energy storage and conversion technologies.[5-11] Among them, significant progress has been made on metal-ion batteries (MIBs),[12-16] particularly the lithium-ion battery (LIB) technology, for which the Nobel Prize in Chemistry in 2019 was awarded. However, despite the booming development of MIBs, battery operation in low-temperature environments (< 0 °C) still suffers from distinct power/capacity degradation especially during long-term cycles.[17, 18]

The essential reason for such limited performances can be derived from the difficulties of ion transport in MIB systems operating at low temperatures, which results in huge electrochemical polarization, concentration polarization, and ohmic polarization. These often lead to a series of issues, such as the abnormal evolution of solid electrolyte interphase (SEI) film, dendrite formation, and electrode dissolution in the battery system, negatively influencing the cycling stability and safety of these batteries.[19] For example, when the LIB is operated at low temperatures, the diffusion of lithium ions at the anode becomes extremely slow, and consequently causes strong polarization during charging process.[20] In addition, the metallic lithium would further react with electrolyte,

resulting in the abnormal SEI evolution. Hence, an in-depth understanding of these ion-transport issues, not only in LIBs but also in other MIBs, is required. In the meanwhile, it is also significant to stimulate and facilitate the development of commensurate strategies to improve the ion-transport kinetics and thereby grants MIBs superior performances in low-temperature environments.

To gain a better understanding of these ion-transport issues, tremendous efforts have been made on using diverse kinds of electrochemical measurements, such as cyclic voltammetry (CV), electrochemical impedance spectroscopy (EIS), and galvanostatic intermittent titration technique (GITT), to reveal the ion-transport kinetics in MIBs at low temperature condition.[21] However, these methods could only reveal the overall kinetics properties, but incapable of identifying the rate-limiting steps in the MIB systems, thus leaving the kinetic issues elusive.[22, 23] In view of this, theoretical calculation, with its ability to provide a supplementary information and more detailed kinetic analysis for a specific ion-transport step, has therefore been combined with the electrochemical measurements to provide a more comprehensive and in-depth understanding of the ion-transport kinetics in MIB systems.[24] Using electrochemical measurements and theoretical calculation methods, more and more facts and insights have been garnered regarding the various ion-transport issues currently encountered in MIBs, and many effective strategies have been proposed and demonstrated to boost the low temperature performance of MIBs.

Considering the fast development of the high-performance MIBs operating at low temperature environment and in an attempt to finally obtain a MIB with superior performances under all-climate conditions, it is thus of vital importance to comprehensively understand the low-temperature MIBs from fundamental mechanism

to battery development. Up to now, several review articles germane to the operation of Li-ion/metal batteries at low temperatures have been published.[25-35] Among them, Li et al.[34] focused on the advances of low temperature electrolyte design for LIBs. Zhu et al.[26] and Zhao et al.[35] focused on the designing scheme of electrolyte and electrode materials for low-temperature LIBs, including tuning electrolyte composition and electrode surface modifications. Rodrigues et al.[25] later discussed the material tolerance of low-temperature LIBs, with more emphasis on the passivation and structural degradation issues of electrode materials at low temperatures. More recently, Chen et al.[27] gave a general review of energy storage devices operating under extreme conditions, such as low/high temperature, high moisture/humidity conditions, etc. Other related reviews majorly focused on low-temperature performance of some typical materials, such as $LiFePO_4$.[28] Beyond the common LIBs, till date, there is no systematic review article that covers the operation of other metal-ion batteries, such as sodium-ion batteries (SIBs), potassium-ion batteries (PIBs), aluminum-ion batteries (AIBs), and zinc-ion batteries (ZIBs), at low temperatures. In view of this, a timely review that presents a broad picture of all the types of low temperature MIBs, including but not limited to LIBs, is of great importance. Hence, in this work, a comprehensive review to the latest development and advancements of different kinds of MIBs from fundamental mechanisms to performance improvement strategies is presented. The fundamentals of ion-transport processes in MIB systems are first introduced. Twelve ion-transport steps are elaborately elucidated and the methods for identifying the rate-limiting steps are reviewed. Subsequently, some key steps engendering the undesirable ion-transport issues in these battery systems at low temperature are identified. Finally, the corresponding strategies to tackle these issues, including modifying crystal structure of electrode materials, constructing sufficient ion-diffusion pathways in electrode

materials, exploring new electrode materials with efficient ion diffusion channels, modifying the surface properties of electrode materials to avoid abnormal SEI/cathode electrode interface (CEI) evolution and reduce ion desolvation energy, engineering the composition of SEI/CEI film by catalytic additives, tailoring electrolyte composition with new cosolvent/metal salts and proper additives selection, designing new types of electrolyte, and activating batteries by preheating before operation are summarized. The recent low-temperature developments of all MIB systems, including LIBs, SIBs, PIBs, AIBs and ZIBs, are classified and extensively discussed.

The subsequent sections of this article are organized as follows: Section 2 presents the ion transport steps in a typical MIB system; Section 3 reviews the strategies for enhancing ion diffusion process in electrode materials; Section 4 summarizes other novel thermal activation strategies for preheating MIBs; and finally, Section 6 highlights the remaining challenges and perspectives for low temperature MIB development in the future.

2. Ion-transport steps in a typical MIB system

Ion transport in a typical rechargeable MIB system follows the "rock-chair" mechanism, which achieves energy storage and conversion via ion intercalation/deintercalation.[8] As shown in **Figure 1**, during this process, the metal ions need to travel across the membrane from one side to another, which involves different steps. These steps, though follow different mechanisms, are all sensitive to the operating temperature of the battery. For different types of MIB, due to the different physicochemical properties of their metal ions (**Table 1**), their low-temperature performances are also different. In this section, the mechanisms of each ion-transport step in a typical MIB system are

systematically introduced and the influences of operating temperature on each step are identified.

2.1 Ion diffusion process in electrode

At the beginning of discharge, metal ions are first extracted from the anode, simultaneously releasing electrons to the external circuit. Thereafter, these ions diffuse out of the anode via the channels in the anode materials. At the same time, on the opposite side, metal ions would also diffuse into the cathode and be accommodated at the storage sites, simultaneously accepting the electrons from the external circuit. Hence, to begin with, one of the major reasons that leads to the performance deterioration of MIB systems at low temperatures is the extraction and accommodation of metal ions, which are in accordance with Faradic reactions and can be described by Arrhenius Equation[36]:

$$k = Aexp(-E_A/RT) \quad (1)$$

where E_A represents the activation energy of electrochemical reactions, R stands for the gas constant, and A is the Arrhenius constant. It can be seen that, the decrement of operating temperature would reduce the reaction rate and thereby significantly limit the performance of MIBs.

As for the diffusion of metal ions in electrodes, the frequency of metal ions moving to their neighboring sites can be expressed by the transition-state theory[37]:

$$\Gamma = v^* exp\ (-\Delta E_h/k_B T) \quad (2)$$

where Γ is the movement frequency, v^* is the effective vibrational frequency, k_B is Boltzmann factor, and ΔE_h represents the required activation energy for the ion mobility. Hence, according to the equation, lowering the operating temperature would reduce the movement frequency of metal ions, which thereby would result in a sluggish

solid-state ion diffusion process in electrodes and thus cause the performance degradation of MIBs. Furthermore, the diffusivity of metal ions in electrodes is also related to the ionic size and crystal structures of electrode materials.[38] In general, metal ions with a larger ionic size, such as Na^+ (1.02 Å) and Ca^{2+} (1.00 Å), display more sluggish ion diffusion kinetics in electrodes at low temperatures, compared to Li^+ (0.76 Å) and Mg^{2+} (0.72 Å).[39, 40] Meanwhile, insertion-type electrode materials with narrow interstitial channels generally show sluggish ion diffusion kinetics. In some typical MIB systems, the sluggish ion diffusion in electrode is found to be the rate-limiting step, rather than ion desolvation and ion diffusion in SEI/CEI.[41] For instance, Zhang et al.[42] investigated the lithium/graphite cell and calculated the lithium diffusivity of LIBs at -20 °C, showing a dramatic decrease compared to the lithium diffusivity at 0 °C. It was found that the poor diffusivity of LIBs mainly originates from the sluggish ion diffusion kinetics in graphite. A LIB system constructed with β-$Li_xV_2O_5$ cathode was also investigated at low temperatures.[43] Activation energy for ion-diffusion in cathode is calculated by Arrhenius equation. It was found that the activation energy for solid-state lithium-ion diffusion in β-$Li_xV_2O_5$ cathode kept almost identical with that of electrochemical reaction at low temperature, indicating that poor lithium diffusion dynamic was also dominant cause of electrochemical performance degradation at low temperatures. Hence, the ion diffusion process in electrodes is a key process that needs great attention so as to ensure the stable performance of MIBs at low operating temperature. Strategies such as fabricating electrodes with a larger interstitial to allow a wider channel for metal ions diffusion could therefore be an effective method.

2.2 Ion diffusion process in SEI/CEI

Following the ion diffusion process in the electrode, the metal ions travel across the anode/SEI interface then diffuse through the SEI reaching the SEI/electrolyte interface.

Similarly, on the opposite side, after the desolvation of metal ions at the electrolyte/CEI interface, the metal ions then diffuse through the CEI reaching the CEI/cathode interface. Currently, there are majorly two types of models for the structure of the SEI/CEI, namely the mosaic structure and the two layered structure.[44] The mosaic structure convinced that several compounds precipitated simultaneously to form a mosaic of microphases,[45] while the two layered model believed that the SEI is consisted of two layers, including an inorganic-rich layer near the electrode/SEI interface and an organic-rich layer near the SEI/electrolyte interface. For the two layered structure, when the lithium-ion transport through the organic-rich layer, it mainly follows the pore diffusion mechanism. In contrast, when it travels across the inorganic-rich layer, there are another two possible ion-transport mechanisms, including knock-off mechanism and direct-hopping mechanism.[46] While the knock-off mechanism considers that lithium-ion diffusion is achieved by knocking off the lithium at its neighboring site, the latter mechanism believes that lithium ions directly hop through empty spaces between lattice sites. The activation energies of lithium-ion diffusion in SEI following different mechanisms are calculated and it was found that activation energy of lithium-ion diffusion following knock-off mechanism is 0.31 eV, smaller than that of direct-hopping mechanism (0.54 eV). Therefore, lithium-ion diffusion in SEI is preferable via a knock-off mechanism. Such a process, where the metal ions diffuse across the SEI/CEI, can be expressed as:[46]

$$D = 1/2v^{*}(\Delta x)^{2}\exp\left(-E_m/k_B T\right) \quad (3)$$

where *D* represents the diffusion coefficient, E_m is the activation energy for diffusion, and Δx stands for the distance of each diffusion step. Through this equation, it is easy to know that the decreasing of operating temperature would reduce the diffusion coefficient of metal ions and thus limit the pace of their transport. This change would

lead to the increase in the resistance of ion diffusion in SEI/CEI, resulting in an increased cell impedance, thereby causing severe electrode polarization.[25] Thomas et al.[47] reported the polarization of graphite anode at low temperatures due to the cell impedance increment, in which the SEI film on graphite anode contributes to a large portion.[48] Wang et al. reported that the ion diffusion in SEI layer is the rate-limiting step for graphite-insertion anode of LIBs, as evidenced by GITT results.[49] Hence, there are critical needs to engineer the SEI films for an enhanced ion diffusion.

2.3 Ion solvation/desolvation process

After the metal ions travel across the anode/SEI interface and reach the SEI/electrolyte interface, the solvation process of metal ions occurs by forming solvation sheaths with the solvent molecules. At the same time, on the opposite side, the solvated ions that migrated across the membrane and reach the CEI/electrolyte interface would subsequently start the desolvation process by the rupture of solvation sheath, so that the naked metal ions can then diffuse across the CEI to reach the cathode/CEI interface. In most cases, this ion solvation/desolvation process is considered to be the most important reason for performance deterioration of MIBs at low temperature and have been widely studied.[50, 51] Galvanostatic charge/discharge test, as an effective method, is often served as an auxiliary technique in the kinetics studies to reveal the rate-limiting step of ion transport. For example, Xu et al.[52] by combining the EIS technique with the galvanostatic charge/discharge tests have examined the ion-transport kinetics in LIBs. Two electrolytes were used for low-temperature operation, including LiTFSI in 1,3-dioxolane (DIOX) and lithium hexafluorophosphate ($LiPF_6$)-based commercial electrolyte. During the initial discharge of a fresh cell at - 40 °C, a distinct voltage drop was observed for commercial electrolyte, whereas the voltage drop in DIOX electrolyte is negligible. As the ionic conductivity of the two electrolytes is similar, the difference

in the voltage drop can only be attributed to the difference in kinetics of ion desolvation, which further resulted in a larger charge transfer resistance (R_{ct}) as demonstrated by EIS spectra leading to a much worse battery performance at low temperatures in comparison to the LIBs with DIOX electrolyte. Therefore, it can be concluded that sluggish ion desolvation in commercial electrolyte is a primary reason for performance degradation at low temperatures and thus require great attention.

In addition to the experimental studies, density functional theory (DFT) calculation as one powerful approach for studying the activation energy of a specific ion-transport step such as ion migration in electrolyte, ion diffusion in electrode and ion desolvation,[24] have also provided some theoretical support. Xu et al.[53] calculated the activation energies of lithium-ion desolvation and diffusion in electrolytes with different solvents, including DIOX, methyl ethyl carbonate (EMC), ethylene carbonate (EC), and dimethyl carbonate (DMC). It was found that the activation energies of lithium-ion diffusion across SEI/electrode interface are in the range of 0.15 eV to 0.6 eV. However, for the desolvation of lithium ions, activation energies are much higher, in the range of 2.00 to 2.60 eV, indicating that the ion desolvation is more kinetically sluggish. Using the DFT calculation, Okoshi et al.[24] investigated the desolvation of other metal ions including lithium, sodium, and magnesium cations in 27 types of organic electrolytes. It is reported that, the desolvation energies of different metal ions follow the following sequence: Na (103.2 – 187.5 kJ/mol) < Li (160.7 – 254.1 kJ/mol) < Mg (456.1 – 747.7 kJ/mol), which therefore again justifies its importance on determining the performances not only to LIBs but also to other types of MIBs. Furthermore, a linear dependence between the desolvation energy and reciprocal of temperature (T^{-1}) is also identified in this process,[54] which thus justifies the great impact of low operating temperature on the ion solvation/desolvation process and positions it

to be an important reason for the performance deterioration of MIBs at such environment. Hence, great efforts for further investigation and improvement of the solvation/desolvation process are still needed so as to eventually ensure superior performance of the battery at all-climate conditions.

2.4 Ion migration process in electrolyte

After the solvation of metal ions at the SEI/electrolyte interface, the solvated ions will thereafter migrate across the membrane and reach the CEI/electrolyte interface. Hence, in addition to the ion diffusion process in the electrode, ion migration also has a decisive effect on the low-temperature performance of the MIBs due to the long migration path from the anode to the cathode during the discharge process. Furthermore, the electrolyte viscosity, which is another major factor influencing the ion migration process, is also sensitive to the operating temperature. When the operating temperature decreases, the intermolecular distance would get smaller while the intermolecular force in solvent molecules would be enhanced. Such a change would therefore lead to a more sluggish ion migration kinetics in the electrolyte when an external electric field is applied, and further result in a decreased ionic conductivity according to the following equation:[55]

$$\sigma = \sum_i n_i u_i Z_i e \tag{4}$$

where σ represents the ionic conductivity, n_i represents the free ion number, Z_i stands for the valence order of ionic species *i,* and e is the unit charge of electrons. u_i represents the ionic mobility, which can be influenced by the operating temperature according to the following equation[56]:

$$u_i = \frac{D_i}{k_B T} \tag{5}$$

where D_i represents the diffusivity of ion species *i*.

Overall, this reduced ionic conductivity at low operating temperature would result in a larger ohmic voltage drop leading to an early hitting of the cut-off voltage, and at last limiting the discharge performance of the MIB system.

It is worth mentioning that, when the operating temperature gets even lower (below the melting point of the electrolyte), the electrolyte would even be frozen and thus greatly reducing the ion mobility. For example, commercial liquid electrolyte of LIBs, composed of $LiPF_6$ salt and organic solvents EC and DMC (1:1), has a high conductivity of 1 mS cm^{-1} at room temperature.[57] However, the electrolyte will be frozen below -10 ^oC, resulting in decreased ionic conductivity, thus not capable of low-temperature operation. The decreased ionic conductivity also results in increased polarization of the electrodes, due to the increased ohmic loss and concentration gradient of metal ions in the electrolyte. Such increased polarization may even cause safety problem and capacity loss of MIBs. For example, the increased polarization of anode in LIBs will lead to the formation of lithium dendrite, which will further react with the electrolyte and even penetrate the membrane, causing short circuit. Hence it is of crucial to address this critical problem by developing electrolyte with a lower frozen point not only to facilitate performance improvement of MIBs at low temperature environments but also to ensure a better safety.

3. Strategies for tackling ion-transport issues at low temperatures

As mentioned previously, ion-transport issues in MIBs at low temperature include sluggish ion diffusion in electrode materials or through SEI/CEI film, poor ionic conductivity of electrolyte, and high ion desolvation energies in electrolyte. Till now, various corresponding strategies (**Figure 2**) have been proposed to improve the low-temperature performance of MIBs. In this section, the strategies for tackling ion-

transport issues in MIBs at low temperatures, from anode/cathode electrode materials and SEI/CEI film to electrolyte design, are discussed and summarized.

3.1 Strategies for enhancing ion diffusion process in electrode materials

As discussed previously, the diffusivity of metal ions in anode or cathode materials is associated with the ionic size and crystal structure of the electrode. In general, metal ions with a larger ionic size, such as Na^+ (1.02 Å) and Ca^{2+} (1.00 Å), display worse diffusion kinetics in electrodes at low temperatures, as compared to Li^+ (0.76 Å) and Mg^{2+} (0.72 Å). Additionally, solid-state diffusion of metal ions in electrode materials at low temperature is also limited by insufficient or too long pathways in electrode structure. Moreover, the insertion/extraction of metal ions may even lead to volumetric changes and displacement of electrode materials thereby affecting the electrode structure and long-term stabilities, where such influence is considered to be even exacerbated under the low operating temperature condition due to the reduced interlayer spacing creating a larger barrier.[58] To address this issue, the two effective approaches to improve ion diffusion in electrode materials at low temperature are: (1) modifying crystal structure of electrode materials by heteroatom doping and oxidation to provide sufficient ion diffusion channels; and (2) constructing efficient ion-diffusion pathways via optimization of specific surface area and particle size, and 3D electrode design.

3.1.1 Modification of crystal structures

To enlarge the ion diffusion channels in crystal structure of electrode materials, different methods have been developed and studied, especially heteroatom doping, which is an effective approach for modifying both the anode and cathode material

structures to facilitate the sluggish metal-ion diffusion process inside the battery at low temperature.

To date, diverse kinds of element such as fluorine (F)[59], chromium (Cr)[60] and iron (Fe)[61] have been used as dopants for anode materials in LIBs and achieved improved battery performance at low operating temperature. Take an anode material of LIBs, spinel lithium titanate ($Li_4Ti_5O_{12}$, LTO), as an example. It is been regarded as a promising alternative to carbon-based anode for LIBs due to its excellent lithiation and delithiation reversibility without structure change as well as remarkably secure and reliable cycle stability without lithium dendrite formation, which however shows limited performance in sub-zero environment.[62] Hence, to enable a good electrochemical performance of LTO at low temperature, F atom was doped in LTO structure via a novel ammonium fluoride (NH_4F) based method in air which altered the lattice parameters and formed a protective lithium fluoride (LiF) layer on the surface of LTO anode (**Figure 3a**).[59] With the introduction of F atom, the LTO anode exhibited much higher capacity retention rate (63.3%) than that without F doping at -20 °C (**Figure 3b and c**). Zou et al.[60] studied the low-temperature performance of Cr doped LTO ($Li_{3.9}Cr_{0.3}Ti_{4.8}O_{12}$) nanofibers, and found that the 1D morphology composed of high-impurity nanoparticles facilitated Li^+ ion transport and achieved steady electrochemical performance at -20 °C condition. In another case, Fe was added into carbon nanofibers to enhance the Li^+ diffusion kinetics at low temperature, which exhibited high capacity retention of 250 mAh g^{-1} with the current of 400 mA g^{-1} after 55 cycles at -15 °C.[61] Other than the anode, elements including titanium (Ti),[63, 64] lanthanum (La) and magnesium (Mg),[65] vanadium (V) and F,[66] and Li and molybdenum (Mo)[67] were reported to be used as dopants at the cathode, and attained better battery performance at sub-zero environment. Take the common lithium iron phosphate ($LiFePO_4$, LFP) cathode in LIBs as an example. Liang's group[63]

doped Ti into the LFP cathode, and found that appropriate amount of Ti doping in LFP crystal structure could effectively shorten the deintercalation distance of Li^+ ions, leading to a discharge capacity of 122.3 mAh g^{-1} at -20 °C. However, they also found that the excess Ti atoms would cause a narrowed lithium-ion diffusion channel in LFP structure, which thereby demonstrating that the amount of Ti significantly affects the feature of LFP particles as well as the battery performance. In another type of cathode candidate, ternary metal oxide material ($MNi_xCo_yMn_{1-x-y}O_2$, M=Li, Na, K), which recently draws more and more interests because of its higher energy density, is also proven to achieve better low temperature performance after modification (**Figure 3d**).[68] Wei et al.[67] studied the effect of Li and Mo as co-dopants on $LiNi_{1/3}Co_{1/3}Mn_{1/3}O_2$ (NCM111) for LIBs (**Figure 3e**) and found that the Li/Mo co-doping could increase unit cell volume as well as the reaction activity of NCM111 particles, leading to the best discharge capacity of 65.41 mAh g^{-1} with the current of 5 C at -30 °C for the sample Mo/M = 0.02 and Li/M = 1.16.

In addition to the LIBs, many works have been conducted on modifying the anode and cathode materials by the heteroatom doping method for SIBs and achieved superior battery performance at sub-zero environment. For instance, a nitrogen doped porous carbon nanofiber combined with ultrafine zinc selenide (ZnSe) nanoparticles was applied as anode for SIBs operated at low temperatures within the range from -20 to -40 °C (**Figure 4a and b**). The modified anode attained higher Na^+ diffusion coefficient and thereby enabled the SIBs to maintain a reversible capacity of 122.8 and 55.0 mAh g^{-1} at -20 and -40 °C under 1.0 A g^{-1} after 1000 cycles, respectively.[69] At the cathode side of SIBs, the impact of F doping in tunnel-structured $Na_{0.66}[Mn_{0.66}Ti_{0.34}]O_2$ cathode was studied by Wang et al. (**Figure 4c and d**).[70] The tunnel structure of this cathode materials was expanded by F atoms, which facilitated the solid-state diffusion of

sodium ions, leading to a stable reversible capacity of 84 mAh g^{-1} at 0 °C and 61.5 mAh g^{-1} at -20 °C with 2 C current rate.

Other than the LIBs and SIBs, the cathode of ZIBs has also been modified using the heteroatom doping method and demonstrated improved low temperature performance. Vanadium pentoxide (V_2O_5) is a kind of promising cathode materials for aqueous ZIBs and many elements have been pre-intercalated in layered V_2O_5 structure to enhance ion diffusion kinetics and ensure structural cycling stability at low temperatures. Li's group doped Mn^{2+} [71] and K^{+} [72] into layered V_2O_5 and obtained the cathodes of $Mn_{0.15}V_2O_5{\cdot}nH_2O$ (**Figure 5a and b**) and $K_{0.5}V_2O_5$ (**Figure 5c and d**) to promote zinc ion diffusion and keep structural integrity at low temperatures. It is reported that the ZIBs displayed high reversible specific capacity of 100 mAh g^{-1} with current of 2.0 A g^{-1} after 3000 cycles ($Mn_{0.15}V_2O_5{\cdot}nH_2O$ based cathode) and 241 and 115 mA h g^{-1} after 1000 cycles with current rates of 1 and 5 A g^{-1} ($K_{0.5}V_2O_5$ based cathode) at -20 °C, respectively. In another work, a series of metal ions (Fe^{2+}, Co^{2+}, Ni^{2+}, Mn^{2+}, Zn^{2+} and Cu^{2+}) were doped into the interlayer to enhance the low temperature properties of ZIBs. Among these metal-ions, Cu^{2+} doped cathode is found to deliver the highest average discharge capacities of 320 and 132 mA h g^{-1} under current rates of 0.5 and 10 A g^{-1} at 0 °C due to enhanced zinc ion diffusion kinetics.[73] Similarly, Mg^{2+} was pre-intercalated into layered V_2O_5 ($Mg_{0.19}V_2O_5{\cdot}0.99H_2O$) to expand interlayer spacing up to 13.4 Å (**Figure 5e**), which enabled the ZIBs to display an energy density as high as 48.14 mWh cm^{-3} (1940 μWh cm^{-2}) under the power density of 17.83 mW cm^{-3} (0.72 mW cm^{-2}) coupled at -30 °C with a polyvinyl alcohol/glycerol gel electrolyte (**Figure 5f**).[74]

Apart from heteroatom doping, some other methods are also developed to modify the crystal structure of electrode materials. For LIBs, oxidation was used to expand the

interlayer spacing in mesocarbon microbeads (MCMBs) based anode for LIBs.[75] The commercial MCMBs were first oxidized and then followed with heat treatment in argon, which was found to result in an expanded interlayer from 0.337 to 0.351 nm. The obtained lithium diffusion coefficient of expanded MCMBs was 10^{-15} cm^2 s^{-1}, nearly two orders of magnitude larger than pristine MCMBs. For SIBs, Peng et al.[76] reported an ice-assisted approach to synthesize well-crystallized Prussian blue (PB) type cathode materials with the composition of $Na_{1.58}Fe[Fe(CN)_6]_{0.87}\cdot 2.38H_2O$, which held much lower content of $Fe(CN)_6$ defects (13%) than that (28%) in the PB materials fabricated from conventional method. The suppressed structure defects enable the $Na_{1.58}Fe[Fe(CN)_6]_{0.87}\cdot 2.38H_2O$ cathode to exhibit larger interstices, more cation diffusion channels, and lower Na^+ diffusion energy barrier (0.11 ~ 0.23 eV) than that in defect-rich crystal structure (2.63 ~ 2.81 eV), leading to fast Na^+ diffusion in cathode material, which enabled the SIB to achieve higher capacity retention rate of 93.2% under 50 mA g^{-1} at -10 °C than that with defect-rich PB cathode material (82.3%).

In summary, the heteroatom doping, oxidation, and new ice-assist synthesis methods are proven to be efficient strategies to enhance the electrochemical performance of electrode, which can enlarge the ion diffusion channels to facilitate the ion diffusion process within the electrode materials. Overall, modifying crystal structure is believed to be a facial and effective way that can enable the MIBs to attain a better performance in sub-zero environment. However, till date, though many progress has been achieved, the research on any potential side effects caused by such electrode modification method still needs further investigation.[77]

3.1.2 Construction of ion-diffusion pathways

In addition to the heteroatom doping method, constructing efficient ion-diffusion pathways in electrode materials by particle size and surface area optimization or three-dimensional (3D) electrode design is another effective strategy to allow the ease of ions transport and thereby boost the performance of MIBs at low temperatures.

3.1.2.1 Reduction of particle size

The first method is to enlarge active reaction area by enlarging the specific surface area and reducing the particle size of the electrode materials. For the anode materials of LIBs, many research works have been conducted on analyzing the effect of particle size and surface area on the electrochemical performance of LTO anode for LIBs, where the smaller particles and higher surface area have been found to accelerate lithium intercalation and deintercalation process and also enhance Li^+ diffusion in LTO at low temperature.[78-80] Take the dual-phase hierarchical porous LTO–TiO_2 (LTO–TO) microspheres fabricated by Huang et al.[81] as an example. The LTO–TO anode prepared for LIBs at low temperature were composed of ultra-thin nanosheets with a large specific surface area for interface intercalation reactions, which thereby ensured a much-reduced diffusion path for both electrons and lithium ions. With this novel LTO-TO anode, the discharge capacities of 143 mAh g^{-1} at 0 °C, 130 mAh g^{-1} at -10 °C, and 94 mAh g^{-1} at -40 °C were achieved. Furthermore, a capacity of 77 mAh g^{-1} was also readily attained at -20 °C with a high current rate of 5 C demonstrating the increment of specific surface area as an effective method. In another work, Wang' group synthesized the novel peapoded LTO nanoparticles via sacrificial template method, and it exhibited remarkably improved electrochemical performance (a high Coulombic efficiency of about 99% after 500 cycles at -25 °C with 10 C current rate).[82] In addition to the anode materials of LIBs, at the cathode, many works have been conducted on

increasing the specific surface area and reducing particle size of cathode materials such as LFP,[83-85] NCM,[86, 87] and others,[88, 89] which are all found to demonstrate improved battery performance at low temperature. The impact of particle size and degree of LFP purity on electrochemical performance for LIBs at low temperature was fully studied by Liang's group.[85] The high quality LFP cathode with reduced size exhibited higher diffusion coefficient of 2.73×10^{-13} cm^2 s^{-1} and higher specific capacity of 105.6 mAh g^{-1} at -20 °C as well as better capacity retention rates of 81.5%, 70.2% and 46.6% at 0, -20 and -40 °C, respectively, under 0.2 C. Apart from LFP, for the high energy density NCM cathode materials, Niu et al.[86] demonstrated the electrochemical performance of three different types of spherical $LiNi_{0.6}Co_{0.2}Mn_{0.2}O_2$ (NCM622) cathode with controlled particle size, nanostructure, specific surface area and pore distributions at 0 °C (**Figure 6a**). They discovered that 3 μm-NCM622 sample held the best low-temperature performance with a high specific capacity of 157 mAh g^{-1} and stable capacity retention of 156 mAh g^{-1} after 300 cycles under 1 C at 0 °C (**Figure 6b**). The same group further studied the property of 3 μm-NCM622 cathode at -30 °C in the design of commercial 18650 LIBs coupled with electrochemically exfoliated graphene (EG) anode, with which excellent cycling stability was obtained after 300 cycles without capacity fading at -30 °C under 1 C.[87] For other cathode materials, Martin et al.[88] fabricated V_2O_5 nanofibers with different diameter and proved that nanostructured 70 nm-V_2O_5 nanofiber showed better performance at 0 and -30 °C than micrometer-sized particles. Furthermore, the nanosized nickel-based Prussian blue (NiHCF) cathode (**Figure 6c and d**) was also found to hold a higher diffusion coefficient of 10^{-10} cm^2 s^{-1} at -70 °C and obtained a much higher capacity retention rate of 89% and 82% with the 0.05 C rate at -50 and -70 °C, respectively.[89]

Apart from the LIBs, in other types of MIBs, increasing the specific surface area and reducing particle size of electrode materials has also been demonstrated as an effective method. For instance, in SIB system, hard carbon (HC) derived from longan peel with appropriate surface area and pore size distribution were prepared via a two-step thermal treatment and employed as the anode materials. It is found to exhibit a safe and reversible capacity of 250 mAh g^{-1} without Na plating at -10 °C.[90] In other works, the nanosized PB based cathode materials were also developed for SIBs.[91, 92] Ma et al.[92] synthesized $Na_{1.59}Fe[Fe(CN)_6]_{0.95}$ nanoparticles with diameter of 50-200 nm and examined their low-temperature performance as cathode materials for SIBs (**Figure 6e and f**). The battery is demonstrated to achieve an initial discharge capacity of ~99.2 mAh g^{-1} at -10 °C under 10 mA g^{-1} by controlling the operation voltage less than 3.8V. Furthermore, another type of PB cathode composed of well-crystallinity $Na_2Ni[Fe(CN)_6]$ nanoparticles with size of 20-120 nm was also fabricated and applied for SIBs (**Figure 6g and h**). The battery was found to retain a high structure stability during cycling and provided sufficient diffusion ability for Na^+ and electron, resulting in excellent capacity retention rate of 87% at 0 °C and high capacity value of 54 mAh g^{-1} at -25 °C after 440 cycles.[91] One high-voltage cathode composed of $Na_3V_2(PO_4)_2O_2F$ with morphology of nano-tetraprism (NVPF-NTP) for SIBs prepared by Guo's group,[93] was also found to facilitate the sodium diffusion and exhibit superior cycling stability with a capacity retention rate of 76.4% under 0.2 C at -25 °C (**Figure 7a and b**). On top of these works, Yu's group[94] developed a top-down method to synthesize required anode/cathode materials with proper particle size and porosity based on mechanism implicitly occurring in SIBs during cycling. They prepared bismuth (Bi) nanoparticles coupling with porous carbon as anode material for SIBs and KIBs (**Figure 7c**), which reduced the diffusion path of electron/ion and realized

ultrafast kinetics for ion intercalation/deintercalation process, delivering remarkable rate capability (190 mAh g^{-1} with current rate of 5 A g^{-1} for SIBs and 233 mAh g^{-1} with current rate of 20 A g^{-1} for KIBs) and high cycling stability (205 mAh g^{-1} after 2000 cycles with current rate of 10 A g^{-1} for KIBs) at -20 °C (**Figure 7d and e**). These superior battery performances attained by increasing the specific surface area and reducing particle size of electrode materials thereby demonstrate the effectiveness of this modification strategy not only for LIBs but also for other types of MIB.

Overall, reducing particle size and enlarging the specific surface area is believed to be a promising method for improving the low-temperature battery performance as it can shorten the diffusion paths of metal ions and electrons to facilitate the intercalation/extraction process. Nevertheless, it should also be noted that the reduced particle size may also result in more side reactions and larger binder demand, thereby inevitably leading to a reduced energy.[95]

3.1.2.2 Control of electrode structure

The second method to ensure sufficient ion diffusion pathways in MIBs working in low temperature environment is to design 3D electrode structure and optimize the electrode thickness and porosity. To date, many works have been conducted on modifying the anode and cathode of LIBs using this method and improved battery performance has been achieved at low operating temperature.[96-98] For the anode materials of LIBs, a stacked layered 3D composite composed of uniformly distributed tin-nanoparticles in expanded graphite interlayers (Sn/EG) (**Figure 8a**) was developed by Huang's group,[99] which exhibited higher Li^+ diffusion coefficient and attained faster Li^+ intercalation kinetics, realizing superior capacities of 200 and 130 mAh g^{-1} under 0.1 and 0.2 C at -20 °C, respectively. Another graphite based 3D anode composite was reported by Xu

et al.,[53] consisting of carbon nanotube grown on porous graphite nanosheets with through-holes (PGN/CNT), which remarkably shortened the distance of Li^+ diffusion and contributed to an improved low-temperature performance of LIBs. Some other carbon-free anode materials with 3D structure were also developed. Passerini's group[100] synthesized a Zn-rich porous Cu–Zn alloy via dynamic hydrogen bubble template method as anode for LIBs (**Figure 8b**), and found that with optimal Cu/Zn atomic ratio ($Cu_{18}Zn_{82}$), the alloy anode exhibited higher lithium storage capability of 197 and 137 mAh g^{-1} under the current of 0.1 A g^{-1} at -20 and -30 °C. Beyond the anode materials, Zhang's group[101] also used this method to present a 3D hybrid cathode composite made of $Li_3V_2(PO_4)_3$ and biomass-derived porous carbon for LIBs (**Figure 8c**), which provided abundant channels for the diffusion of Li^+ and also accelerated its transport kinetics, yielding excellent rate capability of 80 mAh g^{-1} and superior capacity retention rate of 97% after 100 cycles under 5C at -20 °C.

Other than the LIBs, this method has also been applied for the fabrication of cathode/anode of other types of MIBs. For instance, Li et al.[102] designed one CNT based 3D anode material for SIBs, consisting of 9,10-phenanthrene quinone (PhQ) molecules encapsulated in single-walled CNT (PhQ@SWCNT) with tube diameters of 1.5 and 2.5 nm. The 2.5 nm- PhQ@SWCNT sample is found to allow efficient sodium ion diffusion at low temperature and exhibit equal capacity at 0 °C compared to of room temperature, indicating its excellent potential as anode for SIBs at low temperature. Another 3D pollen-scaffolded nickel selenide (NiSe) composite encapsulated by metalorganic framework-derived (MOF) carbon shell (**Figure 8d**) was also fabricated as anode for SIBs, which showed high Na^+ diffusion coefficient and stable structure during sodium intercalation/deintercalation, resulting in a decent capacity of 343.8 mAh g^{-1} under 200 mA g^{-1} at -5 °C.[103] In another case, Huang et al.[104] prepared a 3D layer-stacked Sb

nanosheets uniformly pasted graphene (LS-Sb@G) (**Figure 8e**) micro/nanocomposite as anode for SIBs, which demonstrated enhanced Na^+ ion diffusion thereby leading to high capacity retention of 506.6 and 472.5 mAh g^{-1} under 25 and 50 mA g^{-1} at -20 °C, respectively. Apart from the anode, You et al.[105] reported a 3D cathode material nucleating cubic PB nanoparticles on CNT (PB/CNT) (**Figure 8f**) for SIBs, which obtained ultrafast ionic and electronic transport kinetics, resulting in capacity retention rates of 81% and 86% under 2.4 C after 1000 cycles at 0 and -25 °C, respectively. On top of the SIBs, it has also been reported that, one 3D "trihigh tricontinuous design" graphene film cathode (**Figure 9)** for AIBs was developed by Gao's group,[106] which presented high quality, orientation, and channeling for local structures and continuous electron-conducting matrix, ion-diffusion highway, and electroactive mass for the whole electrode. The AIB employing this graphene film cathode achieved steady performance under a temperature range of -40 to 120 °C with excellent flexibility.

It is also worth mentioning that, apart from the 3D electrode structure, the length of ion diffusion pathways in electrode structure is also affected by the thickness and porosity of electrode. Wang's group[107] investigated the influences of electrode thickness on the low-temperature LIB performances. Anodes with different thicknesses (60, 70, 81, and 90 μm) were investigated at -20 °C, showing that a thinner electrode possesses a shorter transport pathway for ions and a decreased voltage loss, thus improving the battery capacity at low temperatures. Furthermore, anodes with different porosities ranging from 0.2 to 0.4 were also studied, showing that anode with higher porosity shortens ion diffusion pathways, thus displaying superior low-temperature performance.

In summary, electrodes with 3D structure are believed to facilitate the ions diffusion process and sometimes even work as a buffer to absorb the volumetric change effect,

especially at low operating temperature.[108] While it is worth noting that the electrode thickness and porosity are also vital for influencing the ion diffusion process inside the electrode and should be given more attention in the future.

3.1.3 Exploration of novel electrode materials

A number of new electrode composites for anode and cathode materials of MIBs operating at low temperature condition have been developed and tested. These materials are found to display better ion diffusion and transport kinetics than the commonly used or conventional materials.

For LIBs, diverse kinds of novel electrode materials have been developed and applied as the anode and cathode and demonstrated superior battery performance at low operating temperature.[109, 110] For example, the combination of carbon with proper ratio of Li alloying or conversion anodes is an efficacious approach to obtain high low-temperature performance anode for LIBs.[111] Using this approach, Marassi's group[112] presented a series of metal-oxidized graphite composites by mixing graphite with about 1% metal nanoparticles (Au, Ag, Ni, Cu, Al, Sn) as anode for low-temperature LIBs. It is found that, the Cu, Al and Sn modified anode exhibited dramatically improved intercalation capacity of ~90 mAh g^{-1} under 0.2 C at -30 °C due to enhanced Li^+ diffusion coefficient and reduced charge transfer resistance in these anodes. Then, drawn by the improved battery performance, Marassi's group later developed other types of novel electrode materials including oxidized graphite composite covered with few-nanometer thick Cu and Sn layers,[113, 114] Cu nanoparticles supported on Super-P carbon with graphite and LTO composites,[115, 116] and Sn nanoparticles embedded porous multichannel carbon microtubes[117], which have all been used as the anode for low-temperature LIBs. It is proved that Cu and Sn nanoparticles possess a positive

effect on improving the Li^+ diffusion kinetics at low temperature. This group also examined the low-temperature performance of Sn-carbon anode in full cell combined with spinel-type $LiNi_{0.5}Mn_{1.5}O_4$ cathode, and proved the Sn-carbon composite could be regarded as promising anode for LIBs at low temperature (**Figure 10a and b**).[118] Another promising anode for LIBs at low temperature is the zinc stannate (Zn_2SnO_4). Gao et al.[119] developed a Co-doped Zn_2SnO_4-graphene-carbon composite anode with accelerated ion and electron transfer properties, which delivered good electrochemical performance at -25 °C. As one of the typical transition-metal sulfide, thin molybdenum sulfide (MoS_2) nanosheets uniformly intermixed in carbon layers was also prepared as alternative anode for LIBs at low temperature condition, which held enhanced ion diffusion ability and faster lithiation kinetics, resulting in high capacities of 854.3 and 497.5 mAh g^{-1} under 100 and 1000 mA g^{-1} at -20 °C.[120] For cathode materials, the $Li_3V_2(PO_4)_3$ material holds higher apparent chemical diffusion coefficient of Li^+ (10^{-10} cm^2 s^{-1}) and lower activation energies of 6.57 kJ mol^{-1} than that of LFP cathode, demonstrating an easier diffusion kinetics during lithium intercalation and extraction at low temperature conditions.[121] Another cathode material, β-$Li_xV_2O_5$, performed remarkably and exhibit ultrahigh capacity retention rates of 82.3%, 79.5%, and 88.6% under 0.1 C at 0, -20, and -40 °C, respectively, which mainly resulted from the more 3D tunnels for Li^+ diffusion formed by three distinct kinds of vanadium polyhedron chains in the crystal structure.[43] In addition to inorganic electrode, organic materials have also drawn increasing attentions in the recent decades due to their good structure flexibility, tunability and wide application temperature range. For example, Zheng et al.[122] demonstrated a covalent amorphous polymer (CAP) cathode for LIBs. The organic cathode successfully reduced the charge transport resistance and enhanced Li^+

diffusion process. Consequently, the battery exhibited a superior capacity of 141 mAh g^{-1} at - 80 °C as well as a high-capacity retention of 61.3%.

In addition to the LIBs, Fan et al.[123] tailored a natural coral-like anode composed of homogeneously distributed Fe_7Se_8 nanoparticles with a well-defined graphitic carbon matrix (cl-Fe_7Se_8@C) for LIBs and SIBs at low temperature conditions (**Figure 10c**). It is demonstrated that, this cl-Fe_7Se_8@C anode possessed fast ionic and electrical diffusion kinetics for both LIBs and SIBs, thereby leading to an outstanding electrochemical performance at -25 °C to room temperature (**Figure 10d**). As for the cathode of SIBs, Mukai et al.[124] developed two novel kinds of cathode materials ($Li_{0.1}Na_{0.7}Co_{0.5}Mn_{0.5}O_2$ and $Li_{0.8}Co_{0.5}Mn_{0.5}O_2$,) and compared their cycling stability and power density at low operating temperature. They concluded that the power density of SIB based on these two cathodes is 21% higher than that of LIB at -30 °C and the capacity retention rate is two times higher for SIB than that of LIB at 0 °C, indicating the better Na^+ diffusion kinetics in $Li_{0.1}Na_{0.7}Co_{0.5}Mn_{0.5}O_2$ and $Li_{0.8}Co_{0.5}Mn_{0.5}O_2$ cathode materials. In another work, Hwang et al.[125]designed a ternary cathode material for SIBs, which is made of aligned hierarchical-columnar assembled spherical particles with a composition gradient of $NaNi_{0.75}Co_{0.02}Mn_{0.23}O_2$ to $NaNi_{0.58}Co_{0.06}Mn_{0.36}O_2$ from the inner to the outer end. This cathode is found to perform an excellent cycling retention as high as 92% under 75 mA g^{-1} at -20 °C after 100 cycles, which is considered to be resulted from the $Ni^{2+/3+/4+}$ redox reaction in O3-type layer compound as well as the radially aligned long columnar structure for ensuring the efficient Na^+ diffusion at low temperature condition.

Other than the LIBs and SIBs, many novel electrodes have also been fabricated for the ZIBs and achieved superior performance. Li's group fabricated two types of nanowire

morphology based materials, $(NH_4)_2V_6O_{16}\cdot 1.5H_2O$ (**Figure 10e and f**)[126] and polyethylene glycol (PEG)-intercalated V_2O_5 nanowires,[127] as cathode for low-temperature ZIBs. It is proved that the one-dimensional (1D) morphology provided enough interlayer distance while the PEG intersection expanded the diffusion channels for fast Zn^{2+} diffusion during intercalation and deintercalation process, which thereby leads to high cycling stability and rate capability at low temperature conditions. Their group also reported hydrangea-like amorphous Fe-V-O oxides ($FeVO_4$) with designed chemical compositions as cathode for low-temperature ZIBs (**Figure 10g**), which held highly noticeable Zn^{2+} diffusion coefficient and fast surface Zn^{2+} storage mechanism, contributing to a high discharge capacity of 80 mAh g^{-1} with the current of 0.1 A g^{-1} at -20 °C (**Figure 10h**).[128] Except for metal oxides, Zhi's group developed few-layer bismuth selenide (Bi_2Se_3) as cathode for low-temperature ZIBs.[129] With the presence of topological surface states and weaker lattice vibrations, the few-layer Bi_2Se_3 enabled the ZIB to deliver superior capacity of 524 mAh g^{-1} (-20 °C) at 0.3 A g^{-1} and high capacity retention rate of 94.6% over 2000 cycles at 0 °C. It is worth to mention that, at the anode of ZIBs, pure Zn metal anode is found to possess superior cycling stability at 0 °C without any protection, which thereby provides the ZIBs with great potential for stable operation at low temperature conditions. Such a special characteristic of the pure Zn anode is due to the inhibited reactivity between Zn metal and water, which resulted in balanced surface electrical field and more uniform deposition morphology of Zn during cycling.[130]

In this section, various electrode modification strategies have been summarized for enhancing the ion diffusion process inside the MIBs under low operating temperature, including: i) modifying crystal structure; ii) constructing efficient ion-diffusion pathways; and iii) exploring other new types of materials. These approaches are

universal for facilitating the ion diffusion processes and thereby can improve the electrochemical performance of MIBs at both room temperature and low operating temperature.[65, 131] While the strategy by modifying crystal structure through heteroatom doping though has been proved to be an effective method, should be careful about the material used, as it is possible to induce compatibility issue with the electrolytes. Another strategy by constructing effective ion-diffusion pathways in contrast may result in a reduced volumetric energy density and thereby play a negative effect on the LIBs used at room temperature.[25] Looking forward to the future, more attention should also be paid to the technical and economic issues in order to achieve the practical commercialization of these advanced electrode materials.

3.2 Strategies for enhancing ion diffusion through SEI/CEI

The SEI/CEI film is a passivation layer formed between anode/cathode and electrolyte, which is always produced by the decomposition of organic solvents and aggressive metal salts during the first charging-discharging cycle of the battery operation.[132] The quality of SEI/CEI film, especially the stability of its microstructure, plays an important role in the capacity retention ability, cycling stability, and rate capability of MIBs at low temperature conditions. Generally, a thin SEI/CEI film with high ionic conductivity and high stability is highly desired for achieving the superior performances of low-temperature MIBs, as it could enable a short diffusion pathway and fast ion diffusion kinetics. There are two approaches to form a stable and effective SEI/CEI film on anode/cathode surface in MIBs: firstly, modifying the surface properties of anode and cathode materials to avoid abnormal SEI/CEI evolution, and secondly engineering the composition of SEI/CEI film by introducing catalytic additives in electrolytes and designing an additional protective layer.

3.2.1 Modification of anode/cathode surface properties

Designing different coating layers on the surface of electrode materials is effective to enhance the properties of the SEI and CEI films. It could not only alter the surface properties of electrode materials and modify the contact resistance between the electrode particles, but also promote the metal deposition morphology and reform the composition of the SEI/CEI film, finally facilitating the ion diffusion through SEI/CEI films.

To date, different kinds of materials, such as carbon, metal oxides, metal fluorides and carbides, have been applied and coated on the electrode surfaces to form a SEI/CEI layer allowing efficient ion diffusion. Among these materials, carbon was the most widely used coating material on the surface of anode and cathode of MIBs due to its apparent electrical conductivity and cost-effective improvement on SEI/CEI formation. For the anode materials of LIBs, Shao's group[133] firstly synthesized carbon-coated LTO oxide electrodes by a cellulose-assisted combustion technique with sucrose as the organic carbon source, which modified the formation of SEI film and further reduced the charge-transfer resistance at the LTO/electrolyte interface, leading to an improved lithium insertion/extraction capacity and diffusion kinetics, especially at low temperature (-20 °C). At the cathode side of LIBs, carbon coating layer is also applied on electrode materials to improve the ion diffusion kinetics through CEI film. Over the years, different materials and designs, such as polystyrene(PS) spheres-originated carbon coating,[134] polyvinylpyrrolidone (PVP) assisted carbon coating,[84] graphitized carbon cage coating,[135] carbon coating coupled with well-crystallized Mn doping,[136] thin carbon coating layer,[137] amorphous and graphene-like carbon coating,[138] and carbon coated porous LFP/graphene composite[139] have been employed to coat the

carbon layer on the cathodes and are found to achieve improved battery performance at low operating temperature. The first work that compared the low-temperature performance of LFP cathode with/without carbon coating layer was reported by Chung et al..[140] It is found that the carbon coating layer could provide fast Li^+ diffusion through CEI film and ensure even distribution of LFP particles during cycling, which thereby enables the carbon coated LFP cathode to deliver 55.6% of theoretical capacity under 0.2 C at -20 °C. In another work, a double nano-carbon made of amorphous carbon coating and graphited conducting carbon decorated LFP cathode composite was designed for low-temperature LIBs (**Figure 11a-c**), in which the uniformly distributed amorphous carbon coating layer not only enhanced the Li^+ diffusion kinetics through the CEI film but also stabilized the CEI interface during cycling, resulting in an even higher capacity retention rate of 71.4% under 0.2 C at -20 °C.[141] The low-temperature performance of $Li_3V_2(PO_4)_3$ based cathode material was also modified by carbon coatings derived from different carbon sources, including sucrose,[142] polyvinyl alcohol,[143] glucose,[144] glucose and CNTs,[145] and citric acid,[146] which were all demonstrated to boost the LIB performances at low operating temperatures.

For SIBs, carbon coated hard carbon prepared from sugar pyrolysis was also investigated as anode,[147] which reduced the resistance in SEI and enhanced Na^+ diffusion, obtaining a high reversible capacity of 265 mAh g^{-1} with the current of 0.1 C at -15 °C. Similarly, porous carbon-coated $NaTi_2(PO_4)_3$ (NTP) particles,[148] N-doped carbon (NDC)-coated $Ni_{1.8}Co_{1.2}Se_4$ nanoparticles encapsulated in NDC nanoboxes,[149] and several graphitic carbon layers coated small FeS sphere[150] were designed and explored as anode for SIBs, which are all found to effectively reduce the charge transfer resistance between anode particles and electrolyte and thus facilitate Na^+ diffusion kinetics through SEI film, resulting in enhanced low-temperature performance.

Apart from carbon coatings, other coating materials were also reported and studied in the recent years. Friesen et al.[151] designed a porous Al_2O_3 based ceramic coating layer directly on graphite surface (**Figure 11d and e**) by a wet coating process in commercial 18650-type LIBs. The layer is composed of 500 nm nanoparticles and were coated to form a porous ceramic layer between anode and electrolyte, which could modify the formation and morphology of SEI on graphite anode and facilitate the lithium deposition/dissolution process during chare and discharge, leading to enhanced low-temperature performance and high safety at mechanical/thermal abuse. For cathode materials, a CeO_2 modified carbon coating layer was synthesized on the surface of $Li_3V_2(PO_4)_3$ particles (Ce-C/LVP), which enabled the Ce-C/LVP cathode to obtain a large Li^+ diffusion coefficient and a low resistance and polarization, delivering a specific capacity of 70.4 and 103.3 mAh g^{-1} within the voltage of 3.0-4.3 V and 3.0-4.8 V, respectively, under 1 C at -20 °C.[152] Although metal oxide coatings were found to effectively reduce the thickness of SEI/CEI films and suppress the phase transition on the surface of electrode materials, it was also proved that the metal oxide coatings would transfer into more stable metal fluoride species and combined with the SEI/CEI film during its formation.[153, 154] Based on this discovery, some metal fluorides were then directly employed as coating layer on the electrode materials, especially the AlF_3 based coatings. For instance, Sun's group[155] fabricated a thin AlF_3 coating layer with ~10 nm thickness (**Figure 11f**) on the surface of $LiNi_{0.8}Co_{0.15}Al_{0.05}O_2$ particles, and found that this AlF_3 coating layer greatly reduced the charge-transfer resistance between the cathode and the electrolyte and enhanced kinetics of Li^+ diffusion through the interface film by stabilizing the CEI structure at -10 °C condition. Another dense AlF_3 layer with a nanoscale thickness was successfully fabricated on the surface of $Li_{1.2}Ni_{0.13}Co_{0.13}Mn_{0.54}O_2$ particles (**Figure 11g**), and this AlF_3 layer activated the

formation of spinel structure and $LiAlO_2$ on the surface of cathode particles and built a rapid lithium ion transport bridge for adjacent active materials, improving the lithium ion diffusion kinetics through CEI film, which resulted in higher capacities of 161.9 and 109.3 mAh g^{-1} with the current of 0.1 C at -10 and -20 °C, respectively.[156] To further enhance the Li^+ diffusion kinetics and reduce charge transfer resistance of the SEI/CEI film at low temperature conditions of LIBs, more conductive coating layers using other materials such as Cu nanoparticle,[157] Ti_3SiC_2 nanoparticles,[158] and benzenediazonium tetrafluoroborate grafted polyphenylene conducting polymer, were reported to be used and achieved superior performances at low operating temperature.[159] It is reported that the electrode coated with the benzenediazonium tetrafluoroborate grafted polyphenylene conducting polymer enables the LIBs to deliver a superior capacity of 113.4 and 83.8 mAh g^{-1} under the current rate of 0.1 and 5 C, respectively, at -20 °C (LFP cathode) along with an outstanding long-term cycling stability with a capacity retention rate up to 90% under 0.5 C for over 1150 cycles at -20 °C (NCM622 cathode).[159]

3.2.2 Engineering of the SEI/CEI film composition

The stability and microstructure of SEI/CEI film play a critical role in the ion diffusion kinetics in MIBs at low temperature, which is always affected by the composition and formation mechanism of SEI/CEI layer during electrochemical testing. Consequently, some catalytic additives and additional protective layers have been developed to form a stable SEI/CEI film with proper composition for enabling stable operation of MIBs at low temperature conditions.

The first effective approach to stabilize the composition of SEI/CEI film is to introduce catalytic additives into the electrolyte of MIBs working at low temperature. The

reported additive materials for this purpose could be mainly divided into organic and inorganic materials, including organic molecules and organic/inorganic salts. For LIBs, Shi et al.[160] evaluated the effects of fluorosulfonyl isocyanate (FI) as an additive on SEI formation (**Figure 12a**) on graphite anode surface with 1.0 M $LiPF_6$ dissolved in EC: DMC (1:1, vol.) based electrolyte at low temperature conditions. It was confirmed that FI would be reduced prior in the electrolyte because of its high reduction potential (above 2.8 V vs. Li^+/Li) and produce highly conductive SEI film which contained thicker and higher content of protective inorganic components (mainly LiF, Li_2SO_4 and $ROSO_2Li$ species) thus ensuring higher Li^+ conductivity and simultaneously inhibiting the reductive decomposition of electrolyte and electrode erosion. The graphite anode displayed a high cycling stability for 20 cycles without capacity degradation at -20 °C with FI based electrolyte (**Figure 12b**). Elsewhere, dimethyl sulfide (DMS) was also applied as additive in 1.0 M $LiPF_6$-EC/EMC based electrolyte to improve the low-temperature performance of a graphite anode.[161] Due to the weak binding energy of its reduction product with Li^+, DMS presented proper reduction activity to ensure sufficient diffusion kinetics for Li^+ transfer and formed a more stable SEI film on graphite anode surface even at -20 °C. Other types of organic molecules and salts were also reported and studied as additives for LIBs, including difluoromethyl acetate,[162] 4-chloromethyl-1,3,2-dioxathiolane 2-oxide,[163] phenyl methanesulfonate,[164] 1,3-propane sultone,[165] vinylene carbonate,[165] N-(trimethylsilyl)diethylamine,[166] lithium bis(oxalate)borate,[167] cesium hexafluorophosphate,[168] lithium difluorophosphate,[169, 170] lithium-modified silica nanosalt,[171] lithium difluorobis(oxalato) phosphate,[172] sodium chloride,[173] and lithium carbonate,[174] which are all proved to effectively improve the low temperature performance of LIBs.

Using this approach, other types of MIBs have also demonstrated improved performance at low operating temperature. For SIBs, adiponitrile (ADN) was selected as a promising electrolyte additive due to its stronger ability of electron donating than carbonate solvents (**Figure 12c**), and since it was easier to be reduced on the surface of the cathode material, it thus could assist with the formation of a uniform and compact SEI film on the $Na_{0.76}Ni_{0.3}Fe_{0.4}Mn_{0.3}O_2$ cathode material surface.[175] The major components of this ADN promoted film contained NaF and NaCN salts, which could stabilize the SEI film and enhance sodium storage capacity at -20 °C. Take the ZIBs as another example, Li's group[176] studied the effect of diethyl ether and ethylene glycol as additives on the low temperature performance of the aqueous electrolyte, and it was found that the diethyl ether and ethylene glycol additives could stabilize the SEI film between zinc metal and electrolyte and further inhibit zinc dendritic growth and side reactions occurring at low-temperature conditions. These works therefore justify the introduction of catalytic additives into the electrolyte of MIBs as an effective method for enhancing the battery performance at low operating temperature.

Another method to improve the ion diffusion kinetics through the SEI/CEI films is to build an additional protective layer on electrode materials. Allyl sulfide (AS)-derived surface film was developed as a protective layer on the graphite anode to enhance low-temperature performance of LIBs.[177] The AS additive could be spontaneously oxidized after soaking into electrolyte and then build a sulfur-containing surface film, which thereafter could be converted into another carbon-rich sulfur-containing inner layer through pre-cycling and hence provide a substrate for the deposition of SEI layer on its outer surface. By incorporating this protective layer, the formed SEI with stable structure can thus facilitate the Li^+ diffusion kinetics and enable the LIBs with a superior reversible capacity at -30 °C. Using the same approach, Chen et al.[178] reported

the construction of a highly uniform SEI film with the assistance of a $SnCl_4$-derived protective layer for SIBs. This build SEI film thus enabled the fast sodium-ion diffusion process and thereby enhanced the cyclic stability and rate capabilities of SIBs at low temperatures. For ZIBs, a reduced graphene oxide film (**Figure 12d**) was placed between the separator and $V_2O_5 \cdot nH_2O$ cathode as a block layer to inhibit extra diffusion of dissolved active materials to the anode side and simultaneously improves the transport of Zn ions and electrons through CEI film. Such a design was found to help the $V_2O_5 \cdot nH_2O$ cathode to deliver a high capacity of 106 mAh g^{-1} after 100 cycles under the current of 100 mA g^{-1} at -20 °C.[179]

In this section, strategies including modifying electrode surface and introducing catalytic additives have been summarized for assisting the formation of stable and robust SEI/CEI layer to improve the ion diffusion process inside. While designing different coating layers on the electrode surface is proved effective for stabilizing SEI/CEI, improving ion diffusion kinetics, and reducing contact resistance, the widespread adoption of this method could be hindered by the difficult and costly manufacturing process.[180] In contrast, introducing additives is therefore believed to be a more feasible strategy for large-scale application with low cost,[181] while the selection of proper additives, however, requires careful attention. It is necessary for the additives to firstly possess suitable reduction potentials to allow them to undergo redox reaction in prior so as to minimize the electrolyte consumption.[182] Meanwhile, the additives are also expected to prevent the dissolution of any active electrode materials as well as other side reactions.

3.3 Strategies for reducing desolvation energy

As mentioned, ion desolvation is one dominating factor causing inferior low-temperature performance of MIBs. Different metal ions always exhibit quite distinct desolvation energy values, and large desolvation energy definitely leads to sluggish ion desolvation step at low temperature. Okoshi et al.[24] investigated the desolvation of lithium, sodium, and magnesium cations in 27 types of organic electrolytes using DFT calculations. Generally, the desolvation energies of different metal ions are according to the following sequence: Na (118.1-186.3 kJ mol^{-1}) < Li (160.7-254.1 kJ mol^{-1}) < Mg (459.2-747.7 kJ mol^{-1}). Mukai et al.[124] compared the power and cycle performance of SIBs and LIBs at low temperature, and they found that the full-cell SIB based on $Li_{0.1}Na_{0.7}Co_{0.5}Mn_{0.5}O_2$ (or $Li_{0.8}Co_{0.5}Mn_{0.5}O_2$) cathode and hard carbon anode displayed ~21% higher power density and two times higher capacity retention rate at -30 °C than LIBs. According to Raman spectroscopy and DFT calculations results, the better low-temperature performance of SIBs mainly arose from the relatively weaker interaction between Na^+ ions and aprotic polar solvents than that of Li^+, which further proved that a weak Lewis acidity of metal ion generally enables a smaller desolvation energy. Hence, to boost the low temperature performances of MIBs, improved ion desolvation kinetics is vital and to address this issue, several methods have been developed, where the major strategies have been summarized and discussed.

3.3.1 Introduction of catalytic additives

In order to reduce the desolvation energy of metal ions in MIBs at low-temperature conditions, some catalytic additives have been employed. For LIBs, Huang et al.[183] prepared graphite-CuO composite anode and confirmed the catalytic impact of CuO on the intercalation process of Li^+ into graphite anode. CuO could enhance the desolvation reaction rate by reducing the electronic density on the SEI film surface. Based on this

discovery, Marassi's group developed partially oxidized graphite mixed with Cu powders (**Figure 13a and b**), for LIBs at low temperature conditions.[113] It is again proved that the Cu metal could catalyze lithium-ion desolvation process on the electrode surface and therefore reduce activation energy of the charge-transfer in SEI film, with which the graphite delivered high reversible capacities of 130 mAh g^{-1} under 0.2 C at -30 °C (**Figure 13c)**. Apart from Cu metal, Sn nanoparticle is also found to exhibit a catalytic activity to the Li^+ ion desolvation process, and is thus used as additive in graphite[114] and porous multichannel carbon microtubes (PMCMT) anode,[117] which enables the graphite and PMCMT anodes to achieve superior long-term cycling stability and reversible specific capacities at low temperature conditions.

3.3.2 Modification of electrode materials surface

Altering the surface properties of electrode materials is another method for reducing ion desolvation energy and enhancing the low-temperature performance of MIBs. Liu et al.[184] introduced sulfide-rich SEI layer into the surface of a SiO/C anode for LIBs to enhance the battery performance at low temperature. The reported modification layer altered the decomposition path for Li ions and thereby promote the desolvation process at low temperature. Overall, the system achieved a capacity retention of 73% at -20 ˚C. In another study, Delaporte et al.[185] modified LTO anode with Li-rich $PTCLi_4$ organic molecule, using spray-dryer technique to create a layer of few-nanometer-thick carbon coating on the electrode surface. It was found that the perylene stacking structure of modified LTO enhanced the electron motion. Meanwhile, the lithiophilic –COO−Li+ groups formed conductive channels to promote the desolvation process. When cycled at C/2 rate at -20 ˚C, the coated electrode was found to deliver comparable specific capacity with the pristine electrode cycled at 25 ˚C.

In addition to LIBs, for ZIBs, Wang et al.[186] demonstrated a Zn foil anode with ZnF_2-Ag nanoparticles coating as hybrid surface (ZnF_2-Ag@Zn). It was found that while the hydrophilic ZnF_2 surface could bind water molecules and promote the desolvation process, the zincophilic Ag surface could reduce the electrode overpotential to facilitate the nucleation processes. Consequently, the battery exhibited ultralong cycling performance for 5000 cycles at -40 ˚C.

3.3.3 Development of weakly solvated electrolytes

In addition to the methods mentioned in the previous sections, another approach to reduce the desolvation energy is to employ weakly solvated electrolytes. By introducing the electrolytes with lower affinity between metal ions and solvent molecules, the ability for solvent molecules to combine with metal ions becomes lower and thereby the desolvation process would be easier.

Up till now, several works have been conducted to develop electrolytes which can reduce desolvation energy.[187-190] Fan et al.[187] developed novel electrolytes for the LIB by dissolving several fluorinated carbonate electrolytes into non-polar stable solvents to tame the affinity between solvent molecules and Li^+ ions. The developed electrolytes were found to possess low Li^+ desolvation energy since the non-polar solvents broke the interactions between the fluorinated polar electrolyte. Consequently, the battery delivered 56% of the room-temperature capacity at -85 °C. Similarly, Yang et al.[189] proposed a fluorinated electrolyte based on ethyl trifluoroacetate (ETFA) solvent. Due to the low binding energy between the ETFA solvent and Li^+ ions (10.05 kJ mol^{-1}), the desolvation process was greatly enhanced and the batteries demonstrated excellent rate performance at subzero operating temperatures lower than -40 ˚C. Similarly, for SIBs, Zheng et al.[188] developed a highly-fluorinated weakly-solvated electrolyte with low-

viscosity, which could successfully knock down the kinetic barriers of Na^+ ion de-solvation process. The designed SIB achieved discharging capacities of 89.2 mA h g^{-1} at a temperature down to -30 ˚C.

In this section, as mentioned, the desolvation process is believed to greatly affect the performance of MIBs at low temperatures. Therefore, up till now, different strategies have been proposed to enhance this process, including the electrode and electrolyte modification methods. While the surface modification of the electrode materials has been proved to effectively promote the charge-transfer process inside the SEI and enhance the desolvation process, it is complicate and difficult for scale-up and still only have limited works therefore requires further comprehensive study.[77] The electrolyte modification method on the contrary is facile and easy for large-scale application thereby presenting it to be a favorable strategy for improving the MIB performances at low temperature.[191]

3.4 Strategies for enhancing ion migration in electrolyte

As the operating temperature gets lower, the liquid electrolyte viscosity increases, and may even get frozen when the operating temperature drops below its melting point. Hence, in MIB systems, the reduced ion mobility in electrolyte due to the decrease of operating temperature would result in more sluggish ion migration kinetics and thereby limit the battery performances.[187] In recent years, different methods including new cosolvent, proper additives selection, and new types of electrolyte alternatives design have been developed to facilitate the ion migration process in electrolyte and further ensure high ion conductivity for MIBs operating at low temperature conditions.

3.4.1 Exploration of novel electrolyte cosolvents

As solvents for traditional electrolytes such as EC or DMC possess relatively high freezing points, the electrolyte conductivity generally decreases rapidly at lower temperatures, which greatly hinders the battery performance. Thereby, in order to improve the ionic conductivity of electrolyte at low temperature conditions, proper cosolvents can be introduced into the mixtures of electrolyte solvents to reduce the freezing points and the viscosity of the electrolytes.[26] To select proper cosolvents, some critical features should be considered, including high dielectric constant, low viscosity, adequate Lewis acid-based coordination behavior, appropriate liquid ranges, salt solubility in the medium, and chemical compatibility with the electrode. In addition, the cosolvents must have adequate electrochemical stability over a wide voltage window, and excellent thermal and chemical stability.

Several ternary or quaternary solvent mixtures based on different ratios of alkyl carbonates, such as EC, DMC, and diethyl carbonate (DEC), ethyl methyl carbonate (EMC), propylene carbonate (PC) and fluoroethylene carbonate (FEC), were developed to enhance the properties of electrolyte solutions at low temperature conditions for MIBs. Among them, the EC+DMC+DEC mixture,[192] EC+DMC+EMC mixture,[193] EC+DMC+DEC+EMC mixture,[194-196] PC+EC+EMC mixture,[197] and FEC+PC+EC +EMC mixture[198] were prepared and studied at low temperature condition, which were all found to exhibit higher ionic conductivity, lower viscosity and improved stability than binary or pure solvent systems for LIBs. In addition, these ternary and quaternary electrolyte systems were also found to modify the LiF content in the SEI layer, which thereby could accelerate the transport of lithium-ion through SEI film and lead to promising reversible capacity and cycling stability for LIBs at low temperature conditions. Wang's group[187] developed fluorinated carbonate electrolytes (LiFSI-

FEC/FEMC or LiBETI-FEC/DEC) mixed with highly fluorinated non-polar solvents (tetrafluoro-1-(2,2,2-trifluoroethoxy)ethane or methoxyperfluorobutane) for wide-temperature LIBs. These new fluorinated electrolytes possess higher conductivity, wider liquid-phase temperature range, lower viscosity and lower Li^+ desolvation energy than pure carbonate-based electrolyte, enabling the $LiNi_{0.8}Co_{0.15}Al_{0.05}O_2$ || Li battery to deliver high-capacity retention rate of ~50% even at -85 °C. In addition to LIBs, they also developed similar electrolytes for SIBs by replacing NaFSI with LiFSI salt, which displayed higher Na^+ conductivity and faster diffusion kinetics than pure carbonate electrolyte. With such fluorinated electrolytes, the $Na_3V_2(PO_4)_2O_2F$ || Na cell delivered a specific capacity of 70 mAh g^{-1} even at -58 °C, which was ~50% of specific capacity at room temperature.

Apart from alkyl carbonate-based solvents, some other solvents were also developed and studied as cosolvents in electrolyte to improve the low-temperature performance of MIBs. Smart et al.[199] chose a series of ester solvents for incorporation into multicomponent electrolyte formulations, including methyl acetate (MA), ethyl acetate (EA), ethyl propionate (EP), and ethyl butyrate (EB). The conductivity of the electrolytes added with these four esters was found to vary with the following trend: EC+DEC+DMC+MA > EC+DEC+DMC+EA > EC+DEC+DMC+EP > EC+DEC+DMC+EB. And the cells containing the (EP and EB) based electrolytes displayed better low-temperature performance compared to the cells containing (MA and EA) based electrolytes. In 2010, the same group investigated other types of esters, including methyl propionate (MP), EP, methyl butyrate (MB), EB, propyl butyrate (PB), and butyl butyrate (BB) as cosolvents into multicomponent carbonate electrolytes of 1.0 M $LiPF_6$ in EC+EMC+X with volume ratio of 20:60:20 % (X = ester cosolvent).[200] They found that these ester cosolvents with lower molecular weight exhibited lower

viscosity and generally displayed better low-temperature performance than the higher molecular weight solvents. Rodrigo's group[201, 202] fully studied the incorporation of IZ as cosolvent in EC and FEC based electrolyte system, and they examined the effect of IZ on ionic conductivity and SEI formation in the lithium-graphite cell (**Figure 14a**). The IZ-based electrolyte exhibited an ionic conductivity 15 mS cm^{-1} at -20 °C, five times higher than those of the baseline electrolytes (3 mS cm^{-1}), which further resulted in delivering a high reversible capacity of 187.5 mAh g^{-1} with a high Coulombic efficiency of 99.7% at -20 °C, nine times higher than that of the cell with baseline electrolytes. Recently, other groups also focused on analyzing the effects of ester as cosolvents with different weight or volume ratios for properties of electrolytes at low-temperature, including MA,[203-206] EA,[51, 207] MP,[208] isopropyl acetate (IPA) and isoamyl acetate (IAA),[209] trifluoroacetate,[210] 2,2,2-Trifluoroethyl n-caproate,[211] methyl 3,3,3-trifluoropionate (MTFP),[212] DMS and diethyl sulfite (DES).[213, 214]

Ether is another promising type of cosolvents to improve the diffusivity of the lithium-ion in low-temperature electrolyte due to their low melting points and nonflammable nature. Different ethers were applied as cosolvents to modify the low-temperature performance of current electrolyte for MIBs, such as sulfolane,[215] 1,1,2,2-tetrafluoroethyl-2,2,3,3-tetrafluoropropyl ether,[216] 1,3-dioxolane,[52] 1,1,2,2-tetrafluoroethyl-2,2,3,3-tetrafluropropyl ether,[217] and 1,2-dimethoxyethane.[218] Naoi et al.[219] investigated a hydrofluoroether, 2-trifluoromethyl-3-methoxyperfluoropentane (TMMP), as nonflammable cosolvent for LIBs. The TMMP mixed electrolyte exhibited a lower melting point (-38 °C) compared to that of EC (37 °C) and modified the SEI composition to ensure rich C–F groups with lower surface energy, with which the MCMB/$LiCoO_2$ cell delivered much higher capacity retention of 60% under 0.2 C within 2.0~4.2V at -20 °C than that with pure carbonate electrolyte (21%).

Overall, various types of cosolvents, such as alkyl carbonate-based and ether-based, have been developed for the performance enhancement of low temperature MIBs. However, while introducing these cosolvents has been proved to be a promising method, it is of vital importance to carefully examine the compatibility of these solvents with electrode materials before large-scale application.[77]

3.4.2 Exploration of novel electrolyte salts

Apart from the solvents, the metal salt is another necessary component in the electrolyte. As a solute of the electrolytes for MIBs, the metal salts are expected to satisfy the following necessary properties: (i) maintain stable composition and ensure no side reactions with electrolyte solvents and electrode materials within the operation voltage windows; (ii) provide high ionic conductivity over wide operating temperature range, (iii) build a thin and stable SEI/CEI film on the electrode surface; and (iv) passivate the surface of current collectors at the anode and cathode sides.

Tremendous efforts have been made to search for suitable salts with adequate low-temperature properties for the electrolyte and thereby ensure superior performance of MIBs. Ein-Eli et al.[220] examined the low-temperature performance of four different salts: lithium hexafluoroarsenate ($LiAsF_6$), lithium hexafluorophosphate ($LiPF_6$), lithium bis(trifluoromethanesulfonyl)imide ($LiN(SO_2CF_3)_2$), and lithium tris(trifluoromethanesulfonyl)methide ($LiC(SO_2CF_3)_3$), in methyl formate (MF) and EC mixed solvent for LIBs. It is found that the $LiAsF_6$ based electrolyte exhibit the best properties with the highest ionic conductivity of 5.6~8.4 mS cm^{-1} at -40 °C. Apart from these salts, borate-based salts have been regarded as another group of promising alternatives due to their relatively high solubility in carbonate-based solvents, less moisture-sensitive, better thermal stability, favorable compatibility with Li metal on Cu

and better passivation on Al current collectors than $LiPF_6$ based salts. Attracted by their superiorities, a series of borate-based salts have been developed and studied to improve the low-temperature performance of LIBs, including lithium tetrafluoroborate ($LiBF_4$),[221, 222] lithium bis(oxalato)borate (LiBOB),[223, 224] lithium oxalyldifluoroborate (LiODFB or $LiBC_2O_4F_2$),[225-228] and lithium pentafluoroethyltrifluoroborate ($LiC_2F_5BF_3$, or LiFAB).[229] It is confirmed that these borate-based salts not only could help with the formation of the SEI film on graphite anode and thus modify the chemical composition and structural stability of SEI film. In addition, the ionic conductivities of these borate-based electrolytes are also much higher than that of conventional $LiPF_6$ based electrolytes at low temperature conditions, which therefore enabled the LIBs to deliver higher reversible capacity and greater cycling stability.

In addition to the LIBs, some borate-based salts were also developed for other types of low-temperature MIBs, such as the ZIBs. Sun et al.[230] have developed a borate salt based electrolyte for ZIBs that consists of 4.0 M of zinc tetrafluoroborate ($Zn(BF_4)_2$) in water. Due to the impact of BF_4^- anions to break the hydrogen-bond networks in pure water molecules by the formed OH/F hydrogen bonds, the new $Zn(BF_4)_2$ based electrolyte has displayed an ultralow freezing point of -122 °C along with an ultrahigh ionic conductivity of 1.47 mS cm^{-1} even at -70 °C. Such a superior low temperature performance therefore allows the Zn || tetrachlorobenzoquinone (TCBQ) battery to exhibit an excellent discharge capacity of 63.5 mA h g^{-1} with an ultrahigh energy density of 76.2 W h kg^{-1} even at -95 °C. Other than the borate-based salts, several metal perchlorates are also well explored for low-temperature ZIBs. Yang's group[231] reported a chaotropic salt based aqueous electrolyte containing 3.0 M zinc perchlorate ($Zn(ClO_4)_2$) salt (**Figure 14b**), which possesses a much lower concentration than the one used in "water-in-salt" electrolyte. The developed electrolyte is found to hold a

superior ionic conductivity of (4.23 mS cm^{-1}) and thereby enables a much faster ion migration even at -50 °C, which is mainly resulted from the newly formed hydrogen bonds between solute anion ClO_4^- and water molecules that could inhibit the ice crystal construction at low temperature. To further improve the low-temperature performance of ClO_4^- based electrolyte for ZIBs, one dual metal perchlorate salts based electrolyte made of 3.5M magnesium perchlorate ($Mg(ClO_4)_2$) + 1.0 M $Zn(ClO_4)_2$ was developed (**Figure 14c**).[232] In this dual-salt electrolyte, synergistic effect was produced by oxygen-ligand Mg^{2+} cation and hydrogen-ligand ClO_4^- anion, which decreased the number of hydrogen bonds in water molecules, making the electrolyte to obtain excellent low-temperature properties including -121 °C freezing point, 1.41 mS cm^{-1} ionic conductivity as well as 22.9 mPa s viscosity at -70 °C.

In summary, exploring and using these novel salts for tailoring the electrolyte composition is an effective strategy for the development of low temperature MIBs with superior performances. While since the introduction of these salts can significantly affect the electrolyte properties including viscosity, conductivity and diffusivity,[233] future research should also pay attention to the compatibility of these novel salts with different solvents especially under the effect of changed operating temperature.

3.4.3 Introduction of electrolyte additives

In addition to the approaches mentioned previously, another effective method to improve electrolyte conductivity is introducing additives into the electrolyte solutions. Generally, the employed additives possess low melting point and high dielectric constant, which thereby can inhibit the freezing of liquid electrolyte and increase its ionic conductivity for MIBs at low-temperature conditions. For LIBs, Kim et al.[234] applied three polydimethylsiloxane (PDMS)-based polymers - poly[dimethylsiloxane-

co-(siloxane-g-acrylate)] (PDMS-A), poly(dimethylsiloxane-co-phenylsiloxane) (PDMS-P), and poly[dimethylsiloxane-co-(siloxane-g-ethylene oxide)] (PDMS-EO) as additives to modify the low-temperature performance of the organic electrolytes (**Figure 14d**). With these three additives, the developed liquid electrolyte is found to be stable under 5.0 V and demonstrated a high ionic conductivity of 0.5 mS cm^{-1} even at -20 °C. Later, the same group continued to improve the low-temperature performance of LIBs by combining PDMS-A with lithium-modified silica nanosalt as additives.[235] With the help of surface functional groups on these two additives, the liquid electrolyte held an electrochemical stability over 5.5V, while the ionic conductivity reached 0.4 mS cm^{-1} even at -20 °C. In another study, the ionic liquid-decorated poly(methyl methacrylate) (PMMA) nanoparticles have been studied and used as additives to improve the ionic conductivity of electrolyte in LIBs.[236] It is found that, the ionic liquid groups induce a plasticizing effect, which favors the expansion of the free volume, thereby contributing to a high ionic conductivity of 0.915 mS cm^{-1} at -40 °C. In another type of MIBs- the ZIB, diethyl ether and ethylene glycol were chosen as additives to improve the anti-freezing property of common aqueous electrolyte (2.0 M $ZnSO_4$ and 0.2 M $MnSO_4$ dissolved in water).[176] With the addition of 1% diethyl ether and 30% ethylene glycol, the aqueous electrolyte exhibited much higher ionic conductivity of 0.42 S cm^{-1} at -10 °C than the one without additives (0.0012 S cm^{-1}).

In summary, introducing electrolyte additives is believed to be one economic method for enhancing the performance of low temperature MIBs.[237] Except introducing single additive, some works have also attempted to adopt multiple additives simultaneously to obtain combined beneficial effects. However, the combination of different additives can also lead to increased cost and more complex electrolyte handling process, which would conversely hamper their practical applications. Moreover, it is worth noting that

the introduction of additives will also exert complex effect on the electrolyte conductivity and viscosity depending on their functional groups, electronegativity and dielectric constant.[238] Therefore, comprehensive study about the interaction between additives and electrolyte solvents is also essential for realizing the development of versatile and efficient additives.

3.4.4 Design of novel electrolytes

Recently, some new types of electrolytes have been designed to improve the low-temperature performance of MIBs. Although the organic electrolytes have been widely used in commercial battery markets, aqueous electrolytes generally possess higher ionic conductivity compared to organic electrolytes due to their lower viscosity. "Water-in-salt" electrolytes are always holding promising high ionic conductivity, which can greatly reduce the freezing point and extend the voltage window of the batteries.[239] One "water-in-salt" electrolyte made of 21.0 m LiTFSI in water is a well-designed low-temperature aqueous electrolyte, capable of operating stably even at -20 °C.[240] The electrolyte is found to display a good cyclic stability in LIBs by virtue of less dissolved oxygen in water and stable SEI film. The similar "water-in-salt" strategy is also extended to other types of MIBs, such as the aqueous SIBs. Reber et al.[239] developed one highly concentrated aqueous electrolyte consisting of asymmetric-anion based salt, sodium (fluorosulfonyl)(trifluoromethylsulfonyl)imide (NaFTFSI), for SIBs to avoid the partial crystallization of "water-in-salt" electrolytes during long-term cycling at low temperature conditions (**Figure 15a**). With the FTFSI anion, the aqueous SIB based on $NaTi_2(PO_4)_3$ anode and $Na_3(VOPO_4)_2F$ cathode exhibits high-capacity retention rate of 74% after 500 cycles under the current of 0.2 C even at -10 °C (**Figure 15b**).

Solid-state electrolyte (SSE) is another type of new electrolytes with great potential, which, however, generally possesses poor ionic conductivity due to the low ions mobility. The ion transport through SSEs can be achieved by hopping between the interstitials and vacancies of crystals. For low-temperature operation, the ionic conductivity of SSEs can be improved by the following methods: i) increasing the mobile ion concentration; ii) increasing the number of vacancies and interstitials; and iii) improving the hopping attempt frequencies. Recently, several groups have attempted to employ SSEs for MIBs at low temperature conditions. For LIBs, Zhu et al.[241] prepared a novel single-ionic conducting SSE, which is prepared by anchoring the large trifluoromethanesulfonyl group on the skeleton of UiO-66-NH_2 metal-organic framework. The single-ionic conducting SSE displays a high ionic conductivity (2.07×10^{-4} S cm^{-1} at 25 °C), a low activation energy of 0.31 eV, a wide electrochemical window up to 4.52 V as well as a high Li^+ transference number of 0.84, which thus enables the Li/LFP cell to exhibit higher capacity retention rates of 98.6, 95.4, and 91.1% under 0.2, 0.5, and 1 C, respectively, at 0 °C than that of polymer SSE based cell (**Figure 15c**). Another solid electrolyte host named boron-starch-silicon (BStSi) has also been fabricated and studied for low temperature LIBs.[242] Through two cross-linking reactions, the BStSi host is found to obtain sufficient orderly ether-bonded net for lithium salt dissolution. Then, after the LiTFSI is added, the SSE exhibits an outstanding ionic conductivity of 3.10×10^{-5} S cm^{-1}, lithium-ion transfer number of 0.72 and decomposition potential of 5.50 V at -20 °C.

Other than the LIBs, some gel electrolytes have also been developed for the low temperature operation of ZIBs. For instance, Li's group[243] designed a concentrated 3.0 M $Zn(CF_3SO_3)_2$ polyacrylamide hydrogel electrolyte (**Figure 15d**) for high-capacity layered magnesium vanadate ($Mg_{0.1}V_2O_5 \cdot H_2O$) nanobelts based cathode. The hydrogel

electrolyte exhibits a high ionic conductivity of 1.9 mS cm^{-1} at -30 °C, enabling the $Mg_{0.1}V_2O_5 \cdot H_2O$ cathode to achieve a high capacity of 272 mAh g^{-1} without capacity fade over 100 cycles at 0.2 A g^{-1} at -30 °C (**Figure 15e**). In another work,[244] a conductive quasi-solid-state iongel electrolyte is synthesized for yarn ZIBs. The iongel electrolyte is prepared by polymerization reaction between 1-vinyl-3-ethylimidazolium dicyanamide ([Veim][DCA]) and N, N'-methylenebisacrylamide (NNMBA), which is found to hold a high conductivity of 0.016 S cm^{-1} and thereby enables the Zn//MnO_2 yarn battery to achieve higher volumetric capacity of 2.4 mAh cm^{-3} and volumetric energy density of 2.0 mWh cm^{-3} at 0 °C. Yuan's group[245] also developed a hydrogel electrolyte composed of 3.0 M $ZnCl_2$/polyacrylamide (PAm) for a coaxial-like integrated flexible ZIB. The $ZnCl_2$/PAm electrolyte exhibits high ionic conductivity of 1.9 mS cm^{-1} at -20 °C with superior mechanical and electrochemical integrity, which allows the flexible ZIB to obtain high-capacity retention of 97.75% after 3000 flexure cycles at -20 °C. Li et al.[246] also reported a flexible ZIB with EG-based organohydrogel electrolytes (OHEs) that could be stable for 1500 cycles with outstanding capacity retentions of 88.8% at -30 °C.

Ionic liquid (IL) with wide operating temperature also offers great opportunities for achieving high-performance low-temperature MIBs. For LIBs, Fujie et al.[247] developed an ionic electrolyte consisting of 1-ethyl-3-methylimidazolium bis(trifluoromethylsulfonyl)amide (EMI-TFSA) ionic liquid incorporated within the ZIF-8 (Zn(MeIM)2, H(MeIM) = 2-methylimidazole) metal-organic framework, which presents much higher ionic conductivity than the pure IL at -23 °C. In another work, the 1-ethyl-3-methylimidazolium tetrafluoroborate (EMI-BF_4) ionic liquid is introduced into an electrolyte as additive for $LiNi_{0.5}Co_{0.2}Mn_{0.3}O_2$ (NCM523)/graphite cells (**Figure 15f and g**), which was found to effectively enhance the electrolyte

conductivity and contributed to the enhanced low-temperature performance.[248] With 1% EMI-BF_4, the cells displayed higher capacity retention of 93.8% after 150 cycles at -10 °C than that without this additive (82.3%). Other than the LIBs, the application of ionic liquid has also been extensively studied in SIBs. For instance, the Na[FSA]-[C_3C_1pyrr][FSA] ionic liquid is been studied and used as the electrolyte in a Na/$NaCrO_2$ full cell, which displays a wide operational temperature range of -20 to 90 °C.[249] In another work,[250] an even wider operational temperature range is enabled by designing a highly concentrated electrolyte, which contains 2.3 M sodium bis(fluorosulfonyl)imide in trimethyl iso-butyl phosphonium bis(fluorosulfonyl)imid ionic liquid. By applying this electrolyte in the Na/$Na_{2/3}(Fe_{2/3}Mn_{1/3})O_2$ full cell, the cell is found to display an operational temperature range from -71 to 305 °C.

Other than the novel designs of low-temperature electrolyte, the liquefied gas is another type of electrolytes which has drawn a lot of attention. Rustomji et al.[251] demonstrated that liquefied gas could serve as low-temperature electrolyte for batteries and electrochemical capacitors. It possesses low viscosity, about three times lower than that of common electrolytes, which therefore endows it with high ionic conductivity. Moreover, it allows the battery with excellent capacity retention at -60 °C. To further improve the application of liquefied gas electrolyte over wider temperature range, the same group then developed a fluoromethane-based liquefied gas electrolyte with acetonitrile (AN) as cosolvent and 1.2 M LiTFSI for lithium metal batteries.[252] The new liquefied gas electrolyte exhibited a high low-temperature ionic conductivity of 5.8 mS cm^{-1} at -60 °C and 4.8 mS cm^{-1} at -78 °C, which is then found to help the Li/NCM full cell to deliver an excellent cycling stability and a capacity retention rate of 36% and 52% under the current of C/5 and C/3 rate, respectively, at -20 °C.

In this section, several electrolyte modification strategies have been summarized for enhancing the ion migration process inside the electrolyte, including adding cosolvents, introducing novel salts and additives. All of these strategies have been proved to be effective making them to be equally important and should not be overlooked. Nevertheless, adding additives may be considered to be a more convenient and economical strategy due to its relatively small amount used.[181] Still, the exploration of novel electrolyte material with excellent electrochemical properties is of great significance. Importantly, attentions should also be given to the compatibility issue between electrolytes and different electrode materials to ensure its follow-up widespread applications.[253] The realization of such good compatibility relies on the formation of robust SEI, the possession of sufficient number of active sites, and the constraints on the variation of electrode volume.[254]

4. Thermal activation by preheating MIBs

Other than using the all these previously discussed strategies to tackle the ion transport issues of MIBs operating at low temperature, there are also some other methods to resolve most of the problems caused by low temperature and thereby enable a better performance i.e., directly heating the battery before operation to elevate its temperature. Batteries can be gradually warmed up during their discharging process, and the heat mainly derives from Joule heat due to the internal resistance of batteries. However, this process is time-consuming and often leads to material degradation. Hence, advanced technologies for thermal activation are required to efficiently warm up the batteries.

An effective preheating technique was developed via a novel "all-climate battery" design.[255-259] An extra component of nickel foil is inserted into the battery and served as the internal heat generator.[260] The inserted nickel foil, with a thickness of 50 μm, has

two tabs. While one is well connected with the negative terminal, the other one is extended outside the battery to form an activation terminal, which is the key for cell activation (**Figure 16**). A switch for cell activation is connected to these two terminals. Thereafter, before the battery starts its operation at low temperatures, the switch will first be turned on to conduct the cell activation process, during which the core of the battery will quickly warm up due to the generation of ohmic heat when electrons pass through the inserted nickel foil. The time for cell activation (from extremely low temperature to 0 °C) is short, which could be estimated by the energy balance equation expressed as:

$$\int_0^{\tau_A} I_A(U_0 - V_A)dt = mc_p\Delta T \quad (6)$$

where τ_A is the activation time, I_A stands for the current, V_A represents the voltage during cell activation, U_0 is the thermal equilibrium potential of the battery, c_p is the specific heat capacity, and ΔT is the temperature difference. Such estimation is further validated by experiments, showing that the cell activation takes about 19.5 s, 29.6 s, and 42.5 s for the environmental temperatures of -20, -30 and -40 °C, respectively, to reach 0 °C. For LIBs operating at -20 °C, a discharge capacity of about 7.5 Ah is obtained at 1 C, while such cell activation process only consumes a minimal amount of discharge capacity (3.8 %). This impressive result showed great enhancements compared to commercialized LIBs without this novel preheating strategy. The low-temperature LIB with this novel design also demonstrates an excellent capacity retention ability with merely about 7.2 % capacity decay after 500 times of activations. Zhang et al.[261] further optimized it by symmetrically inserting 2 nickel foil sheets into the battery. Using an extra nickel foil sheet, about 24 % energy is saved during the self-heating process compared to the previous work,[260] and the activation time (from -20 to 0 °C) was further shortened to 12.5 s. The symmetrically distributed nickel foil (at ¼

and ¾ thickness of the cell) played a significant role in regulating the thermal distribution demonstrating a uniform temperature distribution and thereby allows the whole battery to be activated rapidly (**Figure 17**). It is worth to mention that compared to the battery with one-sheet design, the battery with two-sheet design also presented a much smaller temperature difference between the surface and the nickel foil.

Thermal activation can also be achieved by using external heat generator. Ji et al.[262] employed convective heating strategy to heat the battery. Typically, a resist heat primarily serves as external heat generator, while a fan has been used to accelerate the heat conduction towards the battery (**Figure 18a**). Although effective, it will suffer from significant heat loss during heat conduction via air medium, which leads to poor energy efficiency for such a thermal activation process. In addition, it is not suitable for heating large battery packs, owing to the uneven thermal distribution. In view of this, alternative current (AC) heating is developed to preheat the battery.[263, 264] An additional load is used to apply AC to batteries (**Figure 18b**). It is found that AC with a large amplitude with a suitable frequency is desired for battery heating, as it can enable a high heating power and reduce the heating time. Consequently, it is found that the battery could be heated from -15.4 to 5.6 °C within 338 s. In comparison, another study shows that the thermal activation of battery pack using direct current and AC, could be heated from -20.8 to 2.1 °C within 600 s.[263] In summary, developing novel strategies or modifying battery designs to directly heat the battery before operation is a promising and effective method that could greatly improve the low temperature performances of MIBs and thus requires more attention in the future.

5. Remaining challenges and perspectives

Up to date, various strategies have been proposed and examined to improve the low-temperature performances of MIBs. While some promising results have been obtained and the low temperature performances of MIBs have achieved a great leap forward, there are still some remaining challenges confronting their further development and application. Firstly, the SEI evolution in some electrolyte systems remains elusive. The complex components and structures of SEI film make it difficult to design corresponding strategies for enhancing ion diffusion kinetics through SEI film. Secondly, previous studies separately developed either low-temperature electrolytes or advanced electrode materials resulting in limited studies on the compatibility between the electrolytes and electrodes, which thereby hinder the obtainable performances upon their combination and further obstructs their practical application. Thirdly, some nanostructured materials used for metal-ion batteries only exhibit good low-temperature performance with a very small mass loading (less than 1.0 mg cm^{-2}), which is apparently far away from the industrial standards (10.0 mg cm^{-2}). Meanwhile, their high-mass-loading performance is still uncertain. Moreover, the low-density property of nanomaterials limits their volumetric energy density and thereby restrains their commercialization progress. Fourthly, dendrite formation in LIB or ZIB systems is inevitable at low temperatures, which often leads to severe capacity decay after long-term operation, as the uncontrollable deposition of metal ions would create barrier for the metal ions to transport through the SEI and further inhibit the contact of ions and electrons. Fifthly, the preparation methods for some well-designed nanomaterials are often complex, time-consuming, and difficult for large-scale production, which in turn significantly hinder their industrialization potentials. It worth mentioning that, in addition to all these issues, the large initial capacity loss of MIBs due to the

consumption of active metal ions in low temperature is also pivotal and should not be overlooked.

For these considerations, perspectives on future research directions are as follows: First, the composition of electrolytes designs should be well tailored to suit with the electrode materials so as to form a stable and conductive SEI film on the electrode surface. Designing artificial dielectric SEI is suggested to be a good direction as it could facilitate the ion diffusion in solid SEI and across the SEI/electrolyte interface. Second, electrode designs by engineering vacancies and metal doping are also recommended. These techniques would not only maintain the volumetric energy densities of the batteries, but also simultaneously boost the low-temperature performance by accelerating the solid-state ion diffusion process. Third, more attempts on the use of additives as catalysts to reduce the desolvation energy of metal ions are suggested. Fourth, more efforts are required on the exploration of new electrode materials for low-temperature operation, especially for the newly emerging MIB systems such as AIBs and ZIBs. Fifth, more theoretical calculations targeting the investigations of ion diffusion energy barrier in the interlayers or at the interface are required to enrich the basic understanding and guide the future designs of these battery systems. In addition, theoretical calculations are also useful for performing material screening thereby producing new electrolyte or electrode choices for the design and development of low-temperature MIB systems. Sixth, currently, the self-heating battery is the most promising design for addressing all the issues caused by low operating temperatures and thus more efforts are recommended to extend this technology for battery performance enhancement especially for electric vehicles at low temperatures. Lastly, fabricating post-LIBs is also a promising solution for low-temperature operation due to their small desolvation energy in organic electrolytes. Although large ionic size of these

metal ions might cause sluggish solid-state ion diffusion, this can be improved by using electrodes with open and conductive channels. In conclusion, it is believed that employing these strategies mentioned would significantly enhance the low-temperature performances of MIBs as they are very promising and inspiring to realize the widespread adoptions of MIBs and thus progressively change the landscape in energy storage technologies in the future.

Conflict of interest:

The authors declare no competing interests.

Acknowledgement:

This work is supported by a grant from the Research Institute for Smart Energy (CDA4), a grant from the Research Institute for Advanced Manufacturing (CD8Z), a grant from the Carbon Neutrality Funding Scheme (WZ2R) at The Hong Kong Polytechnic University, and a grant from the Shenzhen Science and Technology Program (No. JCYJ20190808123011253).

References

1. Z. A. Zafar, S. Imtiaz, R. Razaq, S. Ji, T. Huang, Z. Zhang, Y. Huang and J. A. Anderson, Cathode materials for rechargeable aluminum batteries: current status and progress, *Journal of Materials Chemistry A*, 2017, **5**, 5646-5660.
2. L. Wang, M. Xia, H. Wang, K. Huang, C. Qian, C. T. Maravelias and G. A. Ozin, Greening ammonia toward the solar ammonia refinery, *Joule*, 2018, **2**, 1055-1074.
3. C. Guo, J. Ran, A. Vasileff and S.-Z. Qiao, Rational design of electrocatalysts and photo (electro) catalysts for nitrogen reduction to ammonia (NH 3) under ambient conditions, *Energy & Environmental Science*, 2018, **11**, 45-56.
4. H. Li, L. Peng, Y. Zhu, X. Zhang and G. Yu, Achieving high-energy–high-power density in a flexible quasi-solid-state sodium ion capacitor, *Nano Letters*, 2016, **16**, 5938-5943.
5. J. Muldoon, C. B. Bucur and T. Gregory, Quest for nonaqueous multivalent secondary batteries: magnesium and beyond, *Chemical Reviews*, 2014, **114**, 11683-11720.
6. W. Wang, C. Su, Y. Wu, R. Ran and Z. Shao, Progress in solid oxide fuel cells with nickel-based anodes operating on methane and related fuels, *Chemical Reviews*, 2013, **113**, 8104-8151.
7. P. Tan, B. Chen, H. Xu, H. Zhang, W. Cai, M. Ni, M. Liu and Z. Shao, Flexible Zn–and Li–air batteries: recent advances, challenges, and future perspectives, *Energy & Environmental Science*, 2017, **10**, 2056-2080.
8. Y. Gogotsi and R. M. Penner, Energy storage in nanomaterials–capacitive, pseudocapacitive, or battery-like?, *ACS Nano*, 2018, **12**, 2081-2083.
9. X. Ke, J. M. Prahl, J. I. D. Alexander, J. S. Wainright, T. A. Zawodzinski and R. F. Savinell, Rechargeable redox flow batteries: flow fields, stacks and design considerations, *Chemical Society Reviews*, 2018, **47**, 8721-8743.
10. H. Wang, X. Yuan, G. Zeng, Y. Wu, Y. Liu, Q. Jiang and S. Gu, Three dimensional graphene based materials: Synthesis and applications from energy storage and conversion to electrochemical sensor and environmental remediation, *Advances in Colloid and Interface Science*, 2015, **221**, 41-59.
11. P. Tan, W. Kong, Z. Shao, M. Liu and M. Ni, Advances in modeling and simulation of Li–air batteries, *Progress in Energy and Combustion Science*, 2017, **62**, 155-189.
12. G. Li, B. Huang, Z. Pan, X. Su, Z. Shao and L. An, Advances in three-dimensional graphene-based materials: configurations, preparation and application in secondary metal (Li, Na, K, Mg, Al)-ion batteries, *Energy & Environmental Science*, 2019, **12**, 2030-2053.
13. W. Zhao, X. Ma, L. Yue, L. Zhang, Y. Luo, Y. Ren, X.-E. Zhao, N. Li, B. Tang and Q. Liu, A gradient hexagonal-prism Fe 3 Se 4@ SiO 2@ C configuration as a highly reversible sodium conversion anode, *Journal of Materials Chemistry A*, 2022, **10**, 4087-4099.
14. L. Yue, D. Wang, Z. Wu, W. Zhao, Y. Ren, L. Zhang, B. Zhong, N. Li, B. Tang and Q. Liu, Polyrrole-encapsulated Cu2Se nanosheets in situ grown on Cu mesh

for high stability sodium-ion battery anode, *Chemical Engineering Journal*, 2022, **433**, 134477.
15. Q. Liu, Y. Hu, X. Yu, Y. Qin, T. Meng and X. Hu, The pursuit of commercial silicon-based microparticle anodes for advanced lithium-ion batteries: A review, *Nano Research Energy*, 2022, **1**, e9120037.
16. W. Zhao, L. Gao, L. Yue, X. Wang, Q. Liu, Y. Luo, T. Li, X. Shi, A. M. Asiri and X. Sun, Constructing a hollow microflower-like ZnS/CuS@ C heterojunction as an effective ion-transport booster for an ultrastable and high-rate sodium storage anode, *Journal of Materials Chemistry A*, 2021, **9**, 6402-6412.
17. M. R. Palacín and A. de Guibert, Why do batteries fail?, *Science*, 2016, **351**, 1253292.
18. X. Guo, C. Wang, W. Wang, Q. Zhou, W. Xu, P. Zhang, S. Wei, Y. Cao, K. Zhu and Z. Liu, Vacancy manipulating of molybdenum carbide MXenes to enhance Faraday reaction for high performance lithium-ion batteries, *Nano Research Energy*, 2022, **1**, e9120026.
19. T. M. Bandhauer, S. Garimella and T. F. Fuller, A critical review of thermal issues in lithium-ion batteries, *Journal of the Electrochemical Society*, 2011, **158**, R1.
20. Z. Li, J. Huang, B. Y. Liaw, V. Metzler and J. Zhang, A review of lithium deposition in lithium-ion and lithium metal secondary batteries, *Journal of Power Sources*, 2014, **254**, 168-182.
21. C. Li, B. Liu, N. Jiang and Y. Ding, Elucidating the charge-transfer and Li-ion-migration mechanisms in commercial lithium-ion batteries with advanced electron microscopy, *Nano Research Energy*, 2022, **1**, e9120031.
22. T. Abe, H. Fukuda, Y. Iriyama and Z. Ogumi, Solvated Li-ion transfer at interface between graphite and electrolyte, *Journal of the Electrochemical Society*, 2004, **151**, A1120.
23. X.-G. Yang, T. Liu, Y. Gao, S. Ge, Y. Leng, D. Wang and C.-Y. Wang, Asymmetric temperature modulation for extreme fast charging of lithium-ion batteries, *Joule*, 2019, **3**, 3002-3019.
24. M. Okoshi, Y. Yamada, A. Yamada and H. Nakai, Theoretical analysis on de-solvation of lithium, sodium, and magnesium cations to organic electrolyte solvents, *Journal of the Electrochemical Society*, 2013, **160**, A2160.
25. M.-T. F. Rodrigues, G. Babu, H. Gullapalli, K. Kalaga, F. N. Sayed, K. Kato, J. Joyner and P. M. Ajayan, A materials perspective on Li-ion batteries at extreme temperatures, *Nature Energy*, 2017, **2**, 1-14.
26. G. Zhu, K. Wen, W. Lv, X. Zhou, Y. Liang, F. Yang, Z. Chen, M. Zou, J. Li and Y. Zhang, Materials insights into low-temperature performances of lithium-ion batteries, *Journal of Power Sources*, 2015, **300**, 29-40.
27. M. Chen, Y. Zhang, G. Xing, S.-L. Chou and Y. Tang, Electrochemical energy storage devices working in extreme conditions, *Energy & Environmental Science*, 2021, **14**, 3323-3351.

28. W.-J. Zhang, Structure and performance of LiFePO4 cathode materials: A review, *Journal of Power Sources*, 2011, **196**, 2962-2970.
29. A. Gupta and A. Manthiram, Designing advanced lithium-based batteries for low-temperature Conditions, *Advanced Energy Materials*, 2020, **10**, 2001972.
30. J. Hou, M. Yang, D. Wang and J. Zhang, Fundamentals and challenges of lithium ion batteries at temperatures between− 40 and 60° C, *Advanced Energy Materials*, 2020, **10**, 1904152.
31. N. Zhang, T. Deng, S. Zhang, C. Wang, L. Chen, C. Wang and X. Fan, Critical review on low-temperature Li-ion/metal batteries, *Advanced Materials*, 2021, 2107899.
32. Y. Sun, B. Liu, L. Liu and X. Yan, Ions transport in electrochemical energy storage devices at low temperatures, *Advanced Functional Materials*, 2021, 2109568.
33. X. Dong, Y.-G. Wang and Y. Xia, Promoting rechargeable batteries operated at low temperature, *Accounts of Chemical Research*, 2021, **54**, 3883-3894.
34. Q. Li, G. Liu, H. Cheng, Q. Sun, J. Zhang and J. Ming, Low-temperature electrolyte design for lithium-ion batteries: Prospect and challenges, *Chemistry–A European Journal*, 2021, **27**, 15842-15865.
35. Y. Zhao, Z. Chen, F. Mo, D. Wang, Y. Guo, Z. Liu, X. Li, Q. Li, G. Liang and C. Zhi, Aqueous rechargeable metal-ion batteries working at subzero temperatures, *Advanced Science*, 2021, **8**, 2002590.
36. S. Gong and Q. Wang, Boron-doped graphene as a promising anode material for potassium-ion batteries with a large capacity, high rate performance, and good cycling stability, *The Journal of Physical Chemistry C*, 2017, **121**, 24418-24424.
37. K. Persson, V. A. Sethuraman, L. J. Hardwick, Y. Hinuma, Y. S. Meng, A. Van Der Ven, V. Srinivasan, R. Kostecki and G. Ceder, Lithium diffusion in graphitic carbon, *The Journal of Physical Chemistry Letters*, 2010, **1**, 1176-1180.
38. L. Yue, J. Liang, Z. Wu, B. Zhong, Y. Luo, Q. Liu, T. Li, Q. Kong, Y. Liu and A. M. Asiri, Progress and perspective of metal phosphide/carbon heterostructure anodes for rechargeable ion batteries, *Journal of Materials Chemistry A*, 2021, **9**, 11879-11907.
39. Y. Wang, R. Chen, T. Chen, H. Lv, G. Zhu, L. Ma, C. Wang, Z. Jin and J. Liu, Emerging non-lithium ion batteries, *Energy Storage Materials*, 2016, **4**, 103-129.
40. W. Zhao, L. Gao, X. Ma, L. Yue, D. Zhao, Z. Li, S. Sun, Y. Luo, Q. Liu and A. M. Asiri, An exquisite branch–leaf shaped metal sulfoselenide composite endowing an ultrastable sodium-storage lifespan over 10000 cycles, *Journal of Materials Chemistry A*, 2022, **10**, 16962-16975.
41. C. K. Huang, J. Sakamoto, J. Wolfenstine and S. Surampudi, The limits of low-temperature performance of Li-ion cells, *Journal of the Electrochemical Society*, 2000, **147**, 2893.
42. S. Zhang, K. Xu and T. Jow, Low temperature performance of graphite electrode in Li-ion cells, *Electrochimica Acta*, 2002, **48**, 241-246.

43. P.-P. Wang, C.-Y. Xu, W.-D. Li, L. Wang and L. Zhen, Low temperature electrochemical performance of β-LixV2O5 cathode for lithium-ion batteries, *Electrochimica Acta*, 2015, **169**, 440-446.
44. N. Schulz, R. Hausbrand, C. Wittich, L. Dimesso and W. Jaegermann, XPS-surface analysis of SEI layers on Li-ion cathodes: Part II. SEI-composition and formation inside composite electrodes, *Journal of The Electrochemical Society*, 2018, **165**, A833.
45. P. Schwager, H. Bülter, I. Plettenberg and G. Wittstock, Review of local in situ probing techniques for the interfaces of lithium-Ion and lithium–oxygen batteries, *Energy Technology*, 2016, **4**, 1472-1485.
46. S. Shi, P. Lu, Z. Liu, Y. Qi, L. G. Hector Jr, H. Li and S. J. Harris, Direct calculation of Li-ion transport in the solid electrolyte interphase, *Journal of the American Chemical Society*, 2012, **134**, 15476-15487.
47. T. Waldmann, M. Wilka, M. Kasper, M. Fleischhammer and M. Wohlfahrt-Mehrens, Temperature dependent ageing mechanisms in Lithium-ion batteries–A Post-Mortem study, *Journal of Power Sources*, 2014, **262**, 129-135.
48. M. Smart, J. Whitacre, B. Ratnakumar and K. Amine, Electrochemical performance and kinetics of Li1+ x (Co1/3Ni1/3Mn1/3) 1− xO2 cathodes and graphite anodes in low-temperature electrolytes, *Journal of Power Sources*, 2007, **168**, 501-508.
49. C. Wang, A. J. Appleby and F. E. Little, Low-temperature characterization of lithium-ion carbon anodes via microperturbation measurement, *Journal of the Electrochemical Society*, 2002, **149**, A754.
50. Q. Li, D. Lu, J. Zheng, S. Jiao, L. Luo, C.-M. Wang, K. Xu, J.-G. Zhang and W. Xu, Li+-desolvation dictating lithium-ion battery's low-temperature performances, *ACS Applied Materials & Interfaces*, 2017, **9**, 42761-42768.
51. X. Dong, Z. Guo, Z. Guo, Y. Wang and Y. Xia, Organic batteries operated at− 70 C, *Joule*, 2018, **2**, 902-913.
52. J. Xu, X. Wang, N. Yuan, J. Ding, S. Qin, J. M. Razal, X. Wang, S. Ge and Y. Gogotsi, Extending the low temperature operational limit of Li-ion battery to− 80° C, *Energy Storage Materials*, 2019, **23**, 383-389.
53. J. Xu, X. Wang, N. Yuan, B. Hu, J. Ding and S. Ge, Graphite-based lithium ion battery with ultrafast charging and discharging and excellent low temperature performance, *Journal of Power Sources*, 2019, **430**, 74-79.
54. B. M. Castellano and D. K. Eggers, Experimental support for a desolvation energy term in governing equations for binding equilibria, *The Journal of Physical Chemistry B*, 2013, **117**, 8180-8188.
55. K. Xu, Nonaqueous liquid electrolytes for lithium-based rechargeable batteries, *Chemical Reviews*, 2004, **104**, 4303-4418.
56. M. Park, X. Zhang, M. Chung, G. B. Less and A. M. Sastry, A review of conduction phenomena in Li-ion batteries, *Journal of Power Sources*, 2010, **195**, 7904-7929.

57. B. K. Mandal, A. K. Padhi, Z. Shi, S. Chakraborty and R. Filler, New low temperature electrolytes with thermal runaway inhibition for lithium-ion rechargeable batteries, *Journal of Power Sources*, 2006, **162**, 690-695.
58. H. Tavassol, E. M. Jones, N. R. Sottos and A. A. Gewirth, Electrochemical stiffness in lithium-ion batteries, *Nature Materials*, 2016, **15**, 1182-1187.
59. Y. Zhang, Y. Luo, Y. Chen, T. Lu, L. Yan, X. Cui and J. Xie, Enhanced rate capability and low-temperature performance of Li4Ti5O12 anode material by facile surface fluorination, *ACS Applied Materials & Interfaces*, 2017, **9**, 17145-17154.
60. H. Zou, H. Xiang, X. Liang, X. Feng, S. Cheng, Y. Jin and C. Chen, Electrospun Li3. 9Cr0. 3Ti4. 8O12 nanofibers as anode material for high-rate and low-temperature lithium-ion batteries, *Journal of Alloys and Compounds*, 2017, **701**, 99-106.
61. J. Li, W. Wen, G. Xu, M. Zou, Z. Huang and L. Guan, Fe-added Fe3C carbon nanofibers as anode for Li ion batteries with excellent low-temperature performance, *Electrochimica Acta*, 2015, **153**, 300-305.
62. B. Zhang, Y. Liu, Z. Huang, S. Oh, Y. Yu, Y.-W. Mai and J.-K. Kim, Urchin-like Li4Ti5O12–carbon nanofiber composites for high rate performance anodes in Li-ion batteries, *Journal of Materials Chemistry*, 2012, **22**, 12133-12140.
63. Z. Li, X. Ren, Y. Zheng, W. Tian, L. An, J. Sun, R. Ding, L. Wen and G. Liang, Effect of Ti doping on LiFePO4/C cathode material with enhanced low-temperature electrochemical performance, *Ionics*, 2020, **26**, 1599-1609.
64. G. Li, Z. Huang, Z. Zuo, Z. Zhang and H. Zhou, Understanding the trace Ti surface doping on promoting the low temperature performance of LiNi1/3Co1/3Mn1/3O2 cathode, *Journal of Power Sources*, 2015, **281**, 69-76.
65. H. Zhang, Y. Xu, C. Zhao, X. Yang and Q. Jiang, Effects of carbon coating and metal ions doping on low temperature electrochemical properties of LiFePO4 cathode material, *Electrochimica Acta*, 2012, **83**, 341-347.
66. Y.-j. Lv, B. Huang, J.-x. Tan, S.-q. Jiang, S.-f. Zhang and Y.-x. Wen, Enhanced low temperature electrochemical performances of LiFePO4/C by V3+ and F− co-doping, *Materials Letters*, 2018, **229**, 349-352.
67. X. Wei and Y. Ren, Influence of Li and Mo co-doping for electrochemical performance of ternary cathode materials at room and low temperature for Li-ion power battery, *Electrochimica Acta*, 2015, **180**, 323-329.
68. J. Kou, L. Chen, Y. Su, L. Bao, J. Wang, N. Li, W. Li, M. Wang, S. Chen and F. Wu, Role of cobalt content in improving the low-temperature performance of layered lithium-rich cathode materials for lithium-ion batteries, *ACS Applied Materials & Interfaces*, 2015, **7**, 17910-17918.
69. X. Wang, W. Zhao, W. Zhang, K. W. Wong, J. Wu, T. Chen and S. Huang, Ultrafine ZnSe encapsulated in nitrogen-doped porous carbon nanofibers for superior Na-ion batteries with a long lifespan and low-temperature performance, *ACS Sustainable Chemistry & Engineering*, 2021, **9**, 11705-11713.
70. Q.-C. Wang, Q.-Q. Qiu, N. Xiao, Z.-W. Fu, X.-J. Wu, X.-Q. Yang and Y.-N. Zhou, Tunnel-structured Na0. 66 [Mn0. 66Ti0. 34] O2-xFx (x< 0.1) cathode for

high performance sodium-ion batteries, *Energy Storage Materials*, 2018, **15**, 1-7.

71. H. Geng, M. Cheng, B. Wang, Y. Yang, Y. Zhang and C. C. Li, Electronic structure regulation of layered vanadium oxide via interlayer doping strategy toward superior high-rate and low-temperature zinc-ion batteries, *Advanced Functional Materials*, 2020, **30**, 1907684.
72. G. Su, S. Chen, H. Dong, Y. Cheng, Q. Liu, H. Wei, E. H. Ang, H. Geng and C. C. Li, Tuning the electronic structure of layered vanadium pentoxide by pre-intercalation of potassium ions for superior room/low-temperature aqueous zinc-ion batteries, *Nanoscale*, 2021, **13**, 2399-2407.
73. Y. Yang, Y. Tang, S. Liang, Z. Wu, G. Fang, X. Cao, C. Wang, T. Lin, A. Pan and J. Zhou, Transition metal ion-preintercalated V2O5 as high-performance aqueous zinc-ion battery cathode with broad temperature adaptability, *Nano Energy*, 2019, **61**, 617-625.
74. W. Zhou, J. Chen, M. Chen, A. Wang, A. Huang, X. Xu, J. Xu and C.-P. Wong, An environmentally adaptive quasi-solid-state zinc-ion battery based on magnesium vanadate hydrate with commercial-level mass loading and anti-freezing gel electrolyte, *Journal of Materials Chemistry A*, 2020, **8**, 8397-8409.
75. G. Zhao, Z. Wei, N. Zhang and K. Sun, Enhanced low temperature performances of expanded commercial mesocarbon microbeads (MCMB) as lithium ion battery anodes, *Materials Letters*, 2012, **89**, 243-246.
76. J. Peng, W. Zhang, Z. Hu, L. Zhao, C. Wu, G. Peleckis, Q. Gu, J.-Z. Wang, H. K. Liu and S. X. Dou, Ice-assisted synthesis of highly crystallized prussian blue analogues for all-climate and long-calendar-life sodium ion batteries, *Nano Letters*, 2022.
77. H. Luo, Y. Wang, Y.-H. Feng, X.-Y. Fan, X. Han and P.-F. Wang, Lithium-Ion Batteries under Low-Temperature Environment: Challenges and Prospects, *Materials*, 2022, **15**, 8166.
78. D. Abraham, J. Heaton, S.-H. Kang, D. Dees and A. Jansen, Investigating the low-temperature impedance increase of lithium-ion cells, *Journal of the Electrochemical Society*, 2007, **155**, A41.
79. J. Allen, T. Jow and J. Wolfenstine, Low temperature performance of nanophase Li4Ti5O12, *Journal of Power Sources*, 2006, **159**, 1340-1345.
80. E. Pohjalainen, T. Rauhala, M. Valkeapää, J. Kallioinen and T. Kallio, Effect of Li4Ti5O12 particle size on the performance of lithium ion battery electrodes at high C-rates and low temperatures, *The Journal of Physical Chemistry C*, 2015, **119**, 2277-2283.
81. C. Huang, S.-X. Zhao, H. Peng, Y.-H. Lin, C.-W. Nan and G.-Z. Cao, Hierarchical porous Li4Ti5O12–TiO2 composite anode materials with pseudocapacitive effect for high-rate and low-temperature applications, *Journal of Materials Chemistry A*, 2018, **6**, 14339-14351.
82. L. Peng, H. Zhang, L. Fang, Y. Zhang and Y. Wang, Novel peapoded Li4Ti5O12 nanoparticles for high-rate and ultralong-life rechargeable lithium ion batteries at room and lower temperatures, *Nanoscale*, 2016, **8**, 2030-2040.

83. S. Bae, H. D. Song, I. Nam, G.-P. Kim, J. M. Lee and J. Yi, Quantitative performance analysis of graphite-LiFePO4 battery working at low temperature, *Chemical Engineering Science*, 2014, **118**, 74-82.
84. G. Huang, W. Li, H. Sun, J. Wang, J. Zhang, H. Jiang and F. Zhai, Polyvinylpyrrolidone (PVP) assisted synthesized nano-LiFePO4/C composite with enhanced low temperature performance, *Electrochimica Acta*, 2013, **97**, 92-98.
85. N. Zhao, Y. Li, X. Zhao, X. Zhi and G. Liang, Effect of particle size and purity on the low temperature electrochemical performance of LiFePO4/C cathode material, *Journal of Alloys and Compounds*, 2016, **683**, 123-132.
86. Z. Sun, L. Jiao, Y. Fan, F. Li, D. Wang, D. Han and L. Niu, Industrialization of tailoring spherical cathode material towards high-capacity, cycling-stable and superior low temperature performance for lithium-ion batteries, *RSC Advances*, 2016, **6**, 97818-97824.
87. Z. Sun, Z. Li, X.-L. Wu, M. Zou, D. Wang, Z. Gu, J. Xu, Y. Fan, S. Gan and D. Han, A practical Li-ion full cell with a high-capacity cathode and electrochemically exfoliated graphene anode: superior electrochemical and low-temperature performance, *ACS Applied Energy Materials*, 2019, **2**, 486-492.
88. C. R. Sides and C. R. Martin, Nanostructured electrodes and the low-temperature performance of Li-ion batteries, *Advanced Materials*, 2005, **17**, 125-128.
89. X. Dong, Y. Yang, B. Wang, Y. Cao, N. Wang, P. Li, Y. Wang and Y. Xia, Low-Temperature Charge/Discharge of Rechargeable Battery Realized by Intercalation Pseudocapacitive Behavior, *Advanced Science*, 2020, **7**, 2000196.
90. X. Lin, X. Du, P. S. Tsui, J.-Q. Huang, H. Tan and B. Zhang, Exploring room- and low-temperature performance of hard carbon material in half and full Na-ion batteries, *Electrochimica Acta*, 2019, **316**, 60-68.
91. X.-H. Ma, Y.-Y. Wei, Y.-D. Wu, J. Wang, W. Jia, J.-H. Zhou, Z.-F. Zi and J.-M. Dai, High crystalline Na2Ni [Fe(CN)6] particles for a high-stability and low-temperature sodium-ion batteries cathode, *Electrochimica Acta*, 2019, **297**, 392-397.
92. X. Yan, Y. Yang, E. Liu, L. Sun, H. Wang, X.-Z. Liao, Y. He and Z.-F. Ma, Improved cycling performance of Prussian blue cathode for sodium ion batteries by controlling operation voltage range, *Electrochimica Acta*, 2017, **225**, 235-242.
93. J. Z. Guo, P. F. Wang, X. L. Wu, X. H. Zhang, Q. Yan, H. Chen, J. P. Zhang and Y. G. Guo, High-energy/power and low-temperature cathode for sodium-ion batteries: in situ XRD study and superior full-cell performance, *Advanced Materials*, 2017, **29**, 1701968.
94. B. Wang, H. Yang, Y. Feng, S. Zeng, L. Tan, R. Xu, L. Wang, R. Hu and Y. Yu, Boosting low-temperature sodium/potassium storage performance of Bi via novel electrochemical milling process, *Materials Today Energy*, 2021, **20**, 100627.

95. X. Pang, B. An, S. Zheng and B. Wang, Cathode materials of metal-ion batteries for low-temperature applications, *Journal of Alloys and Compounds*, 2022, **912**, 165142.
96. F. Lu, J. Liu, J. Xia, Y. Yang and X. Wang, Engineering C–N moieties in branched nitrogen-doped graphite tubular foam toward stable Li+-storage at low temperature, *Industrial & Engineering Chemistry Research*, 2020, **59**, 5858-5864.
97. B. Hu, X. Zhou, J. Xu, X. Wang, N. Yuan, S. Ge and J. Ding, Excellent rate and low temperature performance of lithium-ion batteries based on binder-free Li4Ti5O12 electrode, *ChemElectroChem*, 2020, **7**, 716-722.
98. D. Xie, G. Cai, Z. Liu, R. Guo, D. Sun, C. Zhang, Y. Wan, J. Peng and H. Jiang, The low temperature electrochemical performances of LiFePO4/C/graphene nanofiber with 3D-bridge network structure, *Electrochimica Acta*, 2016, **217**, 62-72.
99. Y. Yan, L. Ben, Y. Zhan and X. Huang, Nano-Sn embedded in expanded graphite as anode for lithium ion batteries with improved low temperature electrochemical performance, *Electrochimica Acta*, 2016, **187**, 186-192.
100. A. Varzi, L. Mattarozzi, S. Cattarin, P. Guerriero and S. Passerini, 3D porous Cu–Zn alloys as alternative anode materials for Li-Ion batteries with superior low T performance, *Advanced Energy Materials*, 2018, **8**, 1701706.
101. Y. Cheng, K. Feng, H. Wang, H. Zhang, X. Li and H. Zhang, "Three-in-One:" A new 3D hybrid structure of Li3V2(PO4)3@ biomorphic carbon for high-rate and low-temperature lithium ion batteries, *Advanced Materials Interfaces*, 2017, **4**, 1700686.
102. C. Li, Y. Ishii, S. Inayama and S. Kawasaki, Quinone molecules encapsulated in SWCNTs for low-temperature Na ion batteries, *Nanotechnology*, 2017, **28**, 355401.
103. C. Su, Q. Ru, S. Cheng, Y. Gao, F. Chen, L. Zhao and F. C.-C. Ling, 3D pollen-scaffolded NiSe composite encapsulated by MOF-derived carbon shell as a high-low temperature anode for Na-ion storage, *Composites Part B: Engineering*, 2019, **179**, 107538.
104. K.-C. Huang, J.-Z. Guo, H.-H. Li, H.-H. Fan, D.-H. Liu, Y.-P. Zheng, W.-L. Li, X.-L. Wu and J.-P. Zhang, Layer-stacked Sb@ graphene micro/nanocomposite with decent Na-storage, full-cell and low-temperature performances, *Journal of Alloys and Compounds*, 2018, **731**, 881-888.
105. Y. You, H. R. Yao, S. Xin, Y. X. Yin, T. T. Zuo, C. P. Yang, Y. G. Guo, Y. Cui, L. J. Wan and J. B. Goodenough, Subzero-temperature cathode for a sodium-ion battery, *Advanced Materials*, 2016, **28**, 7243-7248.
106. H. Chen, H. Xu, S. Wang, T. Huang, J. Xi, S. Cai, F. Guo, Z. Xu, W. Gao and C. Gao, Ultrafast all-climate aluminum-graphene battery with quarter-million cycle life, *Science Advances*, 2017, **3**, eaao7233.
107. Y. Ji, Y. Zhang and C.-Y. Wang, Li-ion cell operation at low temperatures, *Journal of The Electrochemical Society*, 2013, **160**, A636.

108. W. Liu, J. Wang, J. Wang, X. Guo and H. Yang, Three-dimensional nitrogen-doped carbon coated hierarchically porous silicon composite as lithium-ion battery anode, *Journal of Alloys and Compounds*, 2021, **874**, 159921.
109. R. Raccichini, A. Varzi, V. S. K. Chakravadhanula, C. Kübel, A. Balducci and S. Passerini, Enhanced low-temperature lithium storage performance of multilayer graphene made through an improved ionic liquid-assisted synthesis, *Journal of Power Sources*, 2015, **281**, 318-325.
110. E. Markevich, G. Salitra and D. Aurbach, Low temperature performance of amorphous monolithic silicon anodes: comparative study of silicon and graphite electrodes, *Journal of The Electrochemical Society*, 2016, **163**, A2407.
111. G. A. Collins, H. Geaney and K. M. Ryan, Alternative anodes for low temperature lithium-ion batteries, *Journal of Materials Chemistry A*, 2021, **9**, 14172-14213.
112. F. Nobili, S. Dsoke, T. Mecozzi and R. Marassi, Metal-oxidized graphite composite electrodes for lithium-ion batteries, *Electrochimica Acta*, 2005, **51**, 536-544.
113. M. Mancini, F. Nobili, S. Dsoke, F. D'Amico, R. Tossici, F. Croce and R. Marassi, Lithium intercalation and interfacial kinetics of composite anodes formed by oxidized graphite and copper, *Journal of Power Sources*, 2009, **190**, 141-148.
114. F. Nobili, M. Mancini, S. Dsoke, R. Tossici and R. Marassi, Low-temperature behavior of graphite–tin composite anodes for Li-ion batteries, *Journal of Power Sources*, 2010, **195**, 7090-7097.
115. M. Marinaro, M. Mancini, F. Nobili, R. Tossici, L. Damen and R. Marassi, A newly designed Cu/Super-P composite for the improvement of low-temperature performances of graphite anodes for lithium-ion batteries, *Journal of power sources*, 2013, **222**, 66-71.
116. M. Marinaro, F. Nobili, A. Birrozzi, S. E. Moorthy, U. Kaiser, R. Tossici and R. Marassi, Improved low-temperature electrochemical performance of Li4Ti5O12 composite anodes for Li-ion batteries, *Electrochimica Acta*, 2013, **109**, 207-213.
117. F. Nobili, I. Meschini, M. Mancini, R. Tossici, R. Marassi and F. Croce, High-performance Sn@ carbon nanocomposite anode for lithium-ion batteries: lithium storage processes characterization and low-temperature behavior, *Electrochimica Acta*, 2013, **107**, 85-92.
118. G. A. Elia, F. Nobili, R. Tossici, R. Marassi, A. Savoini, S. Panero and J. Hassoun, Nanostructured tin–carbon/LiNi0. 5Mn1. 5O4 lithium-ion battery operating at low temperature, *Journal of Power Sources*, 2015, **275**, 227-233.
119. Z. Gao, X. Zhang, H. Hu, D. Guo, H. Zhao and H. Yu, Influencing factors of low-and high-temperature behavior of Co-doped Zn2SnO4–graphene–carbon nanocomposite as anode material for lithium-ion batteries, *Journal of Electroanalytical Chemistry*, 2017, **791**, 56-63.

120. X. Liu, Y. Wang, Y. Yang, W. Lv, G. Lian, D. Golberg, X. Wang, X. Zhao and Y. Ding, A MoS2/Carbon hybrid anode for high-performance Li-ion batteries at low temperature, *Nano Energy*, 2020, **70**, 104550.
121. X. Rui, Y. Jin, X. Feng, L. Zhang and C. Chen, A comparative study on the low-temperature performance of LiFePO4/C and Li3V2 (PO4) 3/C cathodes for lithium-ion batteries, *Journal of Power Sources*, 2011, **196**, 2109-2114.
122. Y. Zheng, T. Qian, H. Ji, X. Xia, J. Liu, Y. Zhu and C. Yan, Accelerating ion dynamics under cryogenic conditions by the amorphization of crystalline cathodes, *Advanced Materials*, 2021, **33**, 2102634.
123. H.-H. Fan, H.-H. Li, Z.-W. Wang, W.-L. Li, J.-Z. Guo, C.-Y. Fan, H.-Z. Sun, X.-L. Wu and J.-P. Zhang, Tailoring coral-like Fe7Se8@ C for superior low-temperature Li/Na-ion half/full batteries: synthesis, structure, and DFT studies, *ACS Applied Materials & Interfaces*, 2019, **11**, 47886-47893.
124. K. Mukai, T. Inoue, Y. Kato and S. Shirai, Superior low-temperature power and cycle performances of Na-ion battery over Li-ion battery, *ACS Omega*, 2017, **2**, 864-872.
125. J.-Y. Hwang, S.-M. Oh, S.-T. Myung, K. Y. Chung, I. Belharouak and Y.-K. Sun, Radially aligned hierarchical columnar structure as a cathode material for high energy density sodium-ion batteries, *Nature Communications*, 2015, **6**, 1-9.
126. S. Chen, Y. Zhang, H. Geng, Y. Yang, X. Rui and C. C. Li, Zinc ions pillared vanadate cathodes by chemical pre-intercalation towards long cycling life and low-temperature zinc ion batteries, *Journal of Power Sources*, 2019, **441**, 227192.
127. C. Lin, F. Qi, H. Dong, X. Li, C. Shen, E. H. Ang, Y. Han, H. Geng and C. C. Li, Suppressing vanadium dissolution of V 2 O 5 via in situ polyethylene glycol intercalation towards ultralong lifetime room/low-temperature zinc-ion batteries, *Nanoscale*, 2021, **13**, 17040-17048.
128. Y. Luo, L. Wei, H. Geng, Y. Zhang, Y. Yang and C. C. Li, Amorphous bimetallic oxides Fe–V–O with tunable compositions toward rechargeable Zn-ion batteries with excellent low-temperature performance, *ACS Applied Materials & Interfaces*, 2020, **12**, 11753-11760.
129. Y. Zhao, Y. Lu, H. Li, Y. Zhu, Y. Meng, N. Li, D. Wang, F. Jiang, F. Mo and C. Long, Few-layer bismuth selenide cathode for low-temperature quasi-solid-state aqueous zinc metal batteries, *Nature Communications*, 2022, **13**, 1-12.
130. H. He, H. Qin, F. Shen, N. Hu and J. Liu, Low temperature induced highly stable Zn metal anodes for aqueous zinc-ion batteries, *Chemical Communications*, 2021, **57**, 11477-11480.
131. L. Yue, C. Ma, S. Yan, Z. Wu, W. Zhao, Q. Liu, Y. Luo, B. Zhong, F. Zhang and Y. Liu, Improving the intrinsic electronic conductivity of NiMoO4 anodes by phosphorous doping for high lithium storage, *Nano Research*, 2022, **15**, 186-194.
132. K. Xu, Electrolytes and interphases in Li-ion batteries and beyond, *Chemical Reviews*, 2014, **114**, 11503-11618.

133. T. Yuan, X. Yu, R. Cai, Y. Zhou and Z. Shao, Synthesis of pristine and carbon-coated Li4Ti5O12 and their low-temperature electrochemical performance, *Journal of Power Sources*, 2010, **195**, 4997-5004.
134. Y. Zhou, C. Gu, J. Zhou, L. Cheng, W. Liu, Y. Qiao, X. Wang and J. Tu, Effect of carbon coating on low temperature electrochemical performance of LiFePO4/C by using polystyrene sphere as carbon source, *Electrochimica Acta*, 2011, **56**, 5054-5059.
135. B. Yao, Z. Ding, J. Zhang, X. Feng and L. Yin, Encapsulation of LiFePO4 by in-situ graphitized carbon cage towards enhanced low temperature performance as cathode materials for lithium ion batteries, *Journal of Solid State Chemistry*, 2014, **216**, 9-12.
136. W. Yang, Y. Bi, Y. Qin, Y. Liu, X. Zhang, B. Yang, Q. Wu, D. Wang and S. Shi, LiMn0. 8Fe0. 2PO4/C cathode material synthesized via co-precipitation method with superior high-rate and low-temperature performances for lithium-ion batteries, *Journal of Power Sources*, 2015, **275**, 785-791.
137. F. Zheng, C. Yang, X. Ji, D. Hu, Y. Chen and M. Liu, Surfactants assisted synthesis and electrochemical properties of nano-LiFePO4/C cathode materials for low temperature applications, *Journal of Power Sources*, 2015, **288**, 337-344.
138. Q. Hu, J.-Y. Liao, B.-K. Zou, M.-F. Yu, Z.-F. Tang, Z.-Y. Wen and C.-H. Chen, Improving the rate and low-temperature performance of LiFePO4 by tailoring the form of carbon coating from amorphous to graphene-like, *Journal of Solid State Electrochemistry*, 2018, **22**, 797-805.
139. Q. Fan, Y. Zhang, Q. Xu, J. Wang, L. Lei, Y. Sun and P. D. Lund, Coral-shaped porous LiFePO4/graphene hybrids for high rate and all-climate battery applications, *Energy Storage Materials*, 2019, **21**, 457-463.
140. H. C. Shin, K. W. Nam, W. Y. Chang, B. W. Cho, W.-S. Yoon, X.-Q. Yang and K. Y. Chung, Comparative studies on C-coated and uncoated LiFePO4 cycling at various rates and temperatures using synchrotron based in situ X-ray diffraction, *Electrochimica Acta*, 2011, **56**, 1182-1189.
141. X. L. Wu, Y. G. Guo, J. Su, J. W. Xiong, Y. L. Zhang and L. J. Wan, Carbon-nanotube-decorated nano-LiFePO4@ C cathode material with superior high-rate and low-temperature performances for lithium-ion batteries, *Advanced Energy Materials*, 2013, **3**, 1155-1160.
142. Z. Liu, X. Kang, C. Li, N. Hua, T. Wumair and Y. Han, Low-temperature behavior of Li3V2 (PO4) 3/C as cathode material for lithium ion batteries, *Journal of Solid State Electrochemistry*, 2012, **16**, 1917-1923.
143. Y. Qiao, J. Tu, X. Wang and C. Gu, The low and high temperature electrochemical performances of Li3V2 (PO4) 3/C cathode material for Li-ion batteries, *Journal of Power Sources*, 2012, **199**, 287-292.
144. F. Teng, Z.-H. Hu, X.-H. Ma, L.-C. Zhang, C.-X. Ding, Y. Yu and C.-H. Chen, Hydrothermal synthesis of plate-like carbon-coated Li3V2 (PO4) 3 and its low temperature performance for high power lithium ion batteries, *Electrochimica Acta*, 2013, **91**, 43-49.

145. L.-H. Tai, Q. Zhao, L.-Q. Sun, L.-N. Cong, X.-L. Wu, J.-P. Zhang, R.-S. Wang, H.-M. Xie and X.-H. Chen, A study of the electrochemical behavior at low temperature of the Li 3 V 2 (PO 4) 3 cathode material for Li-ion batteries, *New Journal of Chemistry*, 2015, **39**, 9617-9626.
146. R. Qin, Y. Wei, T. Zhai and H. Li, LISICON structured Li 3 V 2 (PO 4) 3 with high rate and ultralong life for low-temperature lithium-ion batteries, *Journal of Materials Chemistry A*, 2018, **6**, 9737-9746.
147. A. Ponrouch and M. Palacín, On the high and low temperature performances of Na-ion battery materials: Hard carbon as a case study, *Electrochemistry Communications*, 2015, **54**, 51-54.
148. Q. Hu, M. Yu, J. Liao, Z. Wen and C. Chen, Porous carbon-coated NaTi 2 (PO 4) 3 with superior rate and low-temperature properties, *Journal of Materials Chemistry A*, 2018, **6**, 2365-2370.
149. B. H. Hou, Y. Y. Wang, D. S. Liu, Z. Y. Gu, X. Feng, H. Fan, T. Zhang, C. Lü and X. L. Wu, N-doped carbon-coated Ni1. 8Co1. 2Se4 nanoaggregates encapsulated in N-doped carbon nanoboxes as advanced anode with outstanding high-rate and low-temperature performance for sodium-ion half/full batteries, *Advanced Functional Materials*, 2018, **28**, 1805444.
150. H.-H. Fan, H.-H. Li, J.-Z. Guo, Y.-P. Zheng, K.-C. Huang, C.-Y. Fan, H.-Z. Sun, X.-F. Li, X.-L. Wu and J.-P. Zhang, Target construction of ultrathin graphitic carbon encapsulated FeS hierarchical microspheres featuring superior low-temperature lithium/sodium storage properties, *Journal of Materials Chemistry A*, 2018, **6**, 7997-8005.
151. A. Friesen, S. Hildebrand, F. Horsthemke, M. Börner, R. Klöpsch, P. Niehoff, F. M. Schappacher and M. Winter, Al2O3 coating on anode surface in lithium ion batteries: Impact on low temperature cycling and safety behavior, *Journal of Power Sources*, 2017, **363**, 70-77.
152. G. Cai, Y. Yang, R. Guo, C. Zhang, C. Wu, W. Guo, Z. Liu, Y. Wan and H. Jiang, Synthesis and low temperature electrochemical properties of CeO2 and C co-modified Li3V2 (PO4) 3 cathode materials for lithium-ion batteries, *Electrochimica Acta*, 2015, **174**, 1131-1140.
153. J. Zheng, M. Gu, J. Xiao, B. J. Polzin, P. Yan, X. Chen, C. Wang and J.-G. Zhang, Functioning mechanism of AlF3 coating on the Li-and Mn-rich cathode materials, *Chemistry of Materials*, 2014, **26**, 6320-6327.
154. A. Tron, Y. D. Park and J. Mun, AlF3-coated LiMn2O4 as cathode material for aqueous rechargeable lithium battery with improved cycling stability, *Journal of Power Sources*, 2016, **325**, 360-364.
155. B.-C. Park, H.-B. Kim, H. J. Bang, J. Prakash and Y.-K. Sun, Improvement of electrochemical performance of Li [Ni0. 8Co0. 15Al0. 05] O2 cathode materials by AlF3 coating at various temperatures, *Industrial & Engineering Chemistry Research*, 2008, **47**, 3876-3882.
156. B. Zhao, J. Xie, H. Zhuang, X. Liu, W. Li, X. Hu, Y. Jiang and J. Zhang, Improved low-temperature performance of surface modified lithium-rich Li1.

2Ni0. 13Co0. 13Mn0. 54O2 cathode materials for lithium ion batteries, *Solid State Ionics*, 2020, **347**, 115245.
157. Y. Yin, X. Li, X. Mao, X. Ding and S. Yang, Solid state reaction preparation of LiFePO4/(C+ Cu) cathode material and its electrochemical performance, *Journal of Materials Science & Technology*, 2013, **29**, 937-942.
158. G. Cai, R. Guo, L. Liu, Y. Yang, C. Zhang, C. Wu, W. Guo and H. Jiang, Enhanced low temperature electrochemical performances of LiFePO4/C by surface modification with Ti3SiC2, *Journal of Power Sources*, 2015, **288**, 136-144.
159. Z. Sun, Z. Li, L. Gao, X. Zhao, D. Han, S. Gan, S. Guo and L. Niu, Grafting Benzenediazonium Tetrafluoroborate onto LiNixCoyMnzO2 Materials Achieves Subzero-Temperature High-Capacity Lithium-Ion Storage via a Diazonium Soft-Chemistry Method, *Advanced Energy Materials*, 2019, **9**, 1802946.
160. J. Shi, N. Ehteshami, J. Ma, H. Zhang, H. Liu, X. Zhang, J. Li and E. Paillard, Improving the graphite/electrolyte interface in lithium-ion battery for fast charging and low temperature operation: Fluorosulfonyl isocyanate as electrolyte additive, *Journal of Power Sources*, 2019, **429**, 67-74.
161. R. Guo, Y. Che, G. Lan, J. Lan, J. Li, L. Xing, K. Xu, W. Fan, L. Yu and W. Li, Tailoring low-temperature performance of a lithium-ion battery via rational designing interphase on an anode, *ACS Applied Materials & Interfaces*, 2019, **11**, 38285-38293.
162. R. Chandrasekaran, M. Koh, Y. Ozhawa, H. Aoyoma and T. Nakajima, Electrochemical cell studies on fluorinated natural graphite in propylene carbonate electrolyte with difluoromethyl acetate (MFA) additive for low temperature lithium battery application, *Journal of Chemical Sciences*, 2009, **121**, 339-346.
163. A. S. Wotango, W.-N. Su, A. M. Haregewoin, H.-M. Chen, J.-H. Cheng, M.-H. Lin, C.-H. Wang and B. J. Hwang, Designed synergetic effect of electrolyte additives to improve interfacial chemistry of MCMB electrode in propylene carbonate-based electrolyte for enhanced low and room temperature performance, *ACS Applied Materials & Interfaces*, 2018, **10**, 25252-25262.
164. Y. Lin, X. Yue, H. Zhang, L. Yu, W. Fan and T. Xie, Using phenyl methanesulfonate as an electrolyte additive to improve performance of LiNi0. 5Co0. 2Mn0. 3O2/graphite cells at low temperature, *Electrochimica Acta*, 2019, **300**, 202-207.
165. B. Liu, Q. Li, M. H. Engelhard, Y. He, X. Zhang, D. Mei, C. Wang, J.-G. Zhang and W. Xu, Constructing robust electrode/electrolyte interphases to enable wide temperature applications of lithium-ion batteries, *ACS Applied Materials & Interfaces*, 2019, **11**, 21496-21505.
166. J.-P. Jones, M. C. Smart, F. C. Krause and R. V. Bugga, The effect of electrolyte additives upon lithium plating during low temperature charging of graphite-LiNiCoAlO2 lithium-ion three electrode cells, *Journal of The Electrochemical Society*, 2020, **167**, 020536.

167. S. Zhang, K. Xu and T. Jow, Enhanced performance of Li-ion cell with LiBF4-PC based electrolyte by addition of small amount of LiBOB, *Journal of Power Sources*, 2006, **156**, 629-633.
168. Q. Li, S. Jiao, L. Luo, M. S. Ding, J. Zheng, S. S. Cartmell, C.-M. Wang, K. Xu, J.-G. Zhang and W. Xu, Wide-temperature electrolytes for lithium-ion batteries, *ACS Applied Materials & Interfaces*, 2017, **9**, 18826-18835.
169. P. Shi, L. Zhang, H. Xiang, X. Liang, Y. Sun and W. Xu, Lithium difluorophosphate as a dendrite-suppressing additive for lithium metal batteries, *ACS Applied Materials & Interfaces*, 2018, **10**, 22201-22209.
170. B. Yang, H. Zhang, L. Yu, W. Fan and D. Huang, Lithium difluorophosphate as an additive to improve the low temperature performance of LiNi0. 5Co0. 2Mn0. 3O2/graphite cells, *Electrochimica Acta*, 2016, **221**, 107-114.
171. L. Hamenu, H. S. Lee, M. Latifatu, K. M. Kim, J. Park, Y. G. Baek, J. M. Ko and R. B. Kaner, Lithium-silica nanosalt as a low-temperature electrolyte additive for lithium-ion batteries, *Current Applied Physics*, 2016, **16**, 611-617.
172. B. Liao, H. Li, M. Xu, L. Xing, Y. Liao, X. Ren, W. Fan, L. Yu, K. Xu and W. Li, Designing low impedance interface films simultaneously on anode and cathode for high energy batteries, *Advanced Energy Materials*, 2018, **8**, 1800802.
173. B. Wu, Y. Ren, D. Mu, X. Liu, G. Yang and Z. Sun, Lithium insertion/desertion properties of LiFePO4 cathode in a low temperature electrolyte modified with sodium chloride additive, *Solid State Ionics*, 2014, **260**, 8-14.
174. B. Wu, Y. Ren, D. Mu, C. Zhang, X. Liu and F. Wu, Enhanced low temperature performance of LiFePO4 cathode with electrolyte modification, *International Journal of Electrochemical Science*, 2013, **8**, 8502-8512.
175. X. Song, T. Meng, Y. Deng, A. Gao, J. Nan, D. Shu and F. Yi, The effects of the functional electrolyte additive on the cathode material Na0. 76Ni0. 3Fe0. 4Mn0. 3O2 for sodium-ion batteries, *Electrochimica Acta*, 2018, **281**, 370-377.
176. A. Wang, W. Zhou, A. Huang, M. Chen, Q. Tian and J. Chen, Developing improved electrolytes for aqueous zinc-ion batteries to achieve excellent cyclability and antifreezing ability, *Journal of Colloid and Interface Science*, 2021, **586**, 362-370.
177. S. Jurng, S. Park, T. Yoon, H.-s. Kim, H. Jeong, J. H. Ryu, J. J. Kim and S. M. Oh, Low-temperature performance improvement of graphite electrode by allyl sulfide additive and its film-forming mechanism, *Journal of The Electrochemical Society*, 2016, **163**, A1798.
178. Q. Chen, H. He, Z. Hou, W. Zhuang, T. Zhang, Z. Sun and L. Huang, Building an artificial solid electrolyte interphase with high-uniformity and fast ion diffusion for ultralong-life sodium metal anodes, *Journal of Materials Chemistry A*, 2020, **8**, 16232-16237.
179. J.-Q. Huang, X. Lin, H. Tan, X. Du and B. Zhang, Realizing high-performance Zn-ion batteries by a reduced graphene oxide block layer at room and low temperatures, *Journal of Energy Chemistry*, 2020, **43**, 1-7.

180. Y. Na, X. Sun, A. Fan, S. Cai and C. Zheng, Methods for enhancing the capacity of electrode materials in low-temperature lithium-ion batteries, *Chinese Chemical Letters*, 2021, **32**, 973-982.
181. W. Zhao, Y. Ji, Z. Zhang, M. Lin, Z. Wu, X. Zheng, Q. Li and Y. Yang, Recent advances in the research of functional electrolyte additives for lithium-ion batteries, *Current Opinion in Electrochemistry*, 2017, **6**, 84-91.
182. Z.-X. Huang, X.-L. Zhang, X.-X. Zhao, Y.-Y. Zhao, V. Aravindan, Y.-H. Liu, H. Geng and X.-L. Wu, Electrode/electrolyte additives for practical sodium-ion batteries: a mini review, *Inorganic Chemistry Frontiers*, 2023.
183. H. Huang, E. Kelder and J. Schoonman, Graphite–metal oxide composites as anode for Li-ion batteries, *Journal of Power sources*, 2001, **97**, 114-117.
184. X. Liu, T. Zhang, X. Shi, Y. Ma, D. Song, H. Zhang, X. Liu, Y. Wang and L. Zhang, Hierarchical sulfide-rich modification layer on SiO/C anode for low-temperature Li-ion batteries, *Advanced Science*, 2022, 2104531.
185. N. Delaporte, P. Chevallier, S. Rochon, G. Lajoie, J.-C. Daigle, V. Gariepy, D. Clément, R. Veillette, M.-C. Mathieu and M. Provencher, A low-cost and Li-rich organic coating on a Li 4 Ti 5 O 12 anode material enabling Li-ion battery cycling at subzero temperatures, *Materials Advances*, 2020, **1**, 854-872.
186. D. Wang, D. Lv, H. Peng, N. Wang, H. Liu, J. Yang and Y. Qian, Site-selective adsorption on ZnF2/Ag coated Zn for advanced aqueous zinc–metal batteries at low temperature, *Nano Letters*, 2022, **22**, 1750-1758.
187. X. Fan, X. Ji, L. Chen, J. Chen, T. Deng, F. Han, J. Yue, N. Piao, R. Wang and X. Zhou, All-temperature batteries enabled by fluorinated electrolytes with non-polar solvents, *Nature Energy*, 2019, **4**, 882-890.
188. X. Zheng, Z. Gu, J. Fu, H. Wang, X. Ye, L. Huang, X. Liu, X. Wu, W. Luo and Y. Huang, Knocking down the kinetic barriers towards fast-charging and low-temperature sodium metal batteries, *Energy & Environmental Science*, 2021, **14**, 4936-4947.
189. Y. Yang, P. Li, N. Wang, Z. Fang, C. Wang, X. Dong and Y. Xia, Fluorinated carboxylate ester-based electrolyte for lithium ion batteries operated at low temperature, *Chemical Communications*, 2020, **56**, 9640-9643.
190. S. Lei, Z. Zeng, M. Liu, H. Zhang, S. Cheng and J. Xie, Balanced solvation/de-solvation of electrolyte facilitates Li-ion intercalation for fast charging and low-temperature Li-ion batteries, *Nano Energy*, 2022, **98**, 107265.
191. L. Chen, H. Wu, X. Ai, Y. Cao and Z. Chen, Toward wide-temperature electrolyte for lithium–ion batteries, *Battery Energy*, 2022, **1**, 20210006.
192. M. Smart, B. Ratnakumar and S. Surampudi, Electrolytes for low-temperature lithium batteries based on ternary mixtures of aliphatic carbonates, *Journal of the Electrochemical Society*, 1999, **146**, 486.
193. E. Plichta and W. Behl, A low-temperature electrolyte for lithium and lithium-ion batteries, *Journal of Power Sources*, 2000, **88**, 192-196.
194. E. Plichta, M. Hendrickson, R. Thompson, G. Au, W. Behl, M. Smart, B. Ratnakumar and S. Surampudi, Development of low temperature Li-ion

electrolytes for NASA and DoD applications, *Journal of power sources*, 2001, **94**, 160-162.
195. M. Smart, B. Ratnakumar, L. Whitcanack, K. Chin, S. Surampudi, H. Croft, D. Tice and R. Staniewicz, Improved low-temperature performance of lithium-ion cells with quaternary carbonate-based electrolytes, *Journal of power sources*, 2003, **119**, 349-358.
196. X.-Z. Liao, Z.-F. Ma, Q. Gong, Y.-S. He, L. Pei and L.-J. Zeng, Low-temperature performance of LiFePO4/C cathode in a quaternary carbonate-based electrolyte, *Electrochemistry Communications*, 2008, **10**, 691-694.
197. S. Zhang, K. Xu, J. Allen and T. Jow, Effect of propylene carbonate on the low temperature performance of Li-ion cells, *Journal of Power Sources*, 2002, **110**, 216-221.
198. L. Liao, P. Zuo, Y. Ma, Y. An, G. Yin and Y. Gao, Effects of fluoroethylene carbonate on low temperature performance of mesocarbon microbeads anode, *Electrochimica Acta*, 2012, **74**, 260-266.
199. M. Smart, B. Ratnakumar and S. Surampudi, Use of organic esters as cosolvents in electrolytes for lithium-ion batteries with improved low temperature performance, *Journal of the Electrochemical Society*, 2002, **149**, A361.
200. M. Smart, B. Ratnakumar, K. Chin and L. Whitcanack, Lithium-ion electrolytes containing ester cosolvents for improved low temperature performance, *Journal of the Electrochemical Society*, 2010, **157**, A1361.
201. N. D. Rodrigo, S. Tan, Z. Shadike, E. Hu, X.-Q. Yang and B. L. Lucht, Improved low temperature performance of graphite/Li cells using isoxazole as a novel cosolvent in electrolytes, *Journal of the Electrochemical Society*, 2021, **168**, 070527.
202. S. Tan, U. N. D. Rodrigo, Z. Shadike, B. Lucht, K. Xu, C. Wang, X.-Q. Yang and E. Hu, Novel low-temperature electrolyte using isoxazole as the main solvent for lithium-ion batteries, *ACS Applied Materials & Interfaces*, 2021, **13**, 24995-25001.
203. H.-C. A. Shiao, D. Chua, H.-p. Lin, S. Slane and M. Salomon, Low temperature electrolytes for Li-ion PVDF cells, *Journal of Power Sources*, 2000, **87**, 167-173.
204. S. Herreyre, O. Huchet, S. Barusseau, F. Perton, J. Bodet and P. Biensan, New Li-ion electrolytes for low temperature applications, *Journal of power sources*, 2001, **97**, 576-580.
205. H. Shu, L. Jie, G.-c. Wang, Z.-a. Zhang and Y.-q. Lai, Effect of linear carboxylic ester on low temperature performance of LiMn2O4–graphite cells, *Transactions of Nonferrous Metals Society of China*, 2015, **25**, 206-210.
206. K. Chen, Z. Yu, S. Deng, Q. Wu, J. Zou and X. Zeng, Evaluation of the low temperature performance of lithium manganese oxide/lithium titanate lithium-ion batteries for start/stop applications, *Journal of Power Sources*, 2015, **278**, 411-419.
207. X. Dong, Y. Lin, P. Li, Y. Ma, J. Huang, D. Bin, Y. Wang, Y. Qi and Y. Xia, High-energy rechargeable metallic lithium battery at− 70 C enabled by a

cosolvent electrolyte, *Angewandte Chemie International Edition*, 2019, **58**, 5623-5627.
208. Y.-G. Cho, M. Li, J. Holoubek, W. Li, Y. Yin, Y. S. Meng and Z. Chen, Enabling the low-temperature cycling of NMC|| graphite pouch cells with an ester-based electrolyte, *ACS Energy Letters*, 2021, **6**, 2016-2023.
209. S. V. Sazhin, M. Y. Khimchenko, Y. N. Tritenichenko and H. S. Lim, Performance of Li-ion cells with new electrolytes conceived for low-temperature applications, *Journal of Power Sources*, 2000, **87**, 112-117.
210. W. Lu, K. Xie, Y. Pan, Z.-x. Chen and C.-m. Zheng, Effects of carbon-chain length of trifluoroacetate co-solvents for lithium-ion battery electrolytes using at low temperature, *Journal of Fluorine Chemistry*, 2013, **156**, 136-143.
211. W. Lu, K. Xie, Z. Chen, S. Xiong, Y. Pan and C. Zheng, A new co-solvent for wide temperature lithium ion battery electrolytes: 2, 2, 2-Trifluoroethyl n-caproate, *Journal of Power Sources*, 2015, **274**, 676-684.
212. J. Holoubek, M. Yu, S. Yu, M. Li, Z. Wu, D. Xia, P. Bhaladhare, M. S. Gonzalez, T. A. Pascal and P. Liu, An all-fluorinated ester electrolyte for stable high-voltage Li metal batteries capable of ultra-low-temperature operation, *ACS Energy Letters*, 2020, **5**, 1438-1447.
213. S. Li, W. Zhao, Z. Zhou, X. Cui, Z. Shang, H. Liu and D. Zhang, Studies on electrochemical performances of novel electrolytes for wide-temperature-range lithium-ion batteries, *ACS Applied Materials & Interfaces*, 2014, **6**, 4920-4926.
214. S. Li, X. Li, J. Liu, Z. Shang and X. Cui, A low-temperature electrolyte for lithium-ion batteries, *Ionics*, 2015, **21**, 901-907.
215. S. Li, W. Zhao, X. Cui, Y. Zhao, B. Li, H. Zhang, Y. Li, G. Li, X. Ye and Y. Luo, An improved method for synthesis of lithium difluoro (oxalato) borate and effects of sulfolane on the electrochemical performances of lithium-ion batteries, *Electrochimica Acta*, 2013, **91**, 282-292.
216. Y. Liu, S. Fang, P. Shi, D. Luo, L. Yang and S.-i. Hirano, Ternary mixtures of nitrile-functionalized glyme, non-flammable hydrofluoroether and fluoroethylene carbonate as safe electrolytes for lithium-ion batteries, *Journal of Power Sources*, 2016, **331**, 445-451.
217. X. Zhang, L. Zou, Y. Xu, X. Cao, M. H. Engelhard, B. E. Matthews, L. Zhong, H. Wu, H. Jia and X. Ren, Advanced electrolytes for fast-charging high-voltage lithium-ion batteries in wide-temperature range, *Advanced Energy Materials*, 2020, **10**, 2000368.
218. A. C. Thenuwara, P. P. Shetty, N. Kondekar, S. E. Sandoval, K. Cavallaro, R. May, C.-T. Yang, L. E. Marbella, Y. Qi and M. T. McDowell, Efficient low-temperature cycling of lithium metal anodes by tailoring the solid-electrolyte interphase, *ACS Energy Letters*, 2020, **5**, 2411-2420.
219. K. Naoi, E. Iwama, N. Ogihara, Y. Nakamura, H. Segawa and Y. Ino, Nonflammable hydrofluoroether for lithium-ion batteries: Enhanced rate capability, cyclability, and low-temperature performance, *Journal of the Electrochemical Society*, 2009, **156**, A272.

220. Y. Ein-Eli, S. Thomas, R. Chadha, T. Blakley and V. Koch, Li-ion battery electrolyte formulated for low-temperature applications, *Journal of the Electrochemical Society*, 1997, **144**, 823.
221. S. Zhang, K. Xu and T. Jow, A new approach toward improved low temperature performance of Li-ion battery, *Electrochemistry Communications*, 2002, **4**, 928-932.
222. S. Zhang, K. Xu and T. Jow, Low-temperature performance of Li-ion cells with a LiBF4-based electrolyte, *Journal of Solid State Electrochemistry*, 2003, **7**, 147-151.
223. K. Xu, S. S. Zhang, U. Lee, J. L. Allen and T. R. Jow, LiBOB: Is it an alternative salt for lithium ion chemistry?, *Journal of Power Sources*, 2005, **146**, 79-85.
224. S. Zhang, K. Xu and T. Jow, An improved electrolyte for the LiFePO4 cathode working in a wide temperature range, *Journal of power sources*, 2006, **159**, 702-707.
225. S. S. Zhang, An unique lithium salt for the improved electrolyte of Li-ion battery, *Electrochemistry Communications*, 2006, **8**, 1423-1428.
226. S. S. Zhang, Electrochemical study of the formation of a solid electrolyte interface on graphite in a LiBC2O4F2-based electrolyte, *Journal of Power Sources*, 2007, **163**, 713-718.
227. S. S. Zhang, Lithium oxalyldifluoroborate as a salt for the improved electrolytes of Li-ion batteries, *ECS Transactions*, 2007, **3**, 59.
228. L. Zhang, Y. Sun, Y. Zhou, C. Hai, S. Hu, J. Zeng, Y. Shen, S. Dong, G. Qi and F. Li, Investigation of the synergetic effects of LiBF4 and LiODFB as wide-temperature electrolyte salts in lithium-ion batteries, *Ionics*, 2018, **24**, 2995-3004.
229. Z.-B. Zhou, M. Takeda, T. Fujii and M. Ue, Li[C2F5BF3] as an electrolyte salt for 4 V class lithium-ion cells, *Journal of the Electrochemical Society*, 2005, **152**, A351.
230. T. Sun, X. Yuan, K. Wang, S. Zheng, J. Shi, Q. Zhang, W. Cai, J. Liang and Z. Tao, An ultralow-temperature aqueous zinc-ion battery, *Journal of Materials Chemistry A*, 2021, **9**, 7042-7047.
231. G. Yang, J. Huang, X. Wan, B. Liu, Y. Zhu, J. Wang, O. Fontaine, S. Luo, P. Hiralal and Y. Guo, An aqueous zinc-ion battery working at− 50° C enabled by low-concentration perchlorate-based chaotropic salt electrolyte, *EcoMat*, 2022, e12165.
232. T. Sun, S. Zheng, H. Du and Z. Tao, Synergistic effect of cation and anion for low-temperature aqueous zinc-ion battery, *Nano-micro Letters*, 2021, **13**, 1-10.
233. Z. Chen, D. L. Danilov, R. A. Eichel and P. H. Notten, Porous electrode modeling and its applications to Li-ion batteries, *Advanced Energy Materials*, 2022, **12**, 2201506.
234. K. M. Kim, N. V. Ly, J. H. Won, Y.-G. Lee, W. I. Cho, J. M. Ko and R. B. Kaner, Improvement of lithium-ion battery performance at low temperature by adopting polydimethylsiloxane-based electrolyte additives, *Electrochimica Acta*, 2014, **136**, 182-188.

235. J. H. Won, H. S. Lee, L. Hamenu, M. Latifatu, Y. M. Lee, K. M. Kim, J. Oh, W. I. Cho and J. M. Ko, Improvement of low-temperature performance by adopting polydimethylsiloxane-g-polyacrylate and lithium-modified silica nanosalt as electrolyte additives in lithium-ion batteries, *Journal of Industrial and Engineering Chemistry*, 2016, **37**, 325-329.
236. Y. Li, K. W. Wong, Q. Dou, W. Zhang and K. M. Ng, Improvement of lithium-ion battery performance at low temperature by adopting ionic liquid-decorated PMMA nanoparticles as electrolyte component, *ACS Applied Energy Materials*, 2018, **1**, 2664-2670.
237. L. Liao, X. Cheng, Y. Ma, P. Zuo, W. Fang, G. Yin and Y. Gao, Fluoroethylene carbonate as electrolyte additive to improve low temperature performance of LiFePO4 electrode, *Electrochimica Acta*, 2013, **87**, 466-472.
238. M. Qin, Z. Zeng, S. Cheng and J. Xie, Challenges and strategies of formulating low-temperature electrolytes in lithium-ion batteries, *Interdisciplinary Materials*, 2023, **2**, 308-336.
239. D. Reber, R.-S. Kühnel and C. Battaglia, Suppressing crystallization of water-in-salt electrolytes by asymmetric anions enables low-temperature operation of high-voltage aqueous batteries, *ACS Materials Letters*, 2019, **1**, 44-51.
240. L. Suo, O. Borodin, T. Gao, M. Olguin, J. Ho, X. Fan, C. Luo, C. Wang and K. Xu, "Water-in-salt" electrolyte enables high-voltage aqueous lithium-ion chemistries, *Science*, 2015, **350**, 938-943.
241. F. Zhu, H. Bao, X. Wu, Y. Tao, C. Qin, Z. Su and Z. Kang, High-performance metal–organic framework-based single ion conducting solid-state electrolytes for low-temperature lithium metal batteries, *ACS Applied Materials & Interfaces*, 2019, **11**, 43206-43213.
242. Z. Lin and J. Liu, Low-temperature all-solid-state lithium-ion batteries based on a di-cross-linked starch solid electrolyte, *RSC advances*, 2019, **9**, 34601-34606.
243. W. Deng, Z. Zhou, Y. Li, M. Zhang, X. Yuan, J. Hu, Z. Li, C. Li and R. Li, High-capacity layered magnesium vanadate with concentrated gel electrolyte toward high-performance and wide-temperature zinc-ion battery, *ACS nano*, 2020, **14**, 15776-15785.
244. J. Liu, N. Nie, J. Wang, M. Hu, J. Zhang, M. Li and Y. Huang, Initiating a wide-temperature-window yarn zinc ion battery by a highly conductive iongel, *Materials Today Energy*, 2020, **16**, 100372.
245. Y. Liu, X. Zhou, Y. Bai, R. Liu, X. Li, H. Xiao, Y. Wang, X. Wang, Y. Ma and G. Yuan, Engineering integrated structure for high-performance flexible zinc-ion batteries, *Chemical Engineering Journal*, 2021, **417**, 127955.
246. X. Li, H. Wang, X. Sun, J. Li and Y.-N. Liu, Flexible wide-temperature zinc-ion battery enabled by an ethylene glycol-based organohydrogel electrolyte, *ACS Applied Energy Materials*, 2021, **4**, 12718-12727.
247. K. Fujie, K. Otsubo, R. Ikeda, T. Yamada and H. Kitagawa, Low temperature ionic conductor: ionic liquid incorporated within a metal–organic framework, *Chemical science*, 2015, **6**, 4306-4310.

248. W. Wang, T. Yang, S. Li, W. Fan, X. Zhao, C. Fan, L. Yu, S. Zhou, X. Zuo and R. Zeng, 1-ethyl-3-methylimidazolium tetrafluoroborate (EMI-BF4) as an ionic liquid-type electrolyte additive to enhance the low-temperature performance of LiNi0. 5Co0. 2Mn0. 3O2/graphite batteries, *Electrochimica Acta*, 2019, **317**, 146-154.
249. C. Ding, T. Nohira, R. Hagiwara, K. Matsumoto, Y. Okamoto, A. Fukunaga, S. Sakai, K. Nitta and S. Inazawa, Na [FSA]-[C3C1pyrr][FSA] ionic liquids as electrolytes for sodium secondary batteries: Effects of Na ion concentration and operation temperature, *Journal of Power Sources*, 2014, **269**, 124-128.
250. M. Hilder, P. C. Howlett, D. Saurel, E. Gonzalo, M. Armand, T. Rojo, D. R. Macfarlane and M. Forsyth, Small quaternary alkyl phosphonium bis (fluorosulfonyl) imide ionic liquid electrolytes for sodium-ion batteries with P2- and O3-Na2/3 [Fe2/3Mn1/3] O2 cathode material, *Journal of Power Sources*, 2017, **349**, 45-51.
251. C. S. Rustomji, Y. Yang, T. K. Kim, J. Mac, Y. J. Kim, E. Caldwell, H. Chung and Y. S. Meng, Liquefied gas electrolytes for electrochemical energy storage devices, *Science*, 2017, **356**, eaal4263.
252. Y. Yang, Y. Yin, D. M. Davies, M. Zhang, M. Mayer, Y. Zhang, E. S. Sablina, S. Wang, J. Z. Lee and O. Borodin, Liquefied gas electrolytes for wide-temperature lithium metal batteries, *Energy & Environmental Science*, 2020, **13**, 2209-2219.
253. L. Chen, X. Shen, H. Chen, T. Wen, R. Rao, C. Zhang, Q. Meng, J. Zhang, Y. Ding and X. Ai, High-stable nonflammable electrolyte regulated by coordination-number rule for all-climate and safer lithium-ion batteries, *Energy Storage Materials*, 2023, **55**, 836-846.
254. Y. Cao, S. Li, Z. Yang, M. Wu, X. Wang, C. Xu, X. Zhang, R. Lin, X. Ma and G. Huang, Template-directing coupled with chemical activation methodology-derived hexagon-like porous carbon electrode with outstanding compatibility to electrolytes and low-temperature performance, *ACS Applied Materials & Interfaces*, 2021, **13**, 8206-8218.
255. Z. Lei, Y. Zhang and X. Lei, Improving temperature uniformity of a lithium-ion battery by intermittent heating method in cold climate, *International Journal of Heat and Mass Transfer*, 2018, **121**, 275-281.
256. S. Mohan, J. Siegel, A. G. Stefanopoulou, M. Castanier and Y. Ding, Synthesis of an energy-optimal self-heating strategy for Li-ion batteries, 2016 IEEE 55th Conference on Decision and Control (CDC), 2016, 1589-1594.
257. M. Karthikeyan, A. G. Kannan and S. Um, Sub-zero temperature thermo-electrochemical energy harvesting system using a self-heating negative temperature coefficient CNT-vanadium oxide cathode, *Journal of Applied Electrochemistry*, 2017, **47**, 125-132.
258. X.-G. Yang, G. Zhang and C.-Y. Wang, Computational design and refinement of self-heating lithium ion batteries, *Journal of Power Sources*, 2016, **328**, 203-211.

259. C.-Y. Wang, T. Xu, S. Ge, G. Zhang, X.-G. Yang and Y. Ji, A fast rechargeable lithium-ion battery at subfreezing temperatures, *Journal of The Electrochemical Society*, 2016, **163**, A1944.
260. C.-Y. Wang, G. Zhang, S. Ge, T. Xu, Y. Ji, X.-G. Yang and Y. Leng, Lithium-ion battery structure that self-heats at low temperatures, *Nature*, 2016, **529**, 515-518.
261. G. Zhang, S. Ge, T. Xu, X.-G. Yang, H. Tian and C.-Y. Wang, Rapid self-heating and internal temperature sensing of lithium-ion batteries at low temperatures, *Electrochimica Acta*, 2016, **218**, 149-155.
262. Y. Ji and C. Y. Wang, Heating strategies for Li-ion batteries operated from subzero temperatures, *Electrochimica Acta*, 2013, **107**, 664-674.
263. J. Jiang, H. Ruan, B. Sun, L. Wang, W. Gao and W. Zhang, A low-temperature internal heating strategy without lifetime reduction for large-size automotive lithium-ion battery pack, *Applied Energy*, 2018, **230**, 257-266.
264. H. Ruan, J. Jiang, B. Sun, X. Su, X. He and K. Zhao, An optimal internal-heating strategy for lithium-ion batteries at low temperature considering both heating time and lifetime reduction, *Applied Energy*, 2019, **256**, 113797.

Figures:

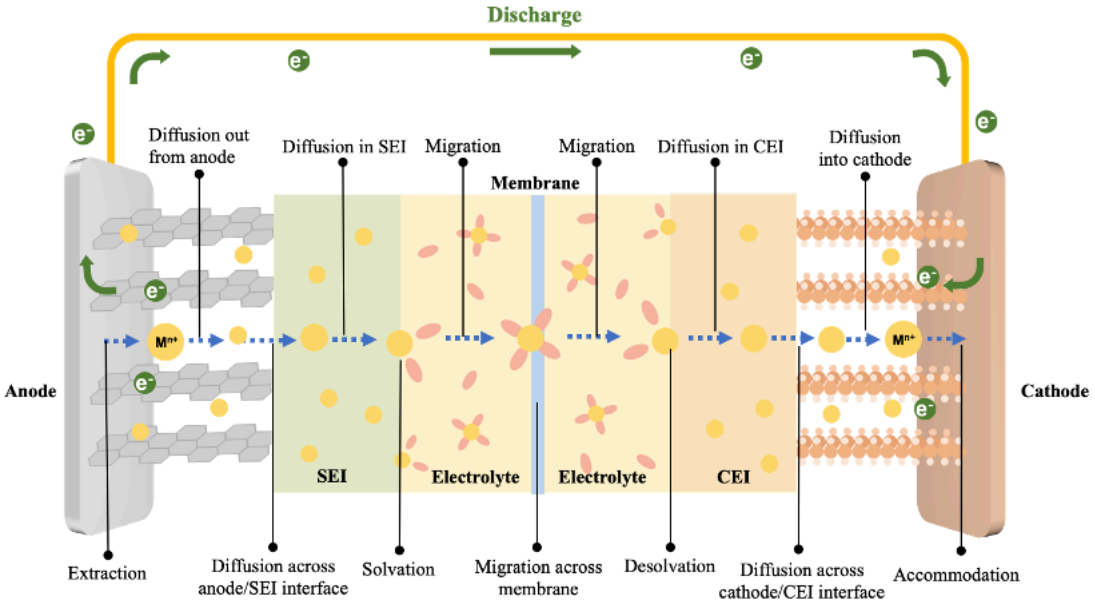

Figure 1. Illustration of the metal-ion transport steps during the battery discharge.

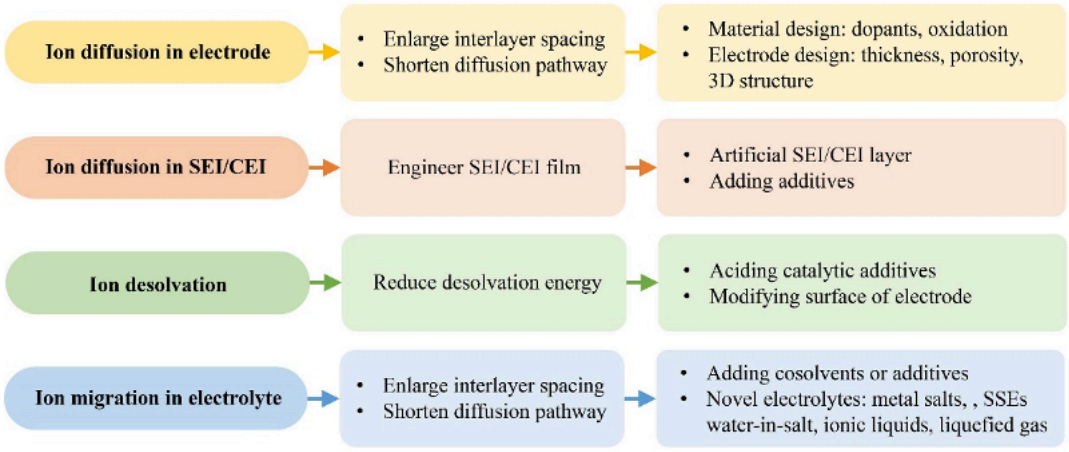

Figure 2. An overview of ion-transport issues in MIBs, corresponding solution strategies and the peculiar methods.

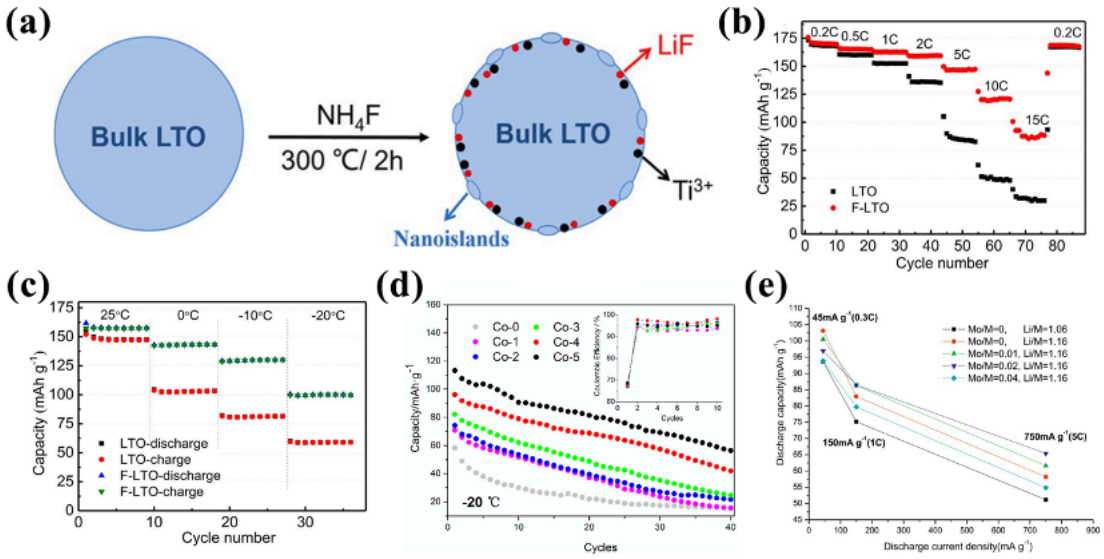

Figure 3. Modifying the crystal structure of electrode materials: (a) illustration of the formation process for F doping LTO anode for LIBs, (b) rate performance of LTO and F-LTO from 0.2 to 15 C, (c) cyclic performance of LTO and F-LTO at various temperatures from 25 to -20 °C at 1 C. Reproduced with permission.[59] Copyright 2017, American Chemical Society. (d) Cycle performance at 0.1 C of the $Li_{1.2}Ni_xCo_yMn_{1-x-y}O_2$ at -20 ˚C. Reproduced with permission.[68] Copyright 2015, American Chemical Society. (e) The high rate discharge capability of Li/Mo co-doped NCM cathode at -30 °C. Reproduced with permission.[67] Copyright 2015, Elsevier.

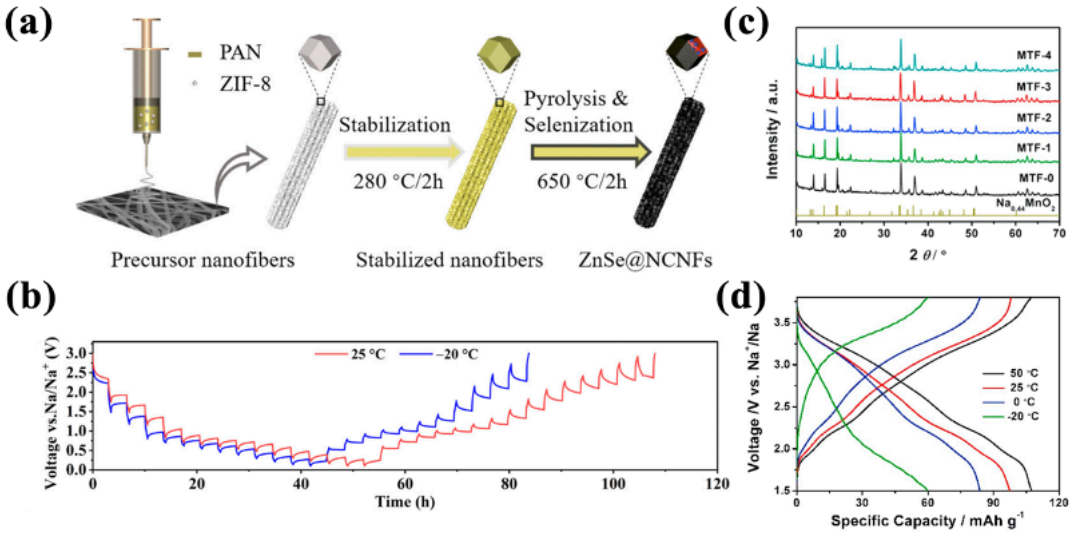

Figure 4. (a) Schematic diagram of the synthesis procedure of N doped ZnSe anode for SIBs, (b) Electrochemistry performance of ZnSe@NCNFs at 25 and -20°C for SIBs. Reproduced with permission.[69] Copyright 2021, American Chemical Society. (c) Composition of F-doped MTF-x cathode (x = 0, 1, 2, 3, 4), (d) galvanostatic charge/discharge curves of MTF-3 at a current rate of 0.2 C at 50, 25, 0 and -20 °C for SIBs. Reproduced with permission,[70] Copyright 2018, Elsevier.

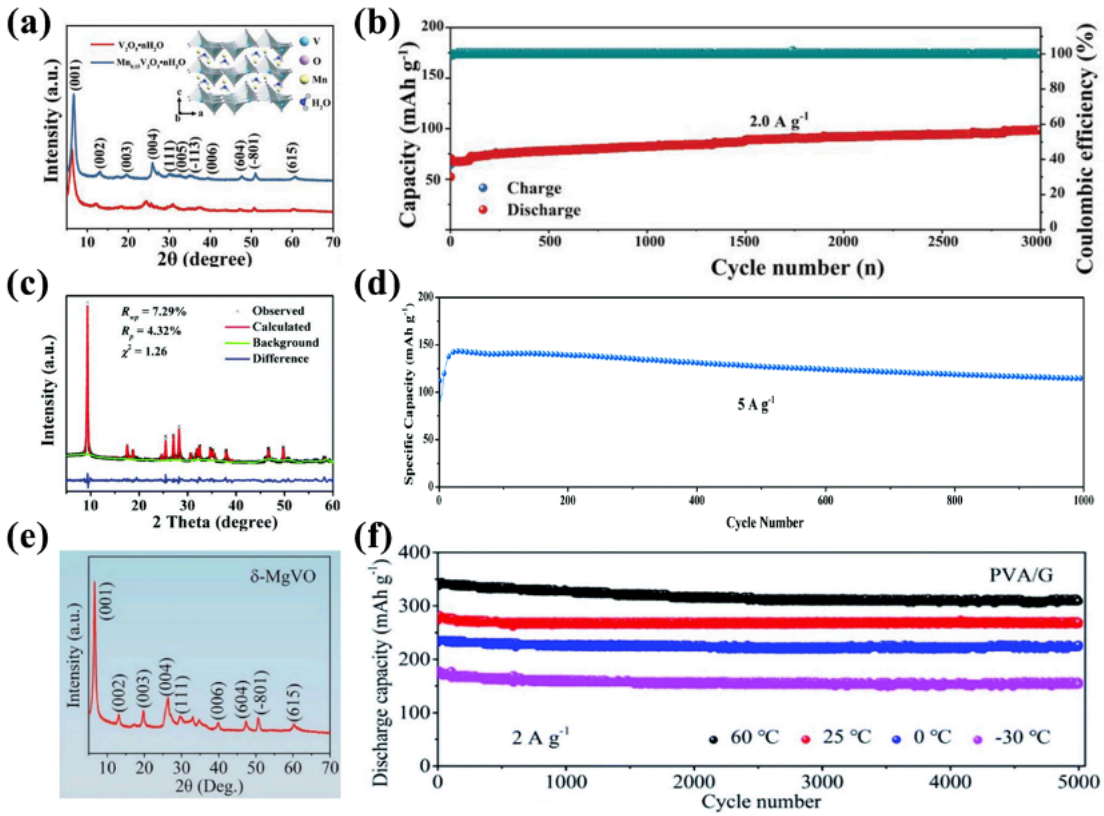

Figure 5. (a) XRD patterns of $Mn_{0.15}V_2O_5{\cdot}nH_2O$ and $V_2O_5{\cdot}nH_2O$, (b) zinc-ion storage performance of $Mn_{0.15}V_2O_5{\cdot}nH_2O$ electrode under 2.0 A g^{-1} at -20 °C. Reproduced with permission.[71] Copyright 2019, Wiley-VCH. (c) The XRD pattern of $K_{0.5}V_2O_5$, (d) long-term cycling performance of $K_{0.5}V_2O_5$ for ZIBs under 5.0 A g^{-1} at -20 °C. Reproduced with permission.[72] Copyright 2021, Royal Society of Chemistry. (e) The XRD pattern of Mg doped on V_2O_5 sample, (f) cycling performances of thin-film PVA/GZn//δ-MgVO battery under 2 A g^{-1} at different temperatures. Reproduced with permission.[74] Copyright 2020, Royal Society of Chemistry.

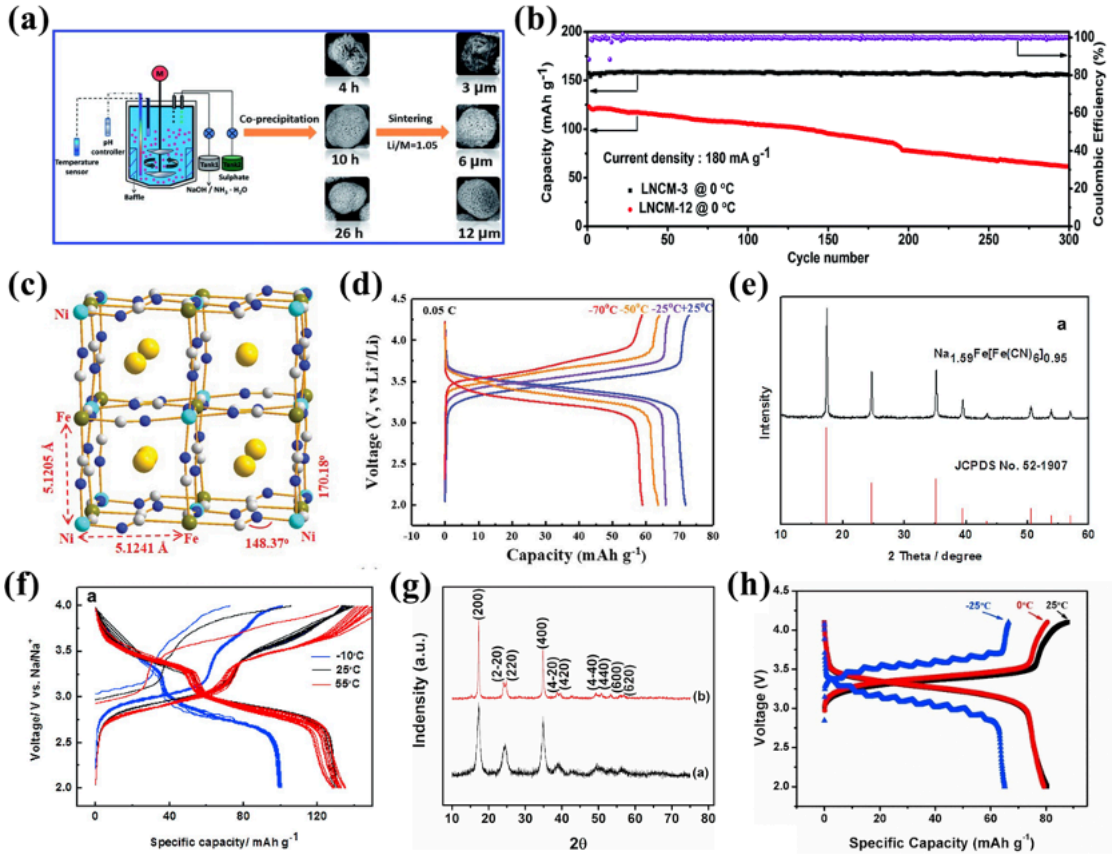

Figure 6. (a) Schematic of the synthesis procedure for NCM cathode with different particle size, (b) charge–discharge profiles of LNCM-3 at 0 °C between 3.0 and 4.4 V. Reproduced with permission.[86] Copyright 2016, Royal Society of Chemistry. (c) Illustration of cell structure and lattice parameter of Ni-based PB nanoparticles, (d) charge/discharge profiles of NiHCF-based LIB with the rate of 0.05 C from +25 to -70 °C. Reproduced with permission.[89] Copyright 2020, Wiley-VCH. (e) Powder XRD pattern of the prepared prussian blue sample, (f) The first 10 cycle charge-discharge profiles of the PB cathode in 2.0–4.0 V under 10 mA g-1 at various temperatures. Reproduced with permission.[92] Copyright 2016, Elsevier. (g) XRD patterns of PBNi and PBNi-ES, (h) the initial charge/discharge profiles of PBNi-ES at different temperatures under 0.1 C. Reproduced with permission.[91] Copyright 2018, Elsevier.

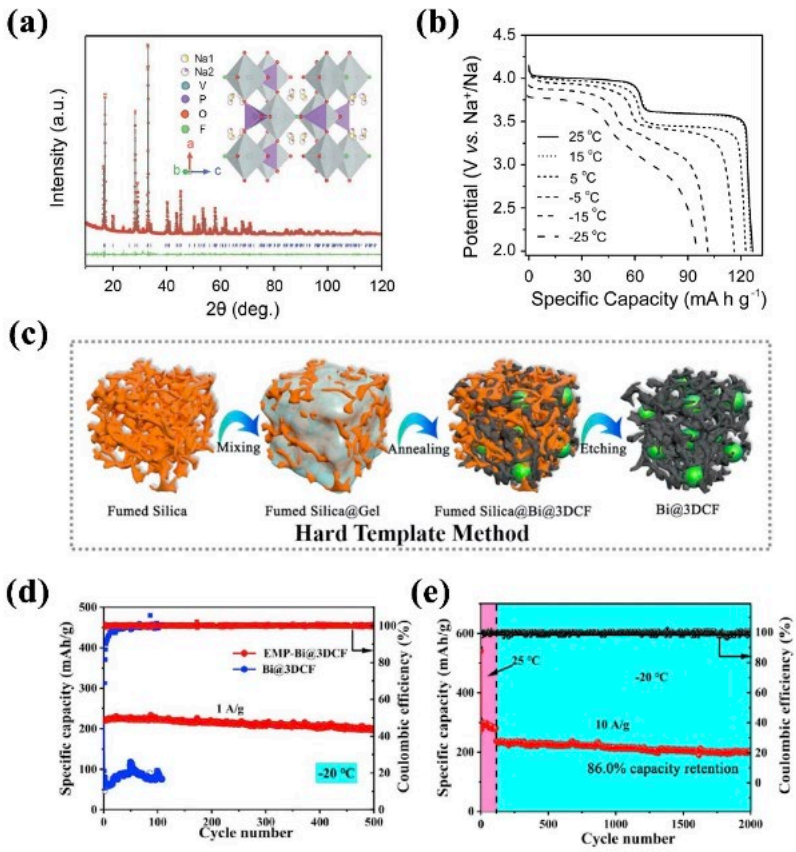

Figure 7. (a) XRD pattern and Le Bail refinements for NVPF-NTP Inset: Schematic of the $Na_3V_2(PO_4)_2O_2F$ crystal structure, (b) galvanostatic discharge curves of NVPF-NTP cycled at 0.2 C in the temperature range from 25 to -25 °C. Reproduced with permission.[93] Copyright 2017, Wiley-VCH. (c) Schematic illustration of the synthesis process of Bi@3DCF, (d) cycling stability under 1 A g^{-1} of EMP-Bi@ 3DCF and Bi@3DCF at -20 °C for SIBs, (e) cycling stability at the current density of 10 A g^{-1} at 25 °C and -20 °C of EMP-Bi@ 3DCF for KIBs. Reproduced with permission.[94] Copyright 2020, Elsevier.

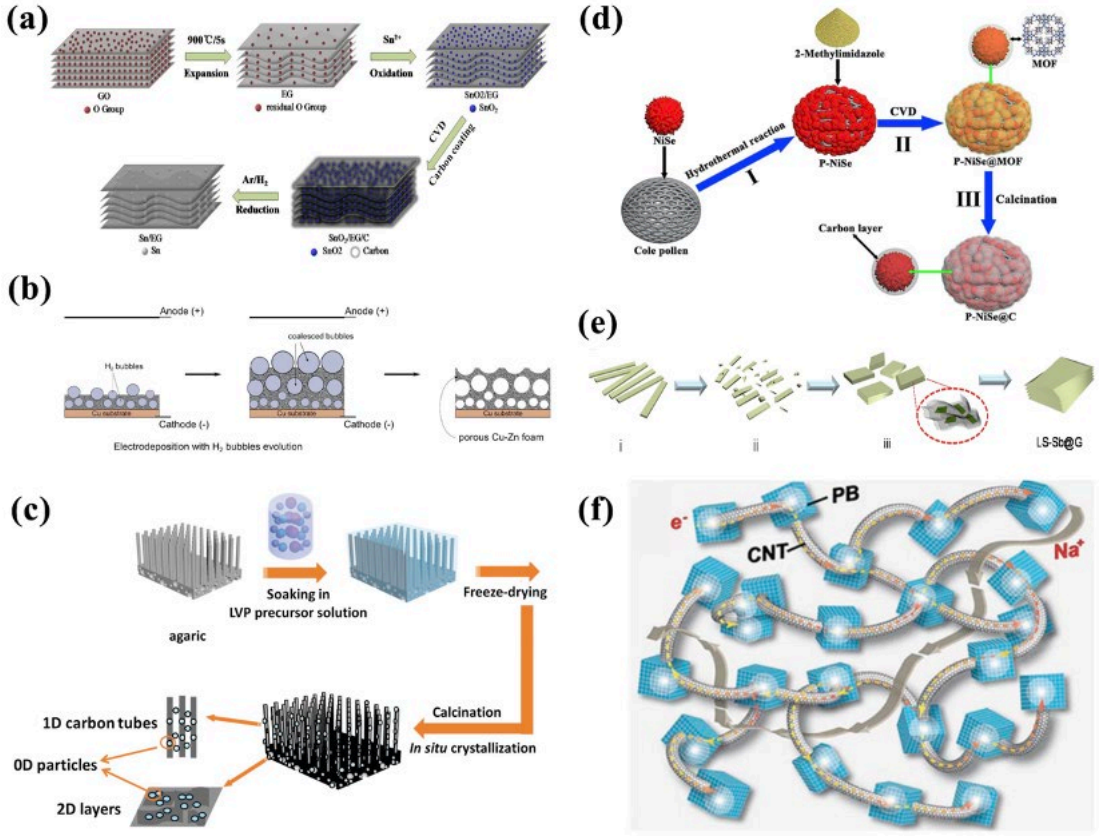

Figure 8. Schematic illustration of the synthesis process of (a) Sn/EG anode materials, Reproduced with permission.[99] Copyright 2015, Elsevier. (b) Cu-Zn 3D anode materials for LIBs. Reproduced with permission.[100] Copyright 2017, Wiley-VCH. (c) 3D LVP and biomass-derived porous carbon as cathode for LIBs. Reproduced with permission.[101] Copyright 2017, Wiley-VCH. (d) 3D P-NiSe@C as anode materials for SIBs. Reproduced with permission.[103] Copyright 2019, Elsevier. (e) Layer-stacked LS-Sb@G anode materials for SIBs via solvothermal route. Reproduced with permission.[104] Copyright 2017, Elsevier. (f) 3D PB/CNT cathode for SIBs. Reproduced with permission.[105] Copyright 2016, Wiley-VCH.

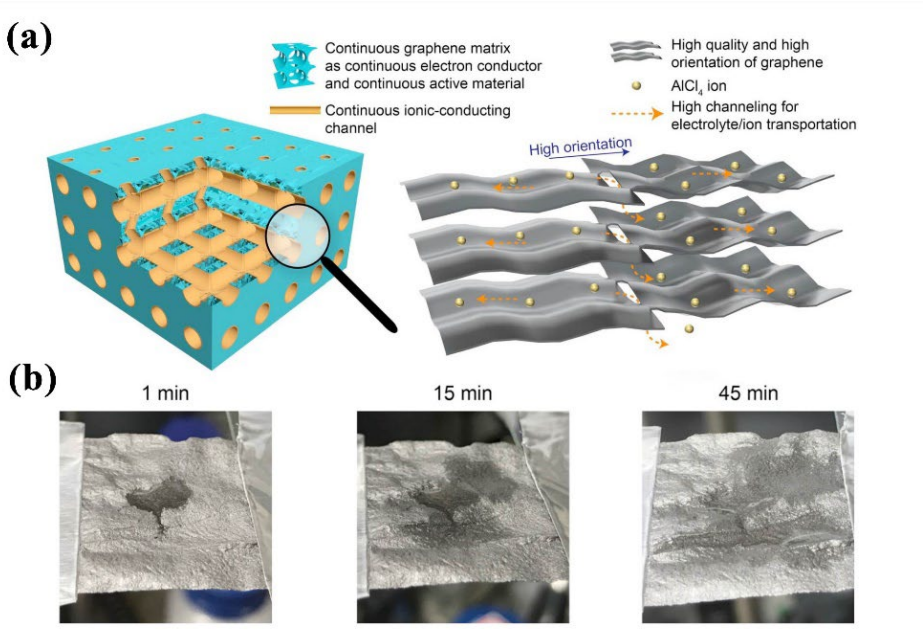

Figure 9. (a) Illustration of tricontinuous (3C, continuous electron conductor, continuous ion-conducting channel, and continuous active material) and trihigh (3H, high-quality graphene, high-orientation assembling, and high channeling) design for 3D graphene film cathode for AIBs. (b) Fast infiltration process of ionic liquid electrolyte in 3D graphene film cathode. Reproduced with permission.[106] Copyright 2017, The American Association for the Advancement of Science.

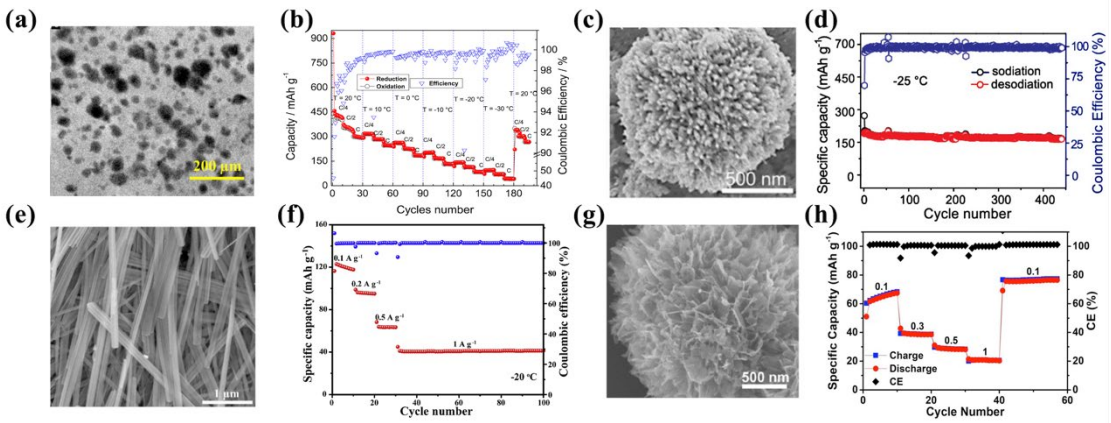

Figure 10. (a) Microstructure and (b) cycling performance of Sn-Carbon anode for LIBs at various temperatures. Reproduced with permission.[118] Copyright 2014, Elsevier. (c) Microstructure of cl-Fe_7Se_8@C anode, (d) long cycling property of cl-Fe_7Se_8@C//NVPOF full SIB at 0.05 A g^{-1} at -25 °C. Reproduced with permission.[123] Copyright 2019, American Chemical Society. (e) Microstructure of $(NH_4)_2V_6O_{16}\cdot 1.5H_2O$ nanowire, (f) cycling performances of Zn//NVO battery at –20 °C. Reproduced with permission.[126] Copyright 2019, Elsevier. (g) Microstructure of hydrangea-like amorphous Fe-V-O oxides (FeVO4) cathode, (h) rate performance of Fe-V-O at –20 °C for ZIBs. Reproduced with permission.[128] Copyright 2020, American Chemical Society.

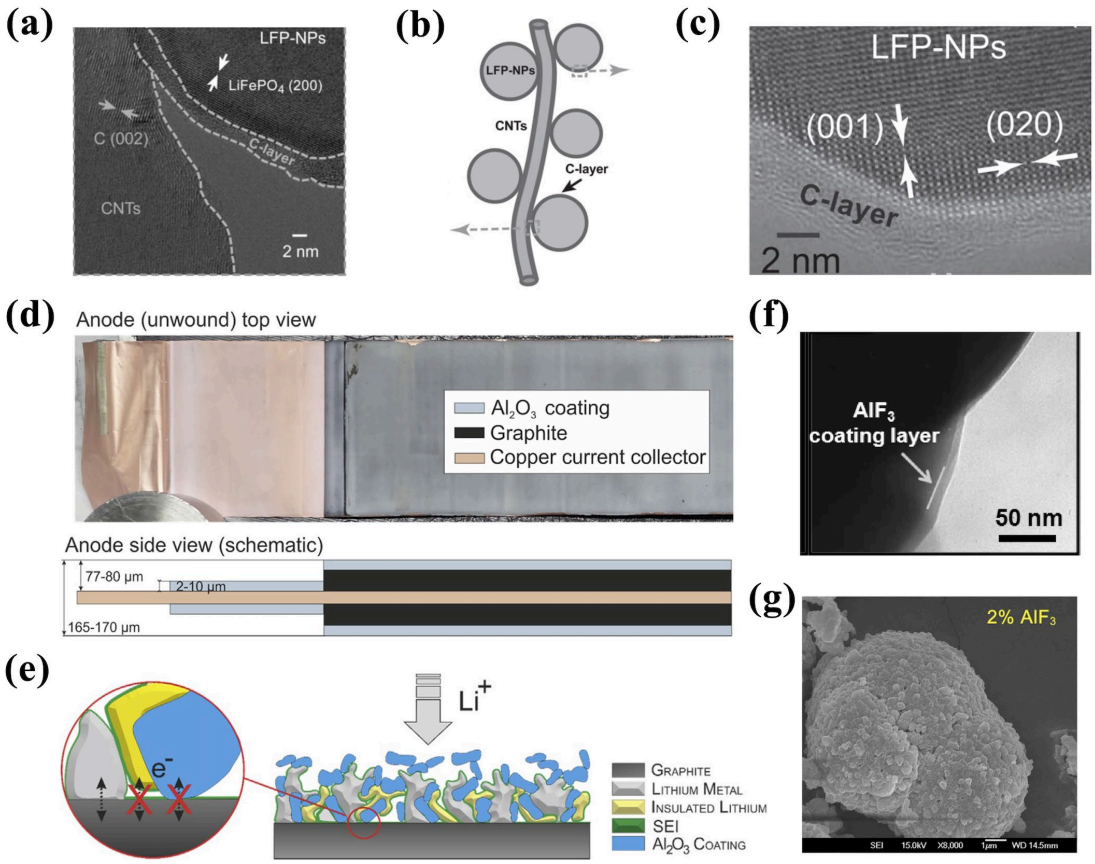

Figure 11. (a-c) The carbon layer in LFP@C/CNT nanocomposite cathode. Reproduced with permission.[141] Copyright 2013, Wiley-VCH. (d) Photos and illustration from top and side view of Al_2O_3 coated anode, (e) lithium metal deposition and dissolution mechanism during charge on anode side. Reproduced with permission.[151] Copyright 2017, Elsevier. (f) The AlF_3 coating layer on $Li[Ni_{0.8}Co_{0.15}Al_{0.05}]O_2$ cathode surface for LIBs. Reproduced with permission.[155] Copyright 2008, American Chemical Society. (g) Microstructure of 2% AlF_3-coated NCM cathode surface for LIBs. Reproduced with permission.[156] Copyright 2020, Elsevier.

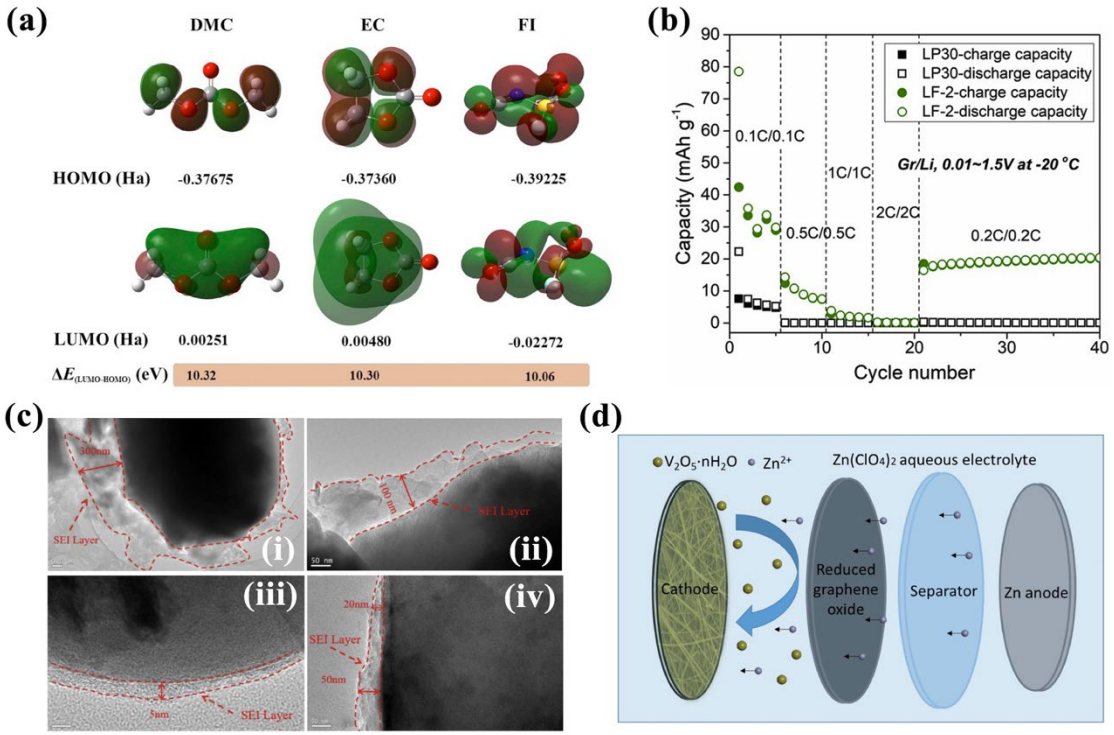

Figure 12. (a) The orbitals of DMC, EC and FI molecules, (b) the electrochemical performance LIBs with normal electrolyte (LP30) and with 2 wt% FI (LF-2) at low temperature. Reproduced with permission.[160] Copyright 2019, Elsevier. (c) SEI layer formed on $Na_{0.76}Ni_{0.3}Fe_{0.4}Mn_{0.3}O_2$ particles (i) without, (ii) with 1%, (iii) 3% and (iv) 5% ADN after working in SIBs. Reproduced with permission.[175] Copyright 2018, Elsevier. (d) The schematic of $V_2O_5 \cdot nH_2O$ migration behavior with rGO block layer in ZIBs. Reproduced with permission.[179] Copyright 2019, Elsevier.

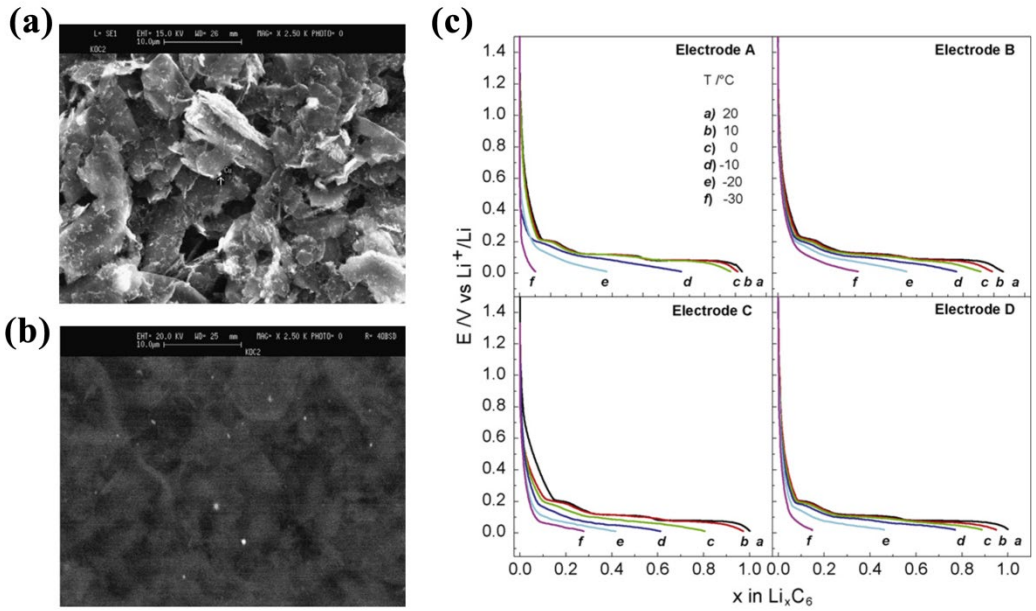

Figure 13. Secondary electrons (a) and backscattered electrons (b) images for Cu-powder/graphite electrode, (c) Galvanostatic intercalation profiles of electrode without Cu (Electrode A), with 1wt% Cu (Electrode B), 50Å Cu layer (Electrode C) and 1wt% Cu/50Å Cu layer (Electrode D) at different temperatures obtained at C/5 rate. Reproduced with permission.[113] Copyright 2008, Elsevier.

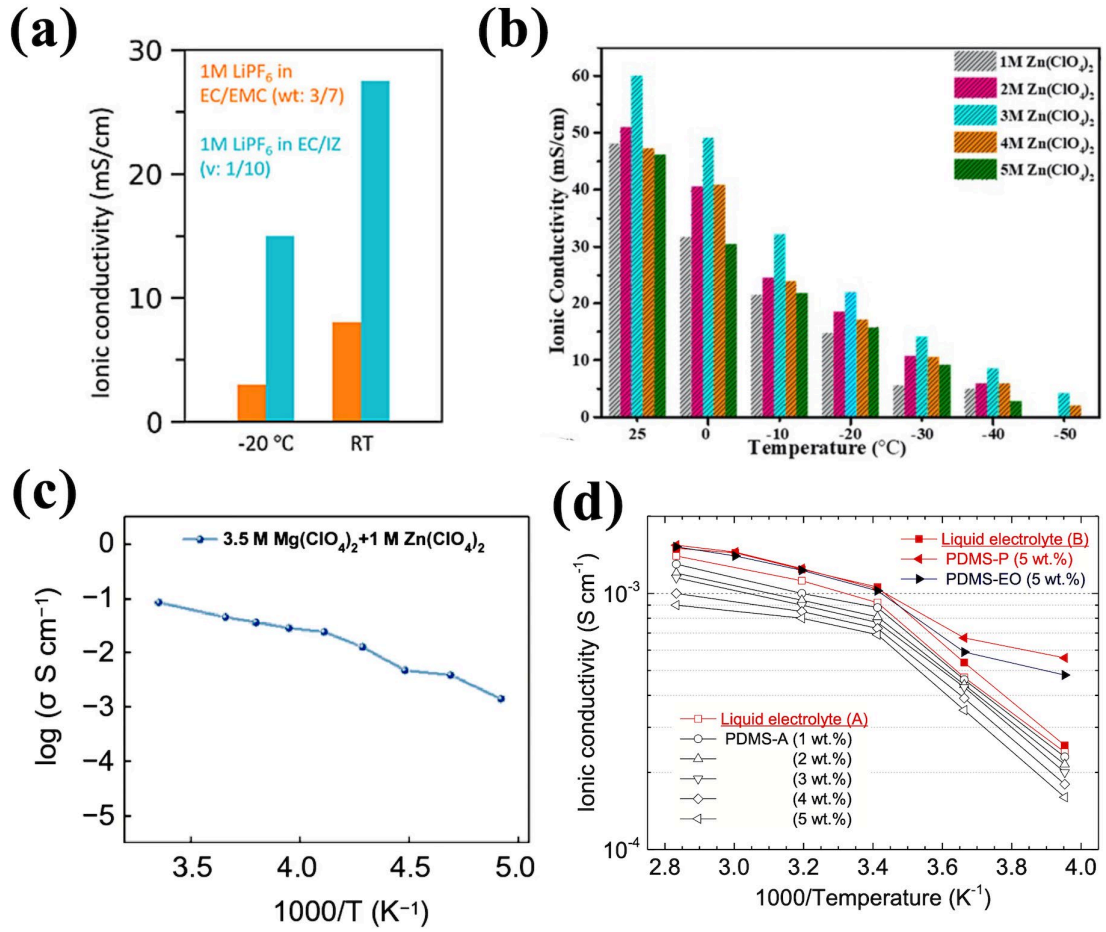

Figure 14. (a) Ionic conductivity of 1 M $LiPF_6$ in EC/EMC (3/7, wt %) and 1 M $LiPF_6$ in EC/IZ (1/10, vol %) electrolytes at room temperature and -20 °C. Reproduced with permission.[202] Copyright 2021, American Chemical Society. (b) Ionic conductivity comparisons of the aqueous $Zn(ClO_4)_2$ aqueous solution with various concentration under different temperatures. Reproduced with permission.[231] Copyright 2022, Wiley-VCH . (c) The ionic conductivity of 3.5 M $Mg(ClO_4)_2$ and $Zn(ClO_4)_2$ based electrolyte for ZIBs at various temperatures. Reproduced with permission.[232] Copyright 2021, Springer Nature. (d) Temperature dependence of ionic conductivities of PDMS-based electrolyte for LIBs at various temperatures. Reproduced with permission.[234] Copyright 2014, Elsevier.

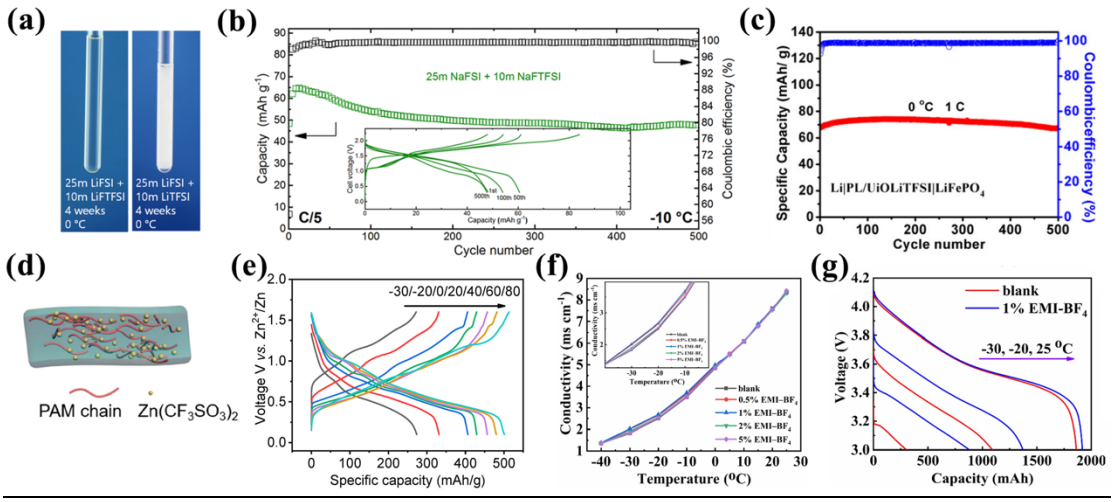

Figure 15. (a) Photographs of 25m LiFSI + 10m LiFTFSI and 25m LiFSI + 10m LiTFSI after storage at 0 °C for 4 weeks, (b) cycling data of $NaTi_2(PO_4)_3|Na_3(VOPO_4)_2F$ full cells under C/5 between 0.3 and 2.2 V at -10 °C. The inset shows voltage profiles for selected cycles. Reproduced with permission.[239] Copyright 2019, American Chemical Society. (c) Cycling performance at 1 C of Li|PL/UiOLiTFSI|LFP at 0 °C. Reproduced with permission.[241] Copyright 2019, American Chemical Society. (d) Schematic illustration of the fabricated 3 M $Zn(CF_3SO_3)_2$PAM gel electrolyte, (e) the electrochemical performance of $Zn(CF_3SO_3)_2$PAM gel electrolyte based ZIBs under 0.2 A g^{-1} at various temperatures. Reproduced with permission.[243] Copyright 2020, American Chemical Society. (f) Ionic conductivity curves of the electrolytes containing 0, 0.5, 1, 2, and 5% EMI-BF_4 from -40 to 25 °C, (g) discharge curves of the NCM523/graphite full cells at the temperatures of -30, -20, and 25 °C at 0.5 C. Reproduced with permission.[248] Copyright 2019, Elsevier.

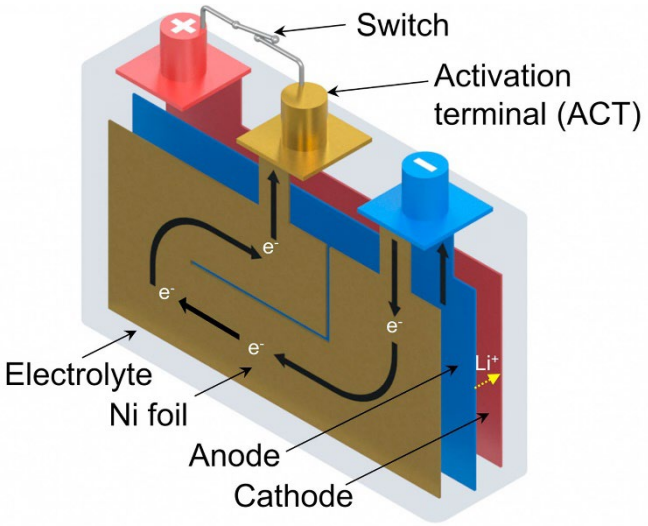

Figure 16. A schematic description of novel battery design in which the nickel foil was inserted into the system to generate heat. Reproduced with permission.[261] Copyright 2016, Elsevier.

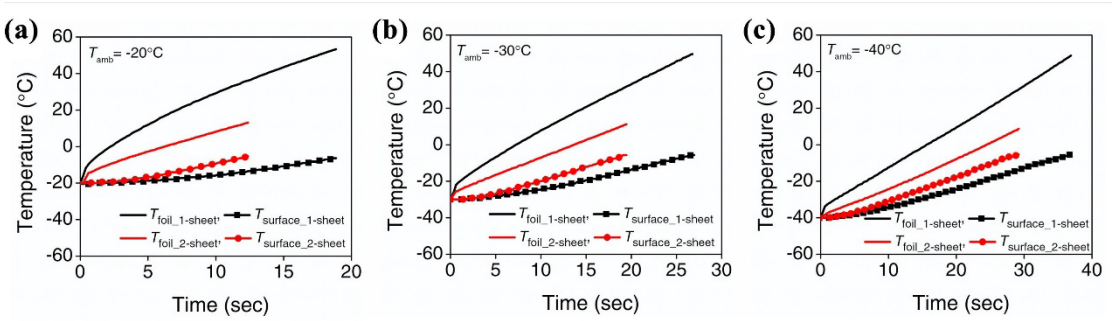

Figure 17. Surface and foil temperatures of the batteries with 1-sheet and 2-sheet designs during self-heating process. (a) -20 ºC. (b) -30 ºC. (c) -40 ºC. Reproduced with permission.[261] Copyright 2016, Elsevier.

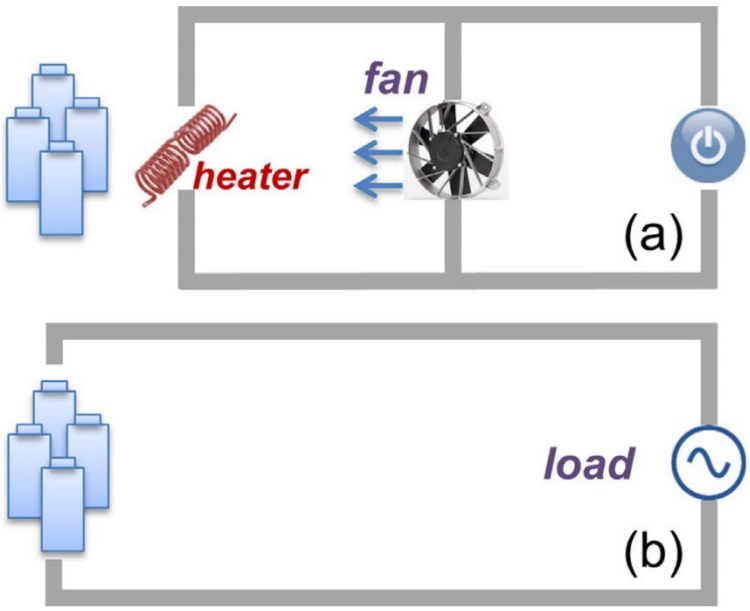

Figure 18. Different heating strategies. (a) External convective heating. (b) AC heating. Reproduced with permission.[262] Copyright 2013, Elsevier.

Tables:

Table 1. Properties of different MIBs.

Properties	Li^+	Na^+	K^+	Zn^{2+}	Mg^{2+}	Al^{3+}
Ionic radii (Å)	0.76	1.02	1.38	0.74	0.72	0.53
Atomic mass	6.94	23.00	39.10	65.38	24.31	26.98
Theoretical capacity (mAh g^{-1})	3861	1166	685	819	2205	8040
Abundance (%)	0.0017	2.8	2.6	0.004	2.4	8.3
E^0 vs. SHE	-3.04	-2.71	-2.931	-0.76	-2.70	-1.66
Desolvation energies (kJ mol^{-1})	160.7 - 254.1	118.1 - 186.3	114.6	/	459.2 - 747.7	/
Ionic conductivity in 1.0 M MFSI (mS cm^{-1})	9.3	9.7	10.7	/	/	/